Université catholique de Louvain

Institute of Neuroscience

Muscle and Exercise Physiology
research group

Regulation of ER stress and insulin pathway by lipids in skeletal muscle

Nicolas Pierre

Thèse présentée en vue de l'obtention du grade
de Docteur en Sciences de la Motricité

Promoteur: Prof. Marc Francaux

Louvain-la-Neuve
2014

JURY

Chair:

Prof. Jean-Louis Thonnard, Université catholique de Louvain, Belgium

Supervisor:

Prof. Marc Francaux, Université catholique de Louvain, Belgium

Committee:

Prof. Pascal Ferré, Université Pierre et Marie Curie, France

Prof. Patrice Cani, Université catholique de Louvain, Belgium

Dr. Xavier Wittebole, Université catholique de Louvain, Belgium

Prof. Jean-Paul Thissen, Université catholique de Louvain, Belgium

Prof. Luc Bertrand, Université catholique de Louvain, Belgium

Remerciements

Cette recherche est le fruit d'un travail collectif. A travers ces quelques lignes, je souhaiterais destiner mes plus chaleureux remerciements à celles et ceux qui ont, de près ou de loin, participé à cette aventure.

En premier lieu Marc, mon promoteur, je tiens à t'exprimer toute ma gratitude pour ton investissement et ton suivi stimulant durant ces six années. En tant que professeur ou promoteur, merci de transmettre ta passion et ton enthousiasme pour la science.
Jean-Marc, merci de m'avoir encadré et encouragé les premières années de ma thèse. Nos discussions scientifiques m'ont accompagné tout au long de mes recherches.

Ma reconnaissance s'adresse ensuite aux membres de mon comité d'accompagnement: Jean-Louis Thonnard, Patrice Cani, Jean-Paul Thissen, Xavier Wittebole, Luc Bertrand. Je vous remercie pour vos critiques constructives et les éclairages que vous avez apportés lors de la défense privée. Merci également à Pascal Ferré, vos remarques m'ont permis d'explorer des mécanismes physiologiques dont je ne soupçonnais pas l'existence.

A mes débuts au laboratoire, Louise, Cécile et Hermann ont été mes guides. Merci à vous pour avoir partagé votre savoir-faire et vos idées.
Je remercie également l'équipe CARD de Luc Bertrand pour m'avoir si bien accueilli, plus particulièrement merci à Audrey, Julien et Edith.

J'ai eu beaucoup de plaisir à collaborer avec Caroline, Pauline et Simon dans le cadre de leurs mémoires. Un grand merci pour votre investissement généreux et nos nombreux échanges stimulants.

Ensuite, mes remerciements s'adressent à mes amis et collègues du laboratoire: Julie, Damien, Céline, Bénédicte. Merci pour votre aide technique, scientifique et aussi pour les bons moments, moins sérieux, passés ensemble.

Je tiens également à remercier toutes les personnes qui participent au bon fonctionnement de l'unité mais aussi à la convivialité de la cafétéria: Sabine, Nico B, Jonathan, Simon, Sophie, Fabian, Elodie, Thierry M, Madeleine, Pascale, Marie-Jo; et les anciens: David, Mathieu, Charles, Gan-Li.

Je tiens à remercier tout particulièrement Rodrigo. Merci « amigo » pour toutes les améliorations, de fond et de forme, que tu as apportées au texte. Cette thèse comporte une touche Chilienne.

Pendant ces six années, j'ai également eu la chance d'enseigner dans de bonnes conditions. C'est pourquoi, je remercie les membres de la FSM, particulièrement Thierry M et Marc, qui m'ont toujours donné toute leur confiance.

Merci à tous ces professeurs passionnés qui, tout au long de mes études, ont stimulé ma curiosité et m'ont donné l'envie de comprendre.

Enfin, il reste à m'adresser à ceux qui me donnent le courage et l'inspiration. Bien qu'ils ne liront probablement jamais cette thèse, ils y sont intégralement associés. Merci à toute ma famille et mes amis.

Je ne pourrais terminer ces remerciements sans parler de toi, Claire. Toujours là, partageant doutes et joies. Merci pour tout.

Table of contents

List of abbreviations

AP-1	activator protein 1
ATF/CREB	activating transcription factor/cyclic AMP response element binding protein
ATF3	activating transcription factor 3
ATF4	activating transcription factor 4
ATF6	activating transcription factor 6
BiP/GRP78	binding immunoglobulin protein/glucose-regulated protein 78 kDa
BSA	bovine serum albumin
bZIP	basic leucine zipper
Cer	ceramide synthase
CD14	cluster of differentiation 14
CHOP	C/EBP homologous protein
DAG	diacylglycerides
DGAT1	acylCoA:diacylglycerol acyltransferase-1
eIF2α	eukaryotic translation-initiation factor 2 alpha
eIF2B	eukaryotic translation-initiation factor 2B
ER	endoplasmic reticulum
ERAD	endoplasmic-reticulum-associated protein degradation
ERKs	extracellular signal-regulated kinases
ERO1	endoplasmic reticulum oxidoreductin-1-like protein
ERSE	ER stress response element
FAD	flavin adenine dinucleotide

FB1	fumonisin B1
FetA	fetuin-A
GCN2	general control non repressed 2
GLUT4	glucose transporter 4
GPx	glutathione peroxidase
GRP94	glucose-regulated protein 94 kDa
GSH	glutathione reduced
GSSG	glutathione oxidized
GSVs	GLUT4 storage vesicles
HFD	high-fat diet
HRI	heme-regulated inhibitor
HSP40	heat-shock protein 40 kDa
HSP70	heat-shock protein 70 kDa
HSP90	heat-shock protein 90 kDa
IκBα	NF-κB inhibitor alpha
IFNβ	interferon beta
IFNγ	interferon gamma
IKK	IκB kinase
IL-1	interleukin 1
IL-6	interleukin 6
IMTG	intramyocellular triglycerides
IP3Rs	inositol trisphosphate receptors
IR	insulin receptor
IRAK	interleukin-1 receptor-associated kinase
IRE1	inositol-requiring 1
IRF3	interferon regulatory factor 3
IRS	insulin receptor substrate

IRESs	internal ribosomal entry sites
ITT	insulin tolerance test
JNKs	c-Jun amino-terminal kinases
LBP	lipopolysaccharide binding protein
LPS	lipopolysaccharide
LRR	leucine-rich repeats
MAM	mitochondria-associated ER membrane
MAMPs	microorganism associated molecular patterns
MAPKs	mitogen-activated protein kinases
MCP1	monocyte chemotactic protein 1
MD-2	myeloid differentiation protein 2
MKK	mitogen-activated protein kinase kinase
mTORC2	mammalian target of rapamycin complex 2
MyD88	myeloid differentiation primary response protein 88
NADPH	nicotinamide adenine dinucleotide phosphate
NEFA	non-esterified fatty acids
NOX	NADPH oxidase
NF-κB	nuclear factor kappa B
NRF2	nuclear factor erythroid 2-related factor 2
OGTT	oral glucose tolerance test
OL	oleate
PA	palmitate
PBA	4-phenyl butyric acid
PDH	pyruvate dehydrogenase
PDI	protein disulfide isomerase
PDK1	phosphoinositide-dependent kinase-1

PERK	double-stranded RNA-dependent protein kinase (PKR)-like ER kinase
PGC-1α	proliferators-activator receptor gamma coactivator-1 alpha
PH	pleckstrin homology
PI3K	phosphatidyl inositol 3-kinase
PIP_2	phosphatidylinositol 4,5-diphosphate
PIP_3	phosphatidylinositol 3,4,5-trisphosphate
PKCζ	protein kinase C zeta
PKCθ	protein kinase C theta
PKR	double-stranded RNA-dependent protein
PL	phospholipids
PLA2	phospholipase A2
PP2A	protein phosphatase 2A
PRRs	pattern recognition receptors
PTB	phosphotyrosine binding
RER	rough endoplasmic reticulum
RIP-1	receptor-interacting protein 1
ROS	reactive oxygen species
RyR1	ryanodine receptor 1
S1P	site-1 protease
S2P	site-2 protease
SCD	stearoyl-CoA-desaturases
SEAP	secreted alkaline phosphatase
SER	smooth endoplasmic reticulum
SERCA1a	sarco/endoplasmic reticulum Ca^{2+} ATPase 1a
SH2	Src homology 2

SOD	superoxide dismutase
SPT	serine palmitoyltransferase
SR	sarcoplasmic reticulum
TAB	TAK-binding proteins
TAD	transcriptional activating domain
TAK1	transforming growth factor-beta-activated kinase 1
TBC1D1	TBC1 family member 1
TBC1D4/AS160	TBC1 family member 4/Akt substrate 160 kDa
TBK1	TANK-binding kinase 1
TC	ternary complex
TG	triglycerides
TIR	toll/interleukin-1 receptor
TIRAP	TIR domain-containing adapter protein
TNFR	tumor necrosis factor receptor
TRAF6	TNF receptor associated factors 6
TRAM	TRIF-related adapter molecule
TRB3	tribbles homolog 3
TRIF	TIR domain-containing adapter-inducing interferon-β
TLR3	toll-like receptor 3
TLR4	toll-like receptor 4
TNFα	tumor necrosis factor alpha
TUDCA	tauroursodeoxycholic acid
Ubc13	ubiquitin-conjugating enzyme
uORFs	upstream open reading frames
UPR	unfolded protein response

Uev1A	ubiquitin-conjugating enzyme
WT	wild-type
XBP1s	X box-binding protein 1, spliced form
XBP1u	X box-binding protein 1, unspliced form
XO	xanthine oxidase

Introduction

From *stapedius* to *sartorius*, skeletal muscle accounts for about 40% of the total body mass. To produce motion, skeletal muscle operates as a motor, which converts chemical energy into mechanical work and heat. Skeletal muscle consumes mainly lipids in basal state as well as during moderate physical exercise (Weber, 2011). In modern society, reduction of physical exercise combined to high energy intake results in a whole body energy storage in the form of fat. In the context of obesity, extracellular and intracellular lipids act as an endogenous toxicant for muscle cells. Lipotoxicity is causally associated with insulin resistance, the principal feature of type 2 diabetes. Recent advances allowed to identify innate immune system and endoplasmic reticulum as key players in lipid-induced insulin resistance.

Chapter 1: Endoplasmic reticulum: from homeostasis to stress response

1.1. General overview

All living organisms as well as virus use proteins in vast array of biological process. Proteins are polymers of units called amino-acids. Linear amino-acids chain is a non-functional structure; protein performances are attributed to their complex three-dimensional shape. In eukaryotic cells, protein folding is mainly achieved in the cytosol and the endoplasmic reticulum (ER). ER lumen provides a unique environment enabling complex reaction which would be impossible in the cytosol. This compartmentalization is essential to fold secreted and

membrane proteins. Inside the ER, cells have evolved a complex machinery to maintain proteostasis (protein homeostasis). A quality control system checks whether proteins are properly folded. Unfolded proteins are degraded either through proteasome or autophagy, whereas correctly folded proteins are exported to the Golgi apparatus. Equilibrium between protein load and folding capacity is delicate. When this balance is upset by physiological or pathological process, unfolded proteins accumulate leading to disturbance of ER homeostasis, this disorder is known as ER stress. To cope with this stress, ER triggers a homeostatic pathway known as unfolded protein response (UPR). After describing the ER and the folding machinery, we will examine UPR signaling.

1.2. Endoplasmic reticulum

ER is a vast eukaryotic organelle surrounding the nucleus. It forms a network of tubules, vesicles and cisternaes delimited by a membrane in continuity with the nucleus. One part of the ER is covered by ribosomes which directly synthesize proteins into the ER lumen. This type of ER is called rough endoplasmic reticulum (RER) since the presence of ribosome makes it visually granular. RER is specialized in the folding of secreted and membrane proteins. RER is more abundant in cells which produce a large amount of secreted proteins (e.g., hepatocyte, plasmocyte, pancreatic β-cells). In contrast to RER, the smooth endoplasmic reticulum (SER) referred to an ER type that is not covered by ribosome. The SER is mainly associated with lipid synthesis. The smooth and striated muscle exhibit a subtype of SER, the sarcoplasmic reticulum (SR). SR has an essential function in

muscle contraction, storing calcium and releasing it in response to action potential. Lastly, depending on the cellular context, ER structures are dynamically interchangeable.

1.3. Endoplasmic reticulum as a protein folding factory

A thought experiment known as Levinthal's paradox highlights the fascinating performances of the cellular folding machinery. A protein of one hundred amino-acid residue, which theoretically has 9^{99} possible conformation, is correctly folded on a subsecond timescale (Stevens and Argon, 1999). Furthermore, the crowded ER environment, about 100 $mg.ml^{-1}$ of macromolecules, makes challenging the folding reaction since unfolded proteins tend to aggregate in such a concentration (Ellis and Minton, 2006, Stevens and Argon, 1999). Much progress has been done since the Nobel Prize, Christian B. Anfinsen, postulated that amino-acid chain contains the native structure information (Sela et al., 1957). However, neither computational science nor *in-vitro* assays are currently able to model or mimic the folding machinery. The protein-folding problem is considered as one of the most challenging question in molecular biology (Ben-Naim, 2012). Its understanding requires a multidisciplinary approach which is beyond the scope of this paragraph. Herein, we will focus on the specificity of ER protein folding. Three main elements drive the folding reaction into the ER: 1) folding factors; 2) oxidative environment; 3) high calcium concentration.

Protein folding reaction are catalyzed or facilitated by a large number of proteins. Inside the ER, around fifty proteins work in an assembly line called the folding pathway (Braakman and Bulleid, 2011). These proteins accomplish multiple functions: chaperone, cochaperone, peptidyl prolyl cis/trans isomerase, oxidoreductase, glycan-binding protein, client-specific folding factor. Native proteins typically have hydrophobic domains buried within their core, whereas hydrophilic domains form a shell around the molecule. On the contrary, the hydrophobic domains of nascent proteins are exposed and tend to aggregate in an amorphous structure (Hartl et al., 2011). Protein aggregation culminates with the formation of a highly toxic structure known as amyloids fibrils (Hartl et al., 2011). To maintain proteostasis, unfolded proteins are segregated by chaperone, a family of proteins which recognize hydrophobic domains (Hartl et al., 2011). A molecular chaperone is defined as: "*any protein which interacts, stabilizes or helps a non-native protein to acquire its native conformation but is not present in the final functional structure*" (Hartl and Hayer-Hartl, 2009). These proteins are found in the ER as well as the cytosol. Among the ER-resident chaperones, the binding immunoglobulin protein (BiP, also known as GRP78 or HSPA5) plays a central role. BiP is a member of the highly conserved heat-shock protein 70 kDa (HSP70) families, which are expressed in probably all eukaryotic cells (Bangs et al., 1993). One remarkable feature of ER-resident chaperone is their ability to perform multiple functions. For instance, BiP is involved in protein folding, UPR regulation, protein translocation, unfolded protein recognition, unfolded protein degradation (Hartl et al., 2011). To perform all these functions, BiP

cooperates with several partners such as HSP40, HSP90 and nucleotide-exchange factors (Buchberger et al., 2010).

The correct folding of proteins is continually evaluated by a quality control system which drives proteins toward folding or degradation processes. Within the ER, N-glycosylation serves as tag to mark the state of protein folding. Most proteins are N-glycosylated once they enter into the ER. This post-translational modification consists of the addition of an oligosaccharide chain to asparagine in the consensus Asn-X-Ser/Thr sequon. N-glycosylation is performed by oligosaccharyltransferase which catalyzes the binding of a $glucose_3$-$mannose_9$-N-$acetylglucosamine_2$ glycan (Needham and Brodsky, 2013). Two glucose molecules are rapidly removed from N-glycosylated proteins by the enzyme glucosidase I and II, enabling the interaction of the polypeptide with the lectin-type chaperones, calnexin and calreticulin. The monoglycosylated protein follows a cycle of deglycosylation and glycosylation mediated by glucosidase II and glycoprotein glucosyl transferase respectively. Native proteins are deglycosylated and enter into the secretory pathway, whereas monoglycosylation serves as a tag for unfolded proteins. Unfolded proteins are eliminated by the endoplasmic-reticulum-associated protein degradation (ERAD) system, a cellular pathway, which culminates with proteasomal degradation. It seems that aggregated proteins are cleared by autophagy but the mechanism remains poorly understood (Buchberger et al., 2010). Finally, glycan binding stabilizes the native protein structure and increases its solubility (Braakman and Bulleid, 2011).

ER provides a unique environment enabling to drive disulfide bond formation. In the cell, reduced glutathione (GSH) is the principal redox buffer (Chakravarthi et al., 2006). Compared to cytosol, ER lumen is highly oxidant. The molar ratio of reduced to oxidized glutathione (GSH/GSSG) ranges from 1:1 to 1:3 in the ER and from 30:1 to 100:1 in the cytosol (Hwang et al., 1992). Oxidative environment allows oxidation of two cysteines to form cystine, resulting thereby in a disulfide bridge. This reaction is catalyzed by the protein disulfide isomerase (PDI), which accepts electrons from thiol groups. Electrons are transferred to another oxidoreductase, the endoplasmic reticulum oxidoreductin-1-like protein (ERO1), which uses flavin adenine dinucleotide (FAD) as a cofactor. Then, ERO1/FAD complex transfers electrons to oxygen and produces hydrogen peroxide (Zhang and Kaufman, 2008). This source of oxidative molecules is not often mentioned in the literature.

Calcium concentration in the ER is several thousand-fold higher than in the cytosol (Schroder and Kaufman, 2005). In the ER of muscle cells, the sarco/endoplasmic reticulum Ca^{2+} ATPase 1a (SERCA1a) regulates calcium entrance, whereas calcium exit depends on the ryanodine receptor 1 (RyR1) and the inositol trisphosphate receptors (IP3Rs) (Csordas and Hajnoczky, 2009). Furthermore, folding factors largely contribute to calcium storage due to their numerous binding sites for the cation (Braakman and Bulleid, 2011). For instance, it has been reported that BiP contributes to 25% of the ER calcium storage in HeLa cells (Lievremont et al., 1997). More

importantly, protein chaperone functions are highly regulated by calcium concentration (Schroder and Kaufman, 2005).

As described above, ER protein folding depends on a subtle interaction between folding factors, redox status and calcium homeostasis. Any perturbation of one of these parameters can disrupt the whole folding machinery and eventually leads to ER stress. The well-known positive controls for ER stress, thapsigargin and tunicamycin, illustrate this fine regulation. Inhibition of SERCA pumps or N-glycosylation by thapsigargin or tunicamycin respectively disrupts ER homeostasis and induced a massive ER stress (Novosyadlyy et al., 2008).

1.4. Unfolded protein response

Accumulation of unfolded proteins into the ER lumen triggers UPR. In eukaryotic cells, UPR includes three pathways initiated by three proteins anchored in the ER membrane, the ER stress sensors: double-stranded RNA-dependent protein kinase (PKR)-like ER kinase (PERK), inositol-requiring 1 (IRE1) and activating transcription factor 6 (ATF6). Each of these proteins is inactivated by BiP binding. Upon ER stress, unfolded proteins competitively recruit BiP leading to activation of the ER stress sensors (Zhang and Kaufman, 2008). UPR mediates an adaptive response via: 1) protein synthesis inhibition; 2) transcriptional upregulation of genes involved in protein folding, transport and ERAD. In the case where these homeostatic responses fail to restore proteostasis, UPR induced cells death through apoptosis. UPR signaling is illustrated in Figure 1.1.

The most immediate response to ER stress is the translational inhibition of protein synthesis (Kaufman, 2004). Upon ER stress, PERK homodimerizes and trans-autophosphorylates. Activated PERK phosphorylates the eukaryotic translation-initiation factor 2α (eIF2α) on serine 51, promoting global inhibition of protein translation and selective protein translation. The mechanism by which eIF2α phosphorylation prevents the initiation stage of protein synthesis have been well described. eIF2 complex (α, β and γ) binds to methionine transfer RNA and GTP to form the ternary complex (TC). This complex assembly is catalyzed by the guanine nucleotide exchange factor eIF2B, which converts inactive eIF2 (eIF2-GDP) to active eIF2 (eIF2-GTP). Phosphorylation of eIF2α on serine 51 inhibits this critical step by stabilizing the inactive complex p-eIF2-GDP-eIF2B (Sudhakar et al., 2000). As a consequence, TC availability decreases, preventing the assembly of the 43S preinitiation complex. Due to the low cellular expression of eIF2B compared to eIF2α (10- to 20-fold lower), inhibition of eIF2B occurs when only 20-30% of eIF2α is phosphorylated (Kaufman et al., 2002, Kaufman, 2004). Consequently, phosphorylation of eIF2α is a key regulator of protein translation.

The initiation step of translation described herein account for the CAP-dependent mechanism. Indeed, mRNAs are recognized by their 5’ CAP end, which successively recruits the 43S preinitiation complex and the 60S ribosomal subunit to form the 80S initiation complex. The 80S ribosomal subunit scans mRNA until to reach the start codon (AUG) (Hashem et al., 2013). Alternatively, unusual mRNA contains internal ribosomal entry sites (IRESs) enabling a CAP-independent

translation (Kaufman, 2004). These cis-acting elements are recognized by the 40S ribosomal subunit which directly starts translation, bypassing thereby the scanning process (Hellen and Sarnow, 2001). Translation of these particular mRNAs is not regulated by eIF2α phosphorylation. This is possibly the case for BiP mRNA, which contains an IRES (Kaufman, 2004).

Paradoxically, eIF2α phosphorylation promotes translation of specific mRNAs by an uncommon mechanism. In eukaryotic cells, upstream open reading frames (uORFs) are short coding sequences present in 5' untranslated region. In human, studies revealed that ~50% of the mRNAs contain at least one uORF (Barbosa et al., 2013). Recognition and translation of uORFs are involved in the regulation of translation initiation. Such mechanism has been initially characterized for the general control non-derepressible 4, the yeast counterpart to activating transcription factor 4 (ATF4). A similar regulation has been found for ATF4 translation response to eIF2α phosphorylation. The mRNA sequence of ATF4 contains two uORFs, which promote (uORF1) or prevent (uORF2) translation (Vattem and Wek, 2004). Upon eIF2α phosphorylation, the reduction in TC level increases time interval required for the scanning ribosome to reinitiate translation at uORF2. This delay allows the ribosomal machinery to skip the inhibitory uORF2 and instead translate the ATF4-coding region (Vattem and Wek, 2004). Thanks to these mechanisms, a single regulator, eIF2α, controls both selective translation and global translation inhibition. In addition to translational control, UPR regulates ATF4 expression at a transcriptional level (Dey et al., 2010).

ATF4 is a transcription factor, which controls most of the effects of the PERK pathway (Schroder and Kaufman, 2005).

In addition to eIF2α, PERK phosphorylates the transcription factor nuclear factor erythroid 2-related factor 2 (NRF2). Phosphorylation of NRF2 by PERK induced its translocation into the nucleus.

The IRE1 pathway is the only UPR branch conserved from yeast to mammalian (Walter and Ron, 2011). In mammalian, two IRE1 paralogs are expressed: IRE1α and IRE1β. IRE1α exhibits ubiquitous expression, whereas IRE1β expression is restricted to intestinal epithelial cells (Iwata and Koizumi, 2012). Activation of IRE1α follows a chronological step, homodimerization then trans-autophosphorylation. These steps are required to activate both functions of IRE1α: kinase and endoribonuclease. When activated, IRE1α triggers a subtle mechanism to regulate activity of the transcription factor X-box-binding protein 1 (XBP1). Such regulation is mediated by a splicing independent of the spliceosome machinery. The unspliced XBP1 (XBP1u) mRNA contains two ORFs partially overlapping (Yoshida et al., 2001). In non-stressed conditions, only the first ORF (ORF1) is translated into a weak transcription factor. Upon ER stress, IRE1α RNase activity results in the splicing of 26-base intron in the overlapping ORFs sequence, generating the spliced form of XBP1 (XBP1s) (Yoshida et al., 2001). Excision of this intronic sequence causes a translational frameshift, which in turn induced a partial translation of both ORFs. The resulting protein contains a basic leucine zipper (bZIP) domain coded by ORF1 and a transcriptional activating domain (TAD) encoded by ORF2

(Nagashima et al., 2011). The presence of a TAD increases drastically XBP1 transcriptional activity (Yoshida et al., 2001). Although non-intuitive, removal of bases from XBP1 transcript results in a protein with a longer amino acid sequence (Iwata and Koizumi, 2012).

The third UPR signaling is initiated by ATF6. In mammalian, all the cells express two ATF6 isoforms, ATF6α and ATF6β (Malhotra and Kaufman, 2007a). Upon ER stress, ATF6 translocates to the Golgi apparatus where it is cleaved by two proteases, the site-1 and site-2 (S1P and S2P) proteases. The proteolysis results in the release of a fragment containing the bZIP domain of ATF6. This fragment migrates to the nucleus and activates transcription (Zhang and Kaufman, 2008).

UPR-regulated transcription factors recognize DNA through a bZIP domain. They act alone or as homodimers or as heterodimers, which are themselves regulated by co-activators and co-repressors (Schroder and Kaufman, 2005). These trans-elements, which bind to cis-elements, constitute the distal step of UPR. XBP1 and ATF6 seem to converge toward the consensus mammalian ER stress response element (ERSE) to control the transcription of chaperones such as BiP and the glucose-regulated protein 94 kDa (GRP94) (Schroder and Kaufman, 2005). ATF4 binds to the activating transcription factor/cyclic AMP response element binding protein (ATF/CREB) site and regulates the transcription of genes encoding proteins involved in antioxidant defense and amino acid biosynthesis (Malhotra and Kaufman, 2007a, Schroder and Kaufman, 2005). ATF4 and ATF6

regulate ER stress-induced apoptosis through induction of the C/EBP homologous protein (CHOP) (Zhang and Kaufman, 2008). Finally, activation of the antioxidant response element by NRF2 regulates the transcription of antioxidant proteins such as subunits of glutathione S-transferase and NAD(P)H:quinone oxidoreductase (Malhotra and Kaufman, 2007a).

In conclusion, eukaryotic cells evolved complex mechanisms to efficiently fold proteins in a highly specialized organelle, i.e., ER. In addition, ER itself is able to defend against stresses through a double-edged weapon, UPR, promoting both survival and the apoptotic death programme.

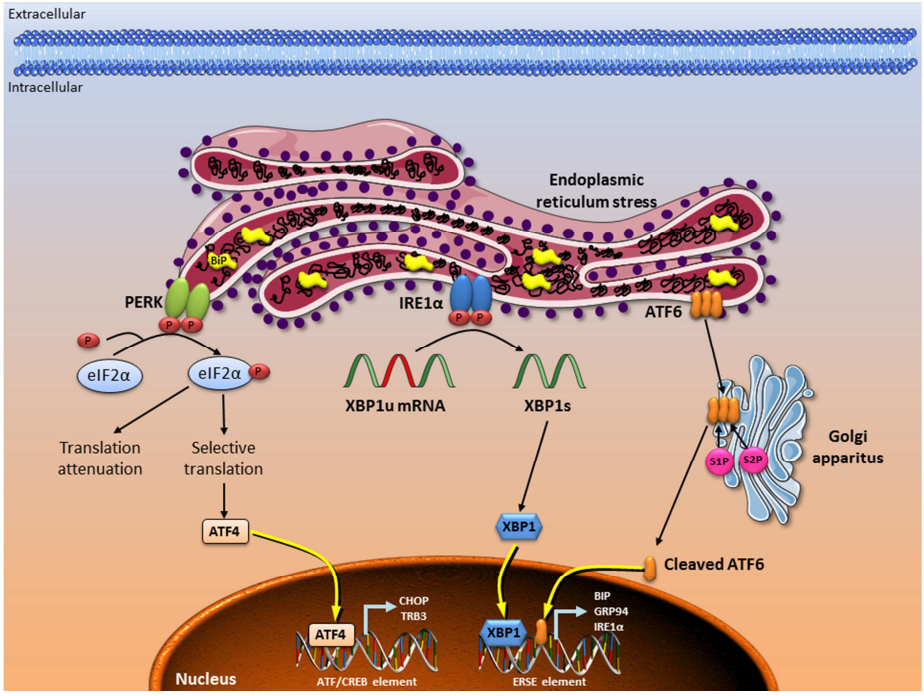

Figure 1.1. UPR signaling. See details in the text.

Chapter 2: Potential mechanisms of lipid-induced endoplasmic reticulum stress

2.1. Toll-like receptor 4 and endoplasmic reticulum stress

2.1.1. Historical overview of toll-like receptor discovery

In 1985, Toll gene was first identified as crucial for *Drosophila* embryogenesis (Anderson et al., 1985). Mutation of this gene induces dorsalized embryos. When the Nobel Laureates Christiane Nüsslein-Volhard observed these abnormal embryos she exclaims: "*Das war ja toll !*" which means in German "That was amazing !", and she gave the name "Toll" to the mutated gene (Hansson and Edfeldt, 2005). At the end of the 1980s, it has been found that *Drosophila* Toll gene encodes a transmembrane protein (Hashimoto et al., 1988). Interestingly, this protein exposes a large extracellular domain that contains leucine-rich repeats (LRR), a consensus sequence involved in protein-ligand interaction (Kobe and Kajava, 2001). In 1996, at the molecular and cellular biology institute of Strasbourg, Jules Hoffman's team showed that a deletion of the *Drosophila* Toll gene reduced survival to fungal infection (Lemaitre et al., 1996). This discovery associated for the first time Toll gene to host defense and was recently rewarded with a Nobel Prize. One year later, the Human Genome Project allowed to identify a human equivalent of the *Drosophila* Toll protein, now called toll-like receptor 4 (TLR4) (Medzhitov et al., 1997). In the wake, Poltorak et al. (1998) discovered that TLR4 mutated mice are resistant to endotoxemia induced by lipopolysaccharide (LPS), a gram-negative bacterial cell wall

component also called endotoxin (Poltorak et al., 1998). This established for the first time that LPS is a TLR4 ligand. All together, these discoveries stimulated research on the innate immune system and led to identify the TLRs family. To date, thirteen mammalian TLRs have been described. The TLRs belong to a large family of proteins, the pattern recognition receptors (PRRs) which recognize highly conserved molecules from pathogens. These molecules are known as microorganism associated molecular patterns (MAMPs) (Kaisho and Akira, 2006).

2.1.2. Toll-like receptor 4 activation and signaling pathways

Besides its expression on immune cells, TLR4 has been found in adipose tissue, liver and skeletal muscle (Reyna et al., 2008, Gustot et al., 2006, Song et al., 2006). TLR4 is a transmembrane protein. Its extracellular N-terminal region consists of LRR modules with a horseshoe-like shape, a motif involved in LPS recognition. On the cytosolic side of the receptor, the C-terminal region exposes a Toll/interleukin-1 receptor (TIR) homology domain orchestrating the downstream signal (Park et al., 2009).

Activation of TLR4 by LPS requires a complex coordination of three accessory proteins (Miyake, 2006): LPS binding protein (LBP), cluster of differentiation 14 (CD14) and myeloid differentiation protein 2 (MD-2). Circulating LPS associates with LBP, a carrier protein synthetized by the liver and the lung. On cell-surface, LBP transfers LPS to CD14. This co-receptor presents LPS to the complex TLR4/MD-2. Crystal structure analysis has revealed interaction

between LPS and the receptor complex (Park et al., 2009). LPS binding to TLR4/MD-2 heterodimer induces the formation of a multimeric receptor composed of two TLR4/MD-2/LPS complexes (Figure 2.1). This complex is internalized into the cytosol, where it initiates the downstream signaling (Kawai and Akira, 2010).

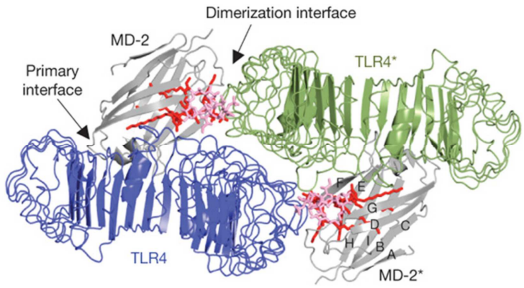

Figure 2.1. Crystal structure of the TLR4-LPS-MD-2 complex (Park et al., 2009)

The interactions between the TIR domain of TLR4 and cytosolic adaptor proteins initiate TLR4 signaling. Activated TLR4 recruits four adaptor proteins: myeloid differentiation primary response protein 88 (MyD88), TIR domain-containing adapter protein (TIRAP), TIR domain-containing adapter-inducing interferon-β (TRIF), and TRIF-related adapter molecule (TRAM). TLR4 triggers two distinct pathways: MyD88-dependent and a MyD88-independent pathways (also called TRIF-dependent pathway). These pathways are illustrated in Figure 2.2.

Except TLR3, all TLRs activate the MyD88-dependent pathway (Patel et al., 2012). Indeed, the production of several cytokines is blocked in MyD88 knockout mice stimulated with TLR ligands (Takeda and Akira, 2004). MyD88-dependent cascade culminates

with the activation of two pro-inflammatory transcription factors: nuclear factor-κB (NF-κB) and activator protein 1 (AP-1). These final effectors control the transcription of cytokines such as tumor necrosis factor α (TNFα), interleukin 1 (IL-1) and interleukin 6 (IL-6) (Takeda and Akira, 2004).

LPS binding to TLR4 leads to the recruitment of a complex formed by MyD88 and TIRAP. This complex associates with two other partners, the interleukin-1 receptor-associated kinase 1 and 4 (IRAK1/4). Phosphorylation of IRAK1 by the kinase IRAK4 enables the association of IRAK1 with the TNF receptor associated factors 6 (TRAF6). The IRAK1/TRAF6 complex separates from the receptor and binds with the transforming growth factor-β-activated kinase 1 (TAK1) and the TAK-binding proteins, TAB1 and TAB2. Activation of TAK1 by TRAF6 is mediated by the ubiquitin-conjugating enzymes, Ubc13 and Uev1A (Wang et al., 2001). Activated TAK1 stimulates NF-κB and AP-1 activity through phosphorylation of the IκB kinase (IKK) and the mitogen-activated protein kinases (MAPKs) respectively. The MAPKs family consists of three kinase subfamilies: extracellular signal-regulated kinases (ERKs), c-Jun amino-terminal kinases (JNKs) and p38. Activation of TAK1 (also called MAP3K7) leads to the MAPK phosphorylation which in turn promotes AP-1 transcriptional activity (Karin, 1995). In the cytosol, NF-κB binds to the NF-κB inhibitor alpha (IκBα) preventing its nuclear translocation. Activated TAK1 phosphorylates IKK complex (IKKα, IKKβ, IKKγ), which in turn phosphorylates IκBα. Subsequently, phosphorylated IκBα is polyubiquitinated and then degraded by the proteasome

system. Once liberated from IκBα, NF-κB can translocate to the nucleus and acts as a transcription factor (Takeda and Akira, 2004).

MyD88 adaptor does not mediate all the TLR4 downstream signaling. In MyD88 knockout macrophages, LPS induces the production of interferon gamma (IFNγ) (Kawai et al., 2001). It is now well established that TLR4 activates the interferon regulatory factor 3 (IRF3) through a MyD88-independent pathway. In response to LPS, TLR4 recruits TRAM and TRIF through their TIR-domain. This event initiates a signaling cascade resulting in the activation the IKK-related kinases IKKε and the TRAF associated NFκB activator TANK-binding kinase 1 (TBK1). These kinases phosphorylate IRF3 leading to its nuclear translocation, where it promotes the transcription IFN-inducible genes such as IFNβ and IFNγ (Clark et al., 2011).

Finally, TLR4 activation induced a delayed activation of NF-κB and AP-1 known as the late-phase response. In other word, redundancy exists between the MyD88-dependent and -independent pathways. TRIF recruits TRAF6 and the receptor-interacting protein 1 (RIP-1) leading to NF-κB and AP-1 activation (Kawai and Akira, 2010).

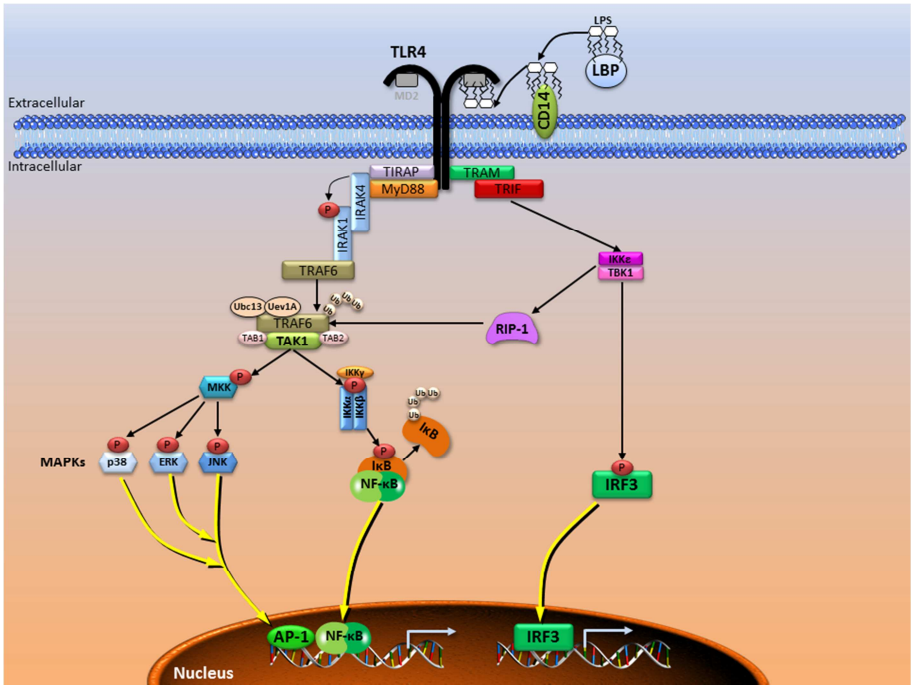

Figure 2.2. TLR4 signaling pathways. See details in the text.

2.1.3. Activation of toll-like receptor 4 by saturated lipids

As its name suggests, LPS is made of lipid and glycan. This biomolecule comprises three parts covalently linked: O-antigen, core polysaccharide and lipid A. Lipid A is responsible for most of the biological activities of LPS. Biologic or synthetic lipid A reproduces the effect of LPS. Lipid A structure is highly conserved among gram-negative bacteria; typically two glucosamines phosphorylated and acylated by four lipid chains, two of them are acylated with two other lipids (Figure 2.3). Lipid A contains six lipid residues, all of them are saturated (Raetz, 1990).

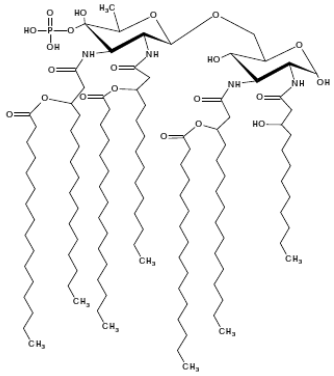

Figure 2.3. LPS from *Brucella* spp (Cardoso et al., 2006)

This hydrophobic region plays a key role in LPS recognition by TLR4 since deacylated lipid A loses its endotoxic activity (Munford and Hall, 1986). All together, these observations had suggested that saturated lipids could be a TLR4 ligand. In 2001, a study demonstrated for the first time that saturated but not unsaturated non-esterified fatty acids (NEFA) activate TLR4 in raw 264.7 macrophages (Lee et al., 2001). This result was confirmed and extended to 3T3-L1 preadipocytes (Shi et al., 2006). In 2009, Errige et al. (2009) casts a doubt on NEFA recognition by TLR4 *in vitro* (Erridge and Samani, 2009). The authors showed that bovine serum albumin (BSA), widely mixed with NEFA in cells culture, is contaminated with TLR4 ligands. The authors concluded: "*LPS and lipopeptide contamination of the widely used reagent fatty-acid-free BSA explains the previously reported stimulation of TLR2 and TLR4 by SFAs*". This conclusion hides important nuances. In this study, three different BSA were used: low endotoxin BSA, fatty acid-free BSA and standard BSA. Only the fatty acid-free BSA stimulated TLRs signaling. Since Lee et al. (2001) used fatty acid-free and low

endotoxin BSA, their findings are probably not an artefact due to BSA contamination. Furthermore, in our lab, we showed that palmitate (16:0) without BSA stimulates TLR4 signaling in C2C12 myotubes (Zbinden-Foncea et al., 2012). Similar results were reported in RAW264.7 macrophages (Huang et al., 2012).

NEFA recognition by TLR4 is also supported by *in vivo* experiments. Some studies showed that $TLR4^{-/-}$ knockout mice are protected against insulin resistance induced by lipid infusion or high-fat diet (HFD) (Shi et al., 2006, Tsukumo et al., 2007).

The mechanism by which NEFA binds to TLR4 remained elusive until 2012. In 2001, Lee et al. (2001) already suggested the presence of an intermediate molecule between NEFA and TLR4: "*Whether saturated fatty acids can directly interact with TLR4 or they interact with molecules associated with either extracellular or intracellular domains of TLR4 remains to be determined*". Recently, such intermediate molecule has been identified. Pal et al. (2012) demonstrated that NEFA alone did not bind to TLR4, this interaction needs a third partner called fetuin-A (FetA) (Pal et al., 2012). In mice adipocytes, FetA as well as TLR4 knockdown prevents NEFA-induced cytokines production and NF-κB activation. In addition, absence of FetA blocks NEFA-induced IL-6 upregulation in RAW 264.7 macrophages. In the TLR4 protein, site-directed mutagenesis revealed that LRR2 and LRR6 are essential for the binding with the NEFA-FetA complex. FetA appears to be the equivalent of LBP for LPS. As LBP, FetA is produced by the liver and acts as an endogenous presenter of NEFA to TLR4.

2.1.4. Regulation of endoplasmic reticulum stress by toll-like receptor 4

Host defense against pathogen invasion activates several stress pathways to orchestrate adaptive response. It appears that TLR4 engagement disrupts ER homeostasis. LPS induced ER stress in different cell types and tissues including lung, liver, adipocytes, human B cells, THP-1 cells and intestinal cells (Endo et al., 2006, Kuribayashi et al., 2008, Kozlov et al., 2009, Coope et al., 2012, Afrazi et al., 2014, Alhusaini et al., 2010). To the best of our knowledge, such experiments have not been carried out in skeletal muscle.

The mechanism by which TLR4 mediates ER stress is still unknown, but probably arises from an increase of ER protein load. In the ER, a greater flux of nascent protein could create an imbalance between protein load and folding capacity leading to ER stress. In skeletal muscle as well as immune cells, TLR4 signaling cascade culminates with the production of a large amount of secreted and membrane proteins including cytokines and TLR4 receptor. In C2C12 myotubes, palmitate and LPS induced a large production of IL-6 in C2C12 (Frost et al., 2006, Jove et al., 2005). TLR4 expression increases in human myotubes incubated with palmitate or lipid A (Reyna et al., 2008).

Furthermore, TLR4-dependent cytokines could indirectly disrupt ER homeostasis. TNFα and IL-1β induced ER stress in L929 cells and liver respectively (Xue et al., 2005, Zhang et al., 2006).

Finally, TLR4 activation could disrupt the folding capacity. It is well established that LPS stimulation is associated with oxidative

stress. In mice injected with LPS, oxidative stress has been detected in skeletal muscle as shown by TBARS assay and GSH/GSSG ratio (Cruzat et al., 2014). In the next part, we will discuss the mechanism by which oxidative stress could induce ER stress.

2.2. Oxidative stress and endoplasmic reticulum stress in muscle cells

2.2.1. Hydrogen peroxide homeostasis

About 2.8 billion years ago, cyanobacteria start to modify atmosphere composition. Thanks to their photosynthetic process, they had converted carbon dioxide into dioxygen leading to a turning point of the evolution. The rise of dioxygen concentration forced life to adapt biochemical processes. Most aerobic organisms used oxygen as a final electron acceptor in a complex chain reaction coupled with energy production. Paradoxically, dioxygen consumption is accompanied by the production of toxic molecules which are involved in most human disorders.

Dioxygen possesses an unusual electron configuration. Ground state dioxygen contains two unpaired electrons with parallel spins, it is a triplet diradical species. To fill its valence shell, dioxygen tends to attract electrons, producing thereby radical species. In other words, dioxygen is an oxidizing agent. In eukaryotic cells, sequential univalent reduction of dioxygen produces molecules known as reactive oxygen species (ROS) (Figure 2.4).

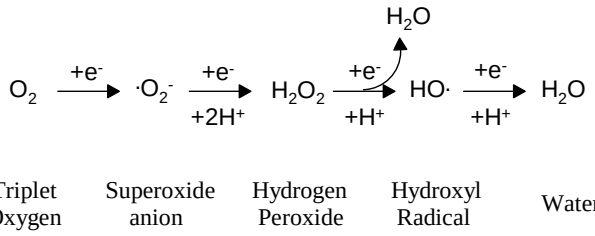

Figure 2.4. Successive monovalent reduction of dioxygen

Among ROS, hydrogen peroxide appears a key molecule in cell physiology and pathology. Because of its relative long half-life and high diffusion capacity, hydrogen peroxide passes through the membrane and, it is recognized as a signaling molecule regulating many physiological processes such as immune response, apoptosis, mitochondria biogenesis, autophagy and differentiation (Powers et al., 2010, Barbieri and Sestili, 2012). On the other hand, univalent reduction of hydrogen peroxide produces hydroxyl radical, the most aggressive ROS (Barbieri and Sestili, 2012). Hydrogen peroxide concentration is tightly regulated by a balance between production and clearance.

The scavenging of hydrogen peroxide depends mainly on glutathione peroxidase (GPx), GSH level and to a lesser extent catalase (Csordas and Hajnoczky, 2009). On the opposite, superoxide dismutation is the principal source of hydrogen peroxide, a reaction catalyzed by the superoxide dismutase (SOD) (Figure 2.5).

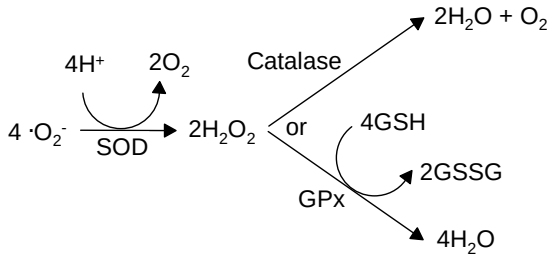

Figure 2.5. Scavenging of hydrogen peroxide by catalase and GPx

Skeletal muscle is particularly exposed to ROS. Indeed, aerobic contraction increases superoxide production due to high oxygen consumption. In muscle cells, superoxide is produced by: 1) mitochondria; 2) nicotinamide adenine dinucleotide phosphate (NADPH) oxidase (NOX); 3) phospholipase A2 (PLA2); 4) xanthine oxidase (XO).

In the mitochondria, electrons from NADH and $FADH_2$ are transferred from electron donor to electron acceptor molecules in a process coupled with energy production. Electrons are transported through four enzymatic complexes known as electrons transport chain. In the cytochrome c oxidase or complex IV, dioxygen undergoes tetravalent reduction to produce water. However, some electrons leak before reaching complex IV, this occurs mainly at complex I and III

(Powers and Jackson, 2008). Free electrons are transferred to dioxygen to produce superoxide. In skeletal muscle, it has been reported that ~0.15% of dioxygen consumed by mitochondria give rise to hydrogen peroxide, this result remains controversial and probably depends on fiber types and oxidized substrates (Barbieri and Sestili, 2012, St-Pierre et al., 2002).

The enzymatic complex NOX transfers electron from NADPH to dioxygen to produce superoxide. Immune cells such as neutrophils and macrophages highly express the phagocyte NADPH oxidase now called NOX2. In these cells, NOX2 is used as a «superoxide gun» to kill pathogen during phagocytosis (Csordas and Hajnoczky, 2009). Recently, six non-phagocytic NOXs have been found: NOX1, NOX3, NOX4, NOX5, DUOX1 and DUOX2 (Kleniewska et al., 2012). Skeletal muscle expressed both NOX2 and NOX4 located in the sarcoplasmic reticulum, the sarcolemma and transverse tubules (Cheng et al., 2001, Powers and Jackson, 2008). It has been reported that NOX4 is constitutively active and produced directly hydrogen peroxide (Nisimoto et al., 2010). In skeletal muscle, NOX clearly contributes to ROS production at rest and during exercise (Powers and Jackson, 2008). However, the physiological function of NOXs in muscle cells remains poorly understood.

PLA2 hydrolyses membrane phospholipid and releases arachidonic acid. This NEFA is a substrate for the lipoxygenases, which reduce dioxygen to produce superoxide. Furthermore, PLA2 could stimulate

NOXs and mitochondria superoxide production (Barbieri and Sestili, 2012).

XO catalyzed the oxidation of hypoxanthine and xanthine to produce xanthine and acid uric, respectively. In these reactions, dioxygen is converted into superoxide. XO contributes to superoxide production in skeletal muscle of rat (Gomez-Cabrera et al., 2005). In human skeletal muscle, generation of superoxide by XO is unclear due to the low expression of this enzyme (Powers and Jackson, 2008).

Finally, ER produces directly hydrogen peroxide during disulfide bond formation (chapter 1).

2.2.2. Induction of oxidative stress by lipids

Oxidative stress results from imbalance between the level of oxidative and antioxidant molecules. In muscle cells, measures of ROS production and oxidative damage demonstrated that lipid excess induced oxidative stress *in vitro, ex vivo* and *in vivo.* In L6 myotubes, palmitate increased mitochondrial ROS production in a dose-dependent manner (Yuzefovych et al., 2010). In *soleus* and *extensor digitorum longus* from rat, palmitate induced ROS production through mitochondria and NOXs but not XO (Lambertucci et al., 2008). Anderson et al. (2009) shown that mitochondrial hydrogen peroxide emission increases in *gastrocnemius* from rats fed with HFD (Anderson et al., 2009). In a similar model, it has been reported that muscle protein carbonyl content, a marker of oxidative protein damage, increases with HFD (Paglialunga et al., 2012). In human fed

with a high-fat meal, mitochondrial hydrogen peroxide production increases in the *vastus lateralis* from lean and obese subjects (Anderson et al., 2009). In addition, the lipid peroxidation content of *vastus lateralis*, a marker of lipid oxidative damage, was 3-fold higher in obese than lean subjects (Russell et al., 2003).

In vitro studies revealed that only saturated NEFA induces ROS production in muscle cells. ROS levels increased in L6 myotubes exposed to palmitate but not palmitoleate (C16:1) (Pillon et al., 2012). In addition, oleate (C18:1) did not change mitochondrial ROS production in L6 myotubes (Yuzefovych et al., 2010). Lipid excess is either stored as triglycerides (TG) or converted into lipid-derived toxic metabolites such as diacylglycerides (DAG) and ceramides. The latter appears a good candidate linking saturated NEFA to ROS production. Ceramides constist of sphingosine amine linked to NEFA. Importantly, ceramide content increases in skeletal muscle from obese subjects and HFD-fed rats (Adams et al., 2004, Zendzian-Piotrowska et al., 2006). As ROS production, ceramide synthesis seems specifically stimulated by saturated NEFA. In C2C12 myotubes as well as human myoblast, palmitate but not oleate increases ceramide levels (Pickersgill et al., 2007, Chavez et al., 2003). Similar results were found in L6 myotubes (Lee et al., 2006). The effect of palmitate on ROS production seems largely mediated by ceramides. C_2-ceramide, an analogue of ceramides, increases dose-dependently mitochondrial ROS production in L6 myotubes (Yuzefovych et al., 2010). In the same study, the authors showed that palmitate-induced mitochondrial ROS accumulation is blocked by fumonisin B1, an

inhibitor of *de novo* ceramide synthesis. All together, these results indicated that saturated NEFA, ceramides and ROS production are closely associated in skeletal muscle.

2.2.3. Oxidative stress and endoplasmic reticulum stress: a vicious circle

The used of antioxidant strategies highlighted the cross-talk between oxidative stress and ER stress in different cell types. In L929 fibroblast cells, TNFα induced ER stress in a ROS-dependent manner (Xue et al., 2005). TNFα as well as tunicamycin activated the PERK and IRE1 pathway as shown by the increase of phospho-eIF2α and XBP1s mRNA, respectively. These effects were completely prevented by butylated hydroxyanisole, an antioxidant molecule. Furthermore, dilatation of ER induced by TNFα and tunicamycin was inhibited by butylated hydroxyanisole. In H9c2 rat cardiomyoblasts, the antioxidant α-tocopherol partially prevents the upregulation of BiP and CHOP protein induced by palmitate exposure (Borradaile et al., 2006). The link between oxidative stress and ER stress is supported in other cell types including murine mesencephalic cells (MN9D), human retinal pigment epithelium (RPE) cells and HeLa cells (Holtz et al., 2006, He et al., 2008, Pallepati and Averill-Bates, 2011). Other report suggested that oxidative stress is uncoupled from ER stress. In endothelial cells, the antioxidants α-tocopherol and ascorbic acids inhibited ROS generation but not ER stress induced by glucotoxicity (Sheikh-Ali et al., 2010). The relation between oxidative stress and ER stress seems cell types-dependent.

In vivo, oxidative stress was induced in mice by adding buthionine sulfoximine, a GSH synthase inhibitor, in drinking water (Guo et al., 2009). After two weeks, ER stress was detected in cardiac muscle as shown by the increase of BiP, phospho-eIF2α, calreticulin and phospho-IRE1α. These effects were abolished in mice with cardiac-specific overexpression of the antioxidant metallothionein (Guo et al., 2009). Although skeletal muscle produces a large amount of ROS, the effect of oxidative stress on ER homeostasis has not been investigated in this organ.

The mechanism by which oxidative stress promotes ER stress is still under investigation. Recently, studies suggested that proximity between ER and mitochondria enables local communication. More precisely, ROS from mitochondria targets ER-based calcium channels leading to leak of calcium from ER. The increase of cytosolic calcium stimulates mitochondria metabolism to produce more ROS, resulting in a vicious circle (Malhotra and Kaufman, 2007b). As noted in chapter 1, calcium concentration tightly regulates ER protein folding.

In different cell types, the gap between ER and mitochondria did not exceed 50 nm (Csordas and Hajnoczky, 2009). Mitochondria appears partially engulfed by ER network as shown by electron microscopy (Mannella, 2000). Cell fractionation demonstrated physical contact between ER and mitochondria. In 1990, Vance found that mitochondria copurifies with some part of the ER in differential centrifugation, this fraction was originally called: «fraction X» (Vance, 1990). Membrane contact site between ER and mitochondria now referred to mitochondria-associated ER membrane (MAM). This

space enables mouth-to-mouth exchange of multiple molecules including calcium and ROS.

ROS from mitochondria can rapidly interact with ER transmembrane protein such as calcium channels. Oxidation of calcium channel in specific Cys thiol group highly regulates their activity (Csordas and Hajnoczky, 2009). ROS increases the activity of RyR1, the calcium release channel essential for excitation-contraction coupling in skeletal muscle (Lanner et al., 2010). In rabbit skeletal muscle, catalase reduced RyR1 activity in a dose-dependent manner (Sun et al., 2011). In C2C12 myotubes, inhibition of NOX4 by siRNA or pharmacological agent abolished RyR1 activity induced by NADPH and high pO_2 (Sun et al., 2011). Calcium flux measurement confirmed these results. Similarly, in cardiac muscle, oxidation of certain thiol groups resulted in irreversible activation of the ryanodine receptor (Xu et al., 1998). Regulation of RyR1 by ROS seems dependent on their concentration. In skeletal muscle from rabbit, hydrogen peroxide up to 10 mM stimulates dose-dependently RyR1 activity while 100 mM totally inhibits the calcium release channel (Favero et al., 1995). Oxidative stress also targets SERCA pumps, IP3Rs and their regulatory partner. Full details are presented in the review by Csordás and Hajnóczky (Csordas and Hajnoczky, 2009).

2.3. Membrane lipid composition and endoplasmic reticulum stress

Cells membranes have been modeled as a “fluid mosaic”, where the phospholipid (PL) bilayer and the anchored proteins represent the fluid and mosaic tiles, respectively (Singer and Nicolson, 1972).

Motions of these proteins depend on the membrane fluidity, i.e., the intermolecular attractive forces of the fluid. This mechanical property is influenced, among others, by the type of NEFA incorporated into PL. More precisely, saturation and length of these NEFA are inversely related to membrane fluidity. Modifications in membrane property are involved in physiological and pathological processes. Indeed, the functioning of membrane-bound proteins is highly regulated by membrane fluidity (Lenaz, 1987). Recently, it has appeared that changes in the composition of ER membrane lipids could be another mechanism by which NEFA disrupts ER homeostasis. Evidences of such a regulation have been demonstrated thanks to manipulation of the stearoyl-CoA-desaturases (SCD). These enzymes are crucial to the biosynthesis of oleate and the formation of unsaturated membrane PL (Lyn et al., 2014). In *Caenorhabditis elegans*, SCD depletion increased BiP expression. This effect was reversed by oleate supplementation (Hou et al., 2014). Similar results were found in 293T cells (Volmer et al., 2013). In addition, PERK activity increased with PL saturation in proteoliposomes (Volmer et al., 2013). This suggests an alternative mechanism by which lipids, particularly saturated NEFA, could disrupt ER homeostasis. Such a mechanism could be physiologically relevant given that dietary lipid intake regulates membrane composition (Abbott et al., 2012).

However, this mechanism seems independent of proteostasis-imbalance. Indeed, SCD depletion did not induce protein aggregation (Hou et al., 2014). Furthermore, deletion of the luminal unfolded protein stress-sensing domain of IRE1α and PERK prevented their activation by thapsigargin but not by membrane lipid saturation

(Volmer et al., 2013). In *Caenorhabditis elegans*, ~90% of the UPR-inducible genes are not regulated through modification of membrane lipid composition, showing thereby an incomplete UPR. Collectively, these results highlight a new type of ER stress and UPR, which are not related to proteostasis. In order to avoid confusion, activation of the ER stress response induced by membrane lipid saturation should bear another name than UPR.

In conclusion, ER is sensitive to various stressful environments including those caused by ROS, innate immune system engagement and changes in membrane lipid content. In this setting, oxidative stress, TLR4 activation and membrane lipid saturation appear as potential mechanisms of NEFA-induced ER stress.

Chapter 3: Mechanisms of lipid-induced insulin resistance in muscle cells

3.1. Regulation of glucose uptake by insulin

Insulin is the master regulator of glycaemia in post-prandial state. After a meal, increase of glycaemia stimulates insulin secretion by the pancreatic β-cells. Insulin promotes glucose uptake mainly in organs widely expressing the insulin sensitive glucose transporter 4 (GLUT4), i.e., skeletal muscle, adipose tissue and cardiac muscle. Insulin action is mediated by several effectors and culminates with the translocation of GLUT4 to the membrane, allowing thereby the entry of glucose into the cell (Figure 3.1).

Insulin binds to its transmembrane receptor, the insulin receptor (IR). IR is a heterotetramer composed by two extracellular α subunits and two transmembrane β subunits linked to each other by disulfide bridges (Chang et al., 2004). Insulin interaction with the α subunits activates the tyrosine kinase domain of the β subunits, resulting in autophosphorylation of several tyrosine residues located in the juxtamembrane region and intracellular C-tail (White and Kahn, 1994). Tyr^{960} of IR is a key residue for the regulation of insulin-stimulated glucose transport (White and Kahn, 1994). This docking site recruits proteins which contain a phosphotyrosine binding (PTB) domain. Among these proteins, the insulin receptor substrates 1 and 2 (IRS-1 and IRS-2) mediate most of the insulin effects. IRS-1/2 contains a PTB domain next to a pleckstrin homology (PH) domain (White, 2003). Due to its high affinity for phospholipids, the PH domain of IRS1/2 stabilizes the protein at the membrane and

facilitates the phosphorylation of its PTB domain by IR. Phosphorylated IRS1/2 on tyrosine residue recruits the regulating subunit (p85) of phosphatidyl inositol 3-kinase (PI3K) through its Src homology 2 (SH2) domains. This interaction leads to the activation of PI3K catalytic subunit (p110), which catalyzes the formation of the membrane phospholipid phosphatidylinositol 3,4,5-trisphosphate (PIP_3) from phosphatidylinositol 4,5-diphosphate (PIP_2) (Chang et al., 2004). PIP_3 recruits Akt (also known as protein kinase B) and phosphoinositide-dependent kinase-1 (PDK1) to the membrane through their PH domains.

The serine/threonine kinase Akt contains a PH domain in its N-terminal end, a kinase domain and a C-terminal hydrophobic domain. In mammalian, three isoforms of Akt have been identified: Akt1, Akt2 and Akt3. Akt1 is widely expressed, whereas Akt3 is principally found in brain and testes. Akt2 expression is predominant in adipocytes and myocytes, where it is responsible of glucose uptake (Hers et al., 2011). In the cytosol, Akt is maintained in an inactive state through an association between its kinase and PH domains. When recruited to the membrane by PIP_3, Akt is phosphorylated by PDK1 and mammalian target of rapamycin complex 2 (mTORC2) on Thr^{308} (kinase domain) and Ser^{473} (C-terminal domain), respectively. Akt activity increases by 100-fold when phosphorylated on Thr^{308}, but full activation requires Ser^{473} phosphorylation (Hers et al., 2011). Activated Akt returns to the cytosol and phosphorylates the TBC1 family member 1 (TBC1D1) and 4 (TBC1D4, formerly known as Akt substrate 160, AS160). TBC1D1/TBC1D4 proteins have GTPase activity toward several Rab proteins (G proteins) associated with

GLUT4 storage vesicles (GSVs). This GTPase activity is inhibited by Akt phosphorylation, leading to an increase of the active forms of Rab, i.e., Rab GTP-bound form (Sakamoto and Holman, 2008). Activated Rab promotes all the steps of GLUT4 exocytosis: approach, tethering, docking and fusion (Stockli et al., 2011). In muscle cells, it seems that Rab8A-Rab13 and Rab14 are under the control of TBC1D4 and TBC1D1, respectively (Klip et al., 2014). Activated Rab8A associated with the myosin Va, a processive motor which promotes GSVs displacement on actin filaments. It seems that Rab13 regulates the tethering of GSVs to the plasma membrane. In skeletal muscle, the role of Rab14 is still unknown. More generally, identification, regulation and individual functions of theses insulin-sensitive Rab proteins remain elusive (Klip et al., 2014).

Recently, actin reorganization has appeared as an essential step of GLUT4 traffic. Independently of Akt downstream signaling, insulin regulates cytoskeletal remodeling through Rac1, another G protein (Chiu et al., 2011). Upon insulin stimulation, PI3K phosphorylation leads to Rac1 GTP loading by a not yet defined mechanism (Klip et al., 2014). Activated Rac1 induces branching of the cortical actin. Actin dynamics regulation seems to promote the tethering of GSVs and insulin effectors to the plasma membrane (Chiu et al., 2011).

The scientific knowledge described in this paragraph is highly dynamic and not homogenous. The signaling from IR to Akt has been well established, whereas regulation of GLUT4 exocytosis by Akt-dependent and -independent mechanisms is less understood and required further explorations.

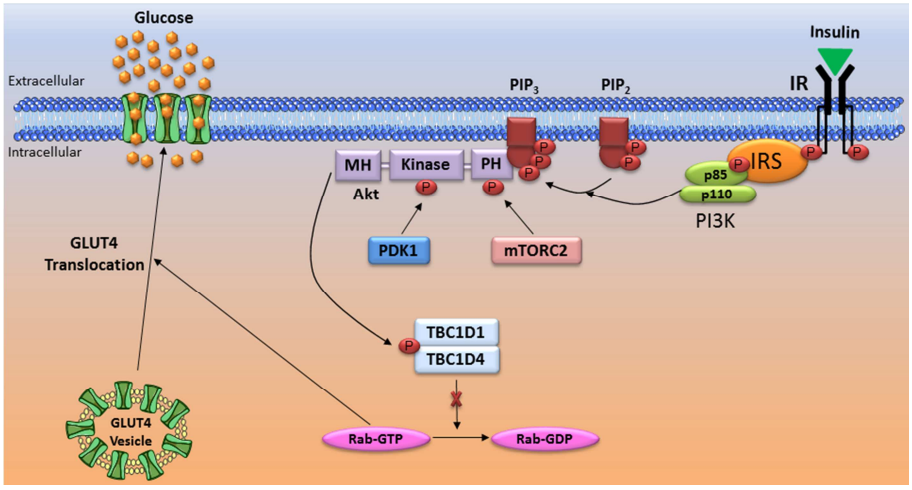

Figure 3.1. Regulation of glucose uptake by insulin. See details in the text.

3.2. Inhibition of insulin-stimulated glucose uptake by lipids: the never ending story

Insulin resistance is generally defined as a reduced ability of insulin to stimulate glucose uptake and to inhibit hepatic glucose production. This pathologic state is associated with obesity and metabolic syndrome. Obesity is characterized by an excess of energy stored as lipids in adipocytes, but also in ectopic tissues such as liver and skeletal muscle. In addition to intracellular deposits, fat accumulates in blood (e.g., NEFA, triglycerides, ceramides and cholesterol). The causal relationship between fat accumulation and insulin resistance is now well established.

In a famous paper published in The Lancet, Randle et al. (1963) were the first to propose that lipids inhibit glucose metabolism, a mechanism known as glucose-fatty acid cycle or Randle cycle (Randle et al., 1963). According to the authors, lipid oxidation alters glucose utilization and conversely. At first sight, it is a happy ending story. Competition between lipids and glucose for oxidation adapts the

energetic substrates to diet composition, regulating thereby lipids and glucose homeostasis. However, Randle et al. (1963) already pointed out that glucose-fatty acid cycle could participate in glucose metabolism disorder such as insulin resistance (Randle et al., 1963).

Fifty-years later, much progress have been done, and we learned that insulin resistance physiopathology differs between liver, muscle and adipose tissue. Herein, we will focus on lipid-induced insulin resistance in skeletal muscle. In human, skeletal muscle accounts for ~80% of insulin-mediated glucose uptake (DeFronzo et al., 1981). This indicates that hyperglycemia, the hallmark of type 2 diabetes, strongly depends on the capacity of skeletal muscle to remove glucose from the circulation.

According to the mechanism proposed by Randle, lipid excess increases acetyl-CoA and citrate concentrations, resulting in the inhibition of pyruvate dehydrogenase (PDH) and phosphofructokinase 1, respectively (Randle, 1998). Then, accumulation of glucose-6-phosphate inhibits hexokinase II and subsequently decreases glucose uptake. This hypothesis was not confirmed in skeletal muscle. In human submitted to an euglycemic-hyperinsulinemic clamp, lipid/heparin infusion inhibited glucose oxidation but failed to increase citrate concentration and to inhibit PDH activity in muscle biopsies (Boden et al., 1991, Saloranta et al., 1993). Another argument against the Randle hypothesis came from Roden et al. (1996) and (1999). They used ^{31}P NMR spectroscopy to continuously monitor *gastrocnemius* glucose-6-phosphate concentration in healthy volunteers during euglycemic-hyperinsulinemic clamp (Roden et al.,

1996, Roden et al., 1999). Lipid infusion increased time-dependently plasma NEFA concentrations and drastically reduced whole-body glucose disposal. In contrast to the Randle hypothesis, glucose-6-phosphate decreased rapidly after lipid infusion. Similar results were found in type 2 diabetic subjects (Rothman et al., 1995). Collectively, these results clearly indicated that the Randle hypothesis does not apply to skeletal muscle. However, it does not totally exclude a direct effect of lipids on glucose metabolism. Indeed, lipids could inhibit hexokinase II, causing a decrease of glucose-6-phosphate and an increase of glucose concentration. To test this hypothesis, Dresner et al. (1999) measured intracellular glucose by ^{13}C NMR spectroscopy in muscle biopsies of healthy volunteers submitted to euglycemic-hyperinsulinemic clamp (Dresner et al., 1999). In this study, lipid infusion reduced intracellular glucose, suggesting that hexokinase II was not inhibited. This indicates that lipids inhibit glucose transport rather than glucose metabolism in skeletal muscle. Inhibition of glucose oxidation and glycogen synthesis by lipids is probably a consequence of a primary defect in glucose transport. It is now well accepted that lipids impair GLUT4 translocation, mainly due to an inhibition of insulin signaling.

Extracellular lipids can disrupt insulin signaling through TLR4, this will be discussed in chapter 8. Furthermore, intracellular lipids are also associated with insulin resistance. In this setting, the case of TG, DAG and ceramides in skeletal muscle will be discussed herein.

Intramyocellular triglycerides (IMTG) concentrations do not seem associated with insulin sensitivity as shown by the “athlete's paradox”.

Endurance-trained athletes are considered highly sensitive to insulin, despite an increase of IMTG levels to the same extent of obese and insulin-resistant subjects (Russell et al., 2003). Although IMTG concentration does not seem a key factor, their peroxidation deserves a particular attention. In the *vastus lateralis*, IMTG peroxidation levels are 6-fold higher in obese subjects than in endurance-trained athletes (Russell et al., 2003). However, a relationship with insulin resistance remains hypothetical.

In vitro experiments demonstrated that saturated NEFA, unlike unsaturated NEFA impairs insulin signaling in C2C12 and L6 myotubes (Yuzefovych et al., 2010, Coll et al., 2008, Peng et al., 2011). The effect of saturated NEFA on insulin pathway seems partially mediated by lipid-derived toxic metabolites such as DAG and ceramides.

The effect of DAG on insulin signaling could be mediated by the novel protein kinase C theta (PKCθ), the most abundant isoform of PKC in muscle cells (Li et al., 2004). DAG is well known to activate (PKCθ), which in turn phosphorylates IRS-1 on an inhibitory serine residue (Ser^{1011}) (Li et al., 2004). Alternatively, PKCθ could act on IKK and JNK as it has been found in T-cells (Altman et al., 2000). Both of these kinases phosphorylate IRS-1 on an inhibitory serine residue, Ser^{307} in rodent and Ser^{312} in human (Morino et al., 2006). Interestingly, HFD increased PKCs activation as well as DAG content in skeletal muscle from rats (Schmitz-Peiffer et al., 1997). In euglycemic-hyperinsulinemic clamp experiment, PKCθ knockout

mice were protected against lipid-induced insulin resistance in skeletal muscle (Kim et al., 2004). However, mice with muscle-specific expression of a dominant-negative PKCθ are obese and insulin-resistant (Serra et al., 2003). Consequently, the involvement of PKCθ in lipid-induced insulin resistance seems controversial.

The implication of DAG in insulin resistance remains unclear in muscle cells. In C2C12 myotubes, palmitate increased DAG content by 6-fold and disrupted insulin signaling. However, inhibition of ceramide synthesis restored insulin signal but had no effect on DAG concentration (Chavez et al., 2003). Consequently, in this study high DAG level were not associated with insulin resistance. In addition, DAG content in skeletal muscle is higher in endurance-trained athletes than obese subjects (Amati et al., 2011). Unexpectedly, DAG concentration was increased in tibialis anterior of rats overexpressing the acylCoA:diacylglycerol acyltransferase-1 (DGAT1), an enzyme that catalyzes the formation of TG from DAG (Timmers et al., 2011). Upon HFD, the insulin-dependent glucose uptake in tibialis anterior was higher in those rats compared to control rats. All together, these results demonstrate a disconnection between DAG content and insulin sensitivity in skeletal muscle. However, the biological effects of DAG depend on their composition, i.e., the length and saturation of the fatty acid chains. Further studies are needed to evaluate the contribution of each DAG species to skeletal muscle insulin resistance. Indeed, if DAG mediates insulin resistance in skeletal muscle, the underlying mechanism is unresolved.

Ceramides are important mediators of lipid-induced insulin resistance in skeletal muscle. Contrary to DAG and IMTG, the “athlete's paradox” does not applies to ceramides. In skeletal muscle, ceramide content is higher in obese than lean sedentary and endurance-trained athletes (Amati et al., 2011). In C2C12 myotubes, palmitate as well as ceramides prevented insulin-stimulated Akt phosphorylation (Chavez et al., 2003, Hage Hassan et al., 2012). On the other hand, the inhibitory effect of palmitate on Akt was restored by the inhibition of *de novo* ceramide synthesis. Importantly, similar results were found with three different inhibitors. Those molecules were myriocin and cycloserine, which inhibit serine palmitoyltransferase (SPT), and fumonisin B1 (FB1) which acts on ceramide synthase (Chavez et al., 2003, Hage Hassan et al., 2012).

At a signaling level, ceramides are well known to inhibit Akt through the protein phosphatase 2A (PP2A) and the atypical PKCζ (Martins et al., 2012). It seems that PKCζ did not impair Akt phosphorylation in muscle cells (Cazzolli et al., 2001). In C2C12 myotubes, inhibition of PP2A with okadaic acid or the SV40 small antigen prevented the inhibitory effect of palmitate on insulin-stimulated Akt phosphorylation (Chavez et al., 2003, Cazzolli et al., 2001). However, in L6 myotubes, okadaic acid failed to restore a loss of Akt phosphorylation and activity induced by ceramides (Hajduch et al., 2001). The role of ceramides in lipid-induced insulin resistance has been assessed *in vivo* by injection of myriocin in HFD-fed and db/db mice (Ussher et al., 2010). In both models, myriocin prevented insulin resistance. However, myriocin increased also energy expenditure. Consequently, it was not clear whether myriocin acted

through ceramides synthesis and/or energetic metabolism. Although ceramides clearly alter insulin signaling *in vitro,* the lack of *in vivo* experiments does not allow strong conclusions.

Alternatively, ceramides could induce insulin resistance via oxidative stress. Indeed, ceramides increase ROS production (chapter 2), and oxidative stress is well known to disrupt insulin signaling in skeletal muscle (Martins et al., 2012). However, this is beyond the scope of this thesis.

3.3. Inhibition of insulin pathway by endoplasmic reticulum stress

In the last decade, ER stress appeared as a key actor in the development of insulin resistance. ER stress has been reported in liver and adipose tissue from leptin deficient (ob/ob) mice and HFD-fed mice (Ozcan et al., 2004). In human, ER stress has been related to body weight (Gregor et al., 2009). Markers of ER stress were measured before and one year after gastric bypass surgery in morbidly obese subjects. After 39% weight loss, phospho-eIF2α, XBP1s and BiP mRNA were reduced in adipose tissue, whereas immunochemistry showed that phospho-eIF2α and BiP levels were decreased in liver. Interestingly, whole-body insulin sensitivity was drastically increased by gastric bypass surgery as shown by the reduction (70%) of the HOMA-IR.

Ozcan et al. (2004) were the first to causally link ER stress to insulin resistance (Ozcan et al., 2004). In Fao liver cells, they showed that ER stress induced by tunycamicin inhibited insulin signaling at the level of IRS-1 and Akt. *In vivo,* deletion of an XBP1 allele in mice

was used to induce ER stress. After 16-weeks HFD, $XBP1^{-/+}$ mice became more insulin-resistant than WT mice as shown by oral glucose tolerance test (OGTT) and insulin tolerance test (ITT) (Ozcan et al., 2004). In the following study, Ozcan et al. (2006) prevented liver ER stress in ob/ob mice by oral administration of the chemical chaperones tauroursodeoxycholic acid (TUDCA) or 4-phenyl butyric acid (PBA) (Ozcan et al., 2006). Upon TUDCA or PBA administrations, ob/ob mice did not developed whole-body insulin resistance. To determine the contribution of each organ, Ozcan et al. (2006) performed euglycemic-hyperinsulinemic clamps. They showed that liver, adipose tissue and skeletal muscle were protected against insulin resistance.

In the paper from Ozcan et al. (2004), ER stress was measured in liver and adipose tissue (Ozcan et al., 2004). They indicated in unpublished observations: "*no indication for ER stress was evident in the muscle tissue of obese animals*". In 2006, they showed in ob/ob mice that TUDCA and PBA increased largely skeletal muscle glucose disposal during euglycemic-hyperinsulinemic clamp (Ozcan et al., 2006). Thus, this suggests that ER stress is involved in the physiopathology of skeletal muscle insulin resistance. Later, studies from our lab as well as others have demonstrated the occurrence of ER stress in muscle cells exposed to high lipid concentration. In C2C12 myotybes, 17 h palmitate (1 mM) incubation increased phospho-PERK, BiP and IRE1α proteins as well as ATF4, CHOP and XBP1s mRNA levels (Deldicque et al., 2010). Similar results were reported in L6 myotubes and human primary myotubes (Hage Hassan et al., 2012, Peter et al., 2009, Peng et al., 2011). Furthermore, after HFD, ER stress was present in skeletal muscle of mice (Deldicque et al., 2010,

Rieusset et al., 2012). However, it seems that short-term HFD did not induce ER stress in human skeletal muscle. In healthy volunteers, 6-weeks HFD diet failed to upregulate ER stress markers in the *vastus lateralis* (Deldicque et al., 2011b).

In muscle cells, ER stress seems implicated in the development of insulin resistance. In C2C12 myotubes, tunicamycin blocked insulin-dependent Akt phosphorylation and glucose uptake (Deldicque et al., 2011a, Panzhinskiy et al., 2013). These deleterious effects were prevented by TUDCA (Panzhinskiy et al., 2013). Similar results were found with PBA in C2C12 myoblast (Peng et al., 2011). However, these findings seem inconsistent with two other reports. In C2C12 myotubes, BiP overexpression as well as TUDCA or PBA treatment did not protect against palmitate-induced insulin resistance (Hage Hassan et al., 2012, Rieusset et al., 2012). Collectively, this suggests that only supraphysiological ER stress could induce insulin resistance in muscle cells.

At a mechanistic level, connections have been reported between UPR and mediators of insulin resistance: JNK/IKK and the tribbles homolog 3 (TRB3). The Figure 3.2 exhibits the potential connections between UPR and insulin signaling.

IRE1α is known to activate JNK and IKK through the adapter protein TRAF2. Both of these kinases phosphorylate IRS-1 on an inhibitory serine residue. IRE1$\alpha^{-/-}$ fibroblasts were protected against JNK activation and IRS-1 serine phosphorylation induced by tunicamycin (Ozcan et al., 2004). In a breast cancer cell line (MCF-7),

IRE1α knockdown prevented IKK activation induced by tunicamycin or thapsigargin (Hu et al., 2006). Similar results were found in fibroblasts (Hu et al., 2006). However, no study investigated whether JNK and IKK are activated by IRE1α in muscle cells. In addition, these mechanisms have been demonstrated only with chemical ER stress inducers.

Recently, TRB3 emerged as a candidate for ER stress-induced insulin resistance. Under ER stress, ATF4 and CHOP cooperate to upregulate TRB3 (Ohoka et al., 2005). Studies demonstrated that TRB3 prevents Akt phosphorylation. TRB3 possesses a kinase-like domain, but lack the ATP binding site and the consensus motif of the catalytic core domain H/Y R D L K/R X X N (Mayumi-Matsuda et al., 1999). Therefore, TRB3 belongs to the pseudokinase family. It has been showed that TRB3 inhibits insulin-stimulated Akt phosphorylation in the liver (Du et al., 2003). In this study, the authors demonstrated that TRB3 binds preferentially with the unphosphorylated kinase domain of Akt. Later, an interaction between TRB3 and the PH domain of Akt has been reported (He et al., 2006). Furthermore, a higher TRB3 expression correlated with a decrease of Akt translocation to the membrane. This effect was restored by TRB3 knockdown (He et al., 2006). Consequently, He et al. (2006) proposed that TRB3 sequesters Akt in the cytosol, preventing thereby its migration to the membrane and subsequent activation. However, interaction of TRB3 with Akt remains controversial. In hepatocytes, TRB3 overexpression did not inhibit insulin-dependent Akt phosphorylation (Iynedjian, 2005).

Interestingly, TRB3 seems involved in the physiopathology of insulin resistance. TRB3 knockout mice were less glucose intolerant than WT mice after a HFD (Koh et al., 2013). Furthermore, the expression of TRB3 in the skeletal muscle has been associated with insulin resistance. TRB3 protein expression is elevated in skeletal muscle from obese subjects, type 2 diabetic patients, leptin receptor deficient (db/db) mice, Zucker fatty rats and streptozotocin-induced diabetic rats (Liu et al., 2010, Koh et al., 2013). Altogether, these results seem to indicate that TRB3 could be implicated in the development of insulin resistance. Nevertheless, its role in lipid-induced insulin resistance has not been evaluated in muscle cells.

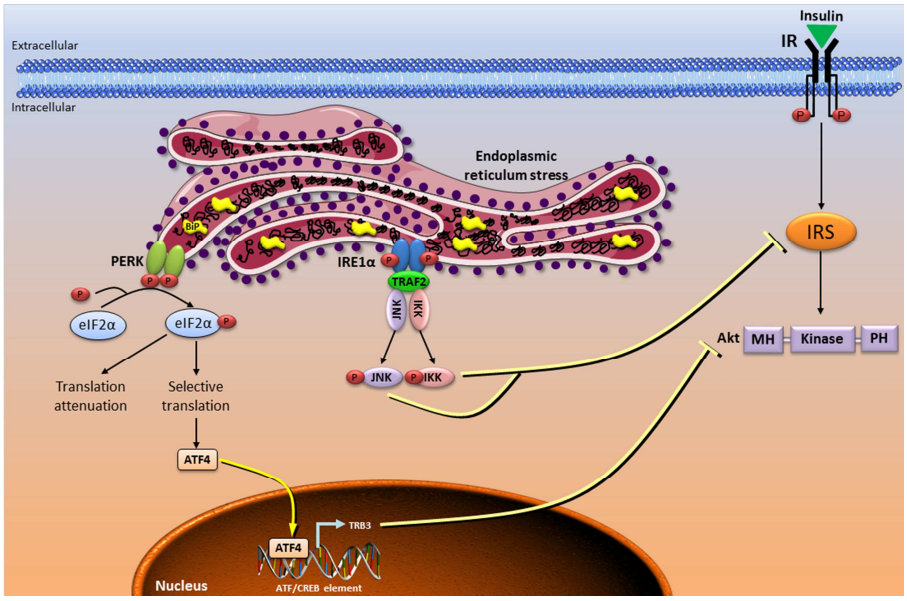

Figure 3.2. Potential connections between UPR and insulin signaling. See details in the text.

Chapter 4: Aim of the thesis

Lipid excess is well known to cause ER stress in many organs including those regulating glucose homeostasis (Flamment et al., 2012). However, the mechanism by which lipids disrupt ER homeostasis remains poorly understood. Interestingly, LPS, a ligand of TLR4 induced ER stress in different cell types (chapter 2). In addition to exogenous ligands, TLR4 recognizes endogenous molecules such as saturated NEFA. The fifth chapter will present a study designed to test whether TLR4 mediates lipid-induced ER stress *in vivo*. This experiment was carried out in WT and $TLR4^{-/-}$ mice submitted to chow or HFD. After HFD, ER stress was measured in skeletal muscle, liver and adipose tissue. In muscle cells, it is particularly unclear how metabolic factors influence ER functions (Hotamisligil, 2010). As noted in chapter 2, high concentrations in lipids is known to trigger oxidative stress, and the use of antioxidant molecules reduced ER stress induced by various conditions. Since muscle cells are great ROS providers, lipids could alter ER equilibrium due to oxidative stress. Chapter six aims to assess whether oxidative stress by itself induces ER stress in C2C12 myotubes.

The inhibitory effect of lipids on glucose uptake is known for over fifty years (Randle et al., 1963), but the underlying mechanisms are not fully unraveled. Although UPR appears as a key mediator of lipid-induced insulin resistance in hepatocytes and adipocytes, this mechanistic link remains controversial in muscle cells. Chapter seven will present a study design to evaluate the connections between UPR and insulin signaling in muscle cells.

References

Abbott, S. K., Else, P. L., Atkins, T. A. & Hulbert, A. J. 2012. Fatty acid composition of membrane bilayers: importance of diet polyunsaturated fat balance. *Biochim Biophys Acta,* **1818,** 1309-17.

Adams, J. M., 2nd, Pratipanawatr, T., Berria, R., Wang, E., DeFronzo, R. A., Sullards, M. C. & Mandarino, L. J. 2004. Ceramide content is increased in skeletal muscle from obese insulin-resistant humans. *Diabetes,* **53,** 25-31.

Afrazi, A., Branca, M. F., Sodhi, C. P., Good, M., Yamaguchi, Y., Egan, C. E., Lu, P., Jia, H., Shaffiey, S., Lin, J., Ma, C., Vincent, G., Prindle, T., Jr., Weyandt, S., Neal, M. D., Ozolek, J. A., *et al.* 2014. Toll-like Receptor 4-mediated Endoplasmic Reticulum Stress in Intestinal Crypts Induces Necrotizing Enterocolitis. *J Biol Chem,* **289,** 9584-99.

Alhusaini, S., McGee, K., Schisano, B., Harte, A., McTernan, P., Kumar, S. & Tripathi, G. 2010. Lipopolysaccharide, high glucose and saturated fatty acids induce endoplasmic reticulum stress in cultured primary human adipocytes: Salicylate alleviates this stress. *Biochem Biophys Res Commun,* **397,** 472-8.

Altman, A., Isakov, N. & Baier, G. 2000. Protein kinase Ctheta: a new essential superstar on the T-cell stage. *Immunol Today,* **21,** 567-73.

Amati, F., Dube, J. J., Alvarez-Carnero, E., Edreira, M. M., Chomentowski, P., Coen, P. M., Switzer, G. E., Bickel, P. E., Stefanovic-Racic, M., Toledo, F. G. & Goodpaster, B. H. 2011. Skeletal muscle triglycerides, diacylglycerols, and ceramides in insulin resistance: another paradox in endurance-trained athletes? *Diabetes,* **60,** 2588-97.

Anderson, E. J., Lustig, M. E., Boyle, K. E., Woodlief, T. L., Kane, D. A., Lin, C. T., Price, J. W., 3rd, Kang, L., Rabinovitch, P. S., Szeto, H. H., Houmard, J. A., Cortright, R. N., Wasserman, D. H. & Neufer, P. D. 2009. Mitochondrial H2O2 emission and cellular redox state link excess fat intake to insulin resistance in both rodents and humans. *J Clin Invest,* **119,** 573-81.

Anderson, K. V., Bokla, L. & Nusslein-Volhard, C. 1985. Establishment of dorsal-ventral polarity in the Drosophila embryo: the induction of polarity by the Toll gene product. *Cell,* **42,** 791-8.

Bangs, J. D., Uyetake, L., Brickman, M. J., Balber, A. E. & Boothroyd, J. C. 1993. Molecular cloning and cellular localization of a BiP homologue in Trypanosoma brucei. Divergent ER retention signals in a lower eukaryote. *J Cell Sci,* **105 (Pt 4),** 1101-13.

Barbieri, E. & Sestili, P. 2012. Reactive oxygen species in skeletal muscle signaling. *J Signal Transduct,* **2012,** 982794.

Barbosa, C., Peixeiro, I. & Romao, L. 2013. Gene expression regulation by upstream open reading frames and human disease. *PLoS Genet,* **9,** e1003529.

Ben-Naim, A. 2012. Levinthal's question revisited, and answered. *J Biomol Struct Dyn,* **30,** 113-24.

Boden, G., Jadali, F., White, J., Liang, Y., Mozzoli, M., Chen, X., Coleman, E. & Smith, C. 1991. Effects of fat on insulin-stimulated carbohydrate metabolism in normal men. *J Clin Invest,* **88,** 960-6.

Borradaile, N. M., Buhman, K. K., Listenberger, L. L., Magee, C. J., Morimoto, E. T., Ory, D. S. & Schaffer, J. E. 2006. A critical role for eukaryotic elongation factor 1A-1 in lipotoxic cell death. *Mol Biol Cell,* **17,** 770-8.

Braakman, I. & Bulleid, N. J. 2011. Protein folding and modification in the mammalian endoplasmic reticulum. *Annu Rev Biochem,* **80,** 71-99.

Buchberger, A., Bukau, B. & Sommer, T. 2010. Protein quality control in the cytosol and the endoplasmic reticulum: brothers in arms. *Mol Cell,* **40,** 238-52.

Cardoso, P. G., Macedo, G. C., Azevedo, V. & Oliveira, S. C. 2006. Brucella spp noncanonical LPS: structure, biosynthesis, and interaction with host immune system. *Microb Cell Fact,* **5,** 13.

Cazzolli, R., Carpenter, L., Biden, T. J. & Schmitz-Peiffer, C. 2001. A role for protein phosphatase 2A-like activity, but not atypical protein kinase Czeta, in the inhibition of protein kinase B/Akt and glycogen synthesis by palmitate. *Diabetes,* **50,** 2210-8.

Chakravarthi, S., Jessop, C. E. & Bulleid, N. J. 2006. The role of glutathione in disulphide bond formation and endoplasmic-reticulum-generated oxidative stress. *EMBO Rep,* **7,** 271-5.

Chang, L., Chiang, S. H. & Saltiel, A. R. 2004. Insulin signaling and the regulation of glucose transport. *Mol Med,* **10,** 65-71.

Chavez, J. A., Knotts, T. A., Wang, L. P., Li, G., Dobrowsky, R. T., Florant, G. L. & Summers, S. A. 2003. A role for ceramide, but not diacylglycerol, in the antagonism of insulin signal transduction by saturated fatty acids. *J Biol Chem,* **278,** 10297-303.

Cheng, G., Cao, Z., Xu, X., van Meir, E. G. & Lambeth, J. D. 2001. Homologs of gp91phox: cloning and tissue expression of Nox3, Nox4, and Nox5. *Gene,* **269,** 131-40.

Chiu, T. T., Jensen, T. E., Sylow, L., Richter, E. A. & Klip, A. 2011. Rac1 signalling towards GLUT4/glucose uptake in skeletal muscle. *Cell Signal,* **23,** 1546-54.

Clark, K., Takeuchi, O., Akira, S. & Cohen, P. 2011. The TRAF-associated protein TANK facilitates cross-talk within the IkappaB kinase family during Toll-like receptor signaling. *Proc Natl Acad Sci U S A,* **108,** 17093-8.

Coll, T., Eyre, E., Rodriguez-Calvo, R., Palomer, X., Sanchez, R. M., Merlos, M., Laguna, J. C. & Vazquez-Carrera, M. 2008. Oleate reverses palmitate-induced insulin resistance and inflammation in skeletal muscle cells. *J Biol Chem,* **283,** 11107-16.

Coope, A., Milanski, M., Arruda, A. P., Ignacio-Souza, L. M., Saad, M. J., Anhe, G. F. & Velloso, L. A. 2012. Chaperone insufficiency links TLR4 protein signaling to endoplasmic reticulum stress. *J Biol Chem,* **287,** 15580-9.

Cruzat, V. F., Bittencourt, A., Scomazzon, S. P., Leite, J. S., de Bittencourt, P. I., Jr. & Tirapegui, J. 2014. Oral free and dipeptide forms of glutamine supplementation attenuate oxidative stress and inflammation induced by endotoxemia. *Nutrition,* **30,** 602-11.

Csordas, G. & Hajnoczky, G. 2009. SR/ER-mitochondrial local communication: calcium and ROS. *Biochim Biophys Acta,* **1787,** 1352-62.

DeFronzo, R. A., Jacot, E., Jequier, E., Maeder, E., Wahren, J. & Felber, J. P. 1981. The effect of insulin on the disposal of intravenous glucose. Results from

indirect calorimetry and hepatic and femoral venous catheterization. *Diabetes,* **30,** 1000-7.

Deldicque, L., Bertrand, L., Patton, A., Francaux, M. & Baar, K. 2011a. ER stress induces anabolic resistance in muscle cells through PKB-induced blockade of mTORC1. *PLoS One,* **6,** e20993.

Deldicque, L., Cani, P. D., Philp, A., Raymackers, J. M., Meakin, P. J., Ashford, M. L., Delzenne, N. M., Francaux, M. & Baar, K. 2010. The unfolded protein response is activated in skeletal muscle by high-fat feeding: potential role in the downregulation of protein synthesis. *Am J Physiol Endocrinol Metab,* **299,** E695-705.

Deldicque, L., Van Proeyen, K., Francaux, M. & Hespel, P. 2011b. The unfolded protein response in human skeletal muscle is not involved in the onset of glucose tolerance impairment induced by a fat-rich diet. *Eur J Appl Physiol,* **111,** 1553-8.

Dey, S., Baird, T. D., Zhou, D., Palam, L. R., Spandau, D. F. & Wek, R. C. 2010. Both transcriptional regulation and translational control of ATF4 are central to the integrated stress response. *J Biol Chem,* **285,** 33165-74.

Dresner, A., Laurent, D., Marcucci, M., Griffin, M. E., Dufour, S., Cline, G. W., Slezak, L. A., Andersen, D. K., Hundal, R. S., Rothman, D. L., Petersen, K. F. & Shulman, G. I. 1999. Effects of free fatty acids on glucose transport and IRS-1-associated phosphatidylinositol 3-kinase activity. *J Clin Invest,* **103,** 253-9.

Du, K., Herzig, S., Kulkarni, R. N. & Montminy, M. 2003. TRB3: a tribbles homolog that inhibits Akt/PKB activation by insulin in liver. *Science,* **300,** 1574-7.

Ellis, R. J. & Minton, A. P. 2006. Protein aggregation in crowded environments. *Biol Chem,* **387,** 485-97.

Endo, M., Mori, M., Akira, S. & Gotoh, T. 2006. C/EBP homologous protein (CHOP) is crucial for the induction of caspase-11 and the pathogenesis of lipopolysaccharide-induced inflammation. *J Immunol,* **176,** 6245-53.

Erridge, C. & Samani, N. J. 2009. Saturated Fatty Acids Do Not Directly Stimulate Toll-Like Receptor Signaling. *Arterioscl Throm Vas,* **29,** 1944-U574.

Favero, T. G., Zable, A. C. & Abramson, J. J. 1995. Hydrogen peroxide stimulates the Ca2+ release channel from skeletal muscle sarcoplasmic reticulum. *J Biol Chem,* **270,** 25557-63.

Flamment, M., Hajduch, E., Ferre, P. & Foufelle, F. 2012. New insights into ER stress-induced insulin resistance. *Trends Endocrinol Metab,* **23,** 381-90.

Frost, R. A., Nystrom, G. J. & Lang, C. H. 2006. Multiple Toll-like receptor ligands induce an IL-6 transcriptional response in skeletal myocytes. *Am J Physiol Regul Integr Comp Physiol,* **290,** R773-84.

Gomez-Cabrera, M. C., Borras, C., Pallardo, F. V., Sastre, J., Ji, L. L. & Vina, J. 2005. Decreasing xanthine oxidase-mediated oxidative stress prevents useful cellular adaptations to exercise in rats. *J Physiol,* **567,** 113-20.

Gregor, M. F., Yang, L., Fabbrini, E., Mohammed, B. S., Eagon, J. C., Hotamisligil, G. S. & Klein, S. 2009. Endoplasmic reticulum stress is reduced in tissues of obese subjects after weight loss. *Diabetes,* **58,** 693-700.

Guo, R., Ma, H., Gao, F., Zhong, L. & Ren, J. 2009. Metallothionein alleviates oxidative stress-induced endoplasmic reticulum stress and myocardial dysfunction. *J Mol Cell Cardiol,* **47,** 228-37.

Gustot, T., Lemmers, A., Moreno, C., Nagy, N., Quertinmont, E., Nicaise, C., Franchimont, D., Louis, H., Deviere, J. & Le Moine, O. 2006. Differential liver sensitization to toll-like receptor pathways in mice with alcoholic fatty liver. *Hepatology,* **43,** 989-1000.

Hage Hassan, R., Hainault, I., Vilquin, J. T., Samama, C., Lasnier, F., Ferre, P., Foufelle, F. & Hajduch, E. 2012. Endoplasmic reticulum stress does not mediate palmitate-induced insulin resistance in mouse and human muscle cells. *Diabetologia,* **55,** 204-14.

Hajduch, E., Balendran, A., Batty, I. H., Litherland, G. J., Blair, A. S., Downes, C. P. & Hundal, H. S. 2001. Ceramide impairs the insulin-dependent membrane recruitment of protein kinase B leading to a loss in downstream signalling in L6 skeletal muscle cells. *Diabetologia,* **44,** 173-83.

Hansson, G. K. & Edfeldt, K. 2005. Toll to be paid at the gateway to the vessel wall. *Arterioscler Thromb Vasc Biol,* **25,** 1085-7.

Hartl, F. U., Bracher, A. & Hayer-Hartl, M. 2011. Molecular chaperones in protein folding and proteostasis. *Nature,* **475,** 324-32.

Hartl, F. U. & Hayer-Hartl, M. 2009. Converging concepts of protein folding in vitro and in vivo. *Nat Struct Mol Biol,* **16,** 574-81.

Hashem, Y., des Georges, A., Dhote, V., Langlois, R., Liao, H. Y., Grassucci, R. A., Hellen, C. U., Pestova, T. V. & Frank, J. 2013. Structure of the mammalian ribosomal 43S preinitiation complex bound to the scanning factor DHX29. *Cell,* **153,** 1108-19.

Hashimoto, C., Hudson, K. L. & Anderson, K. V. 1988. The Toll gene of Drosophila, required for dorsal-ventral embryonic polarity, appears to encode a transmembrane protein. *Cell,* **52,** 269-79.

He, L., Simmen, F. A., Mehendale, H. M., Ronis, M. J. & Badger, T. M. 2006. Chronic ethanol intake impairs insulin signaling in rats by disrupting Akt association with the cell membrane. Role of TRB3 in inhibition of Akt/protein kinase B activation. *J Biol Chem,* **281,** 11126-34.

He, S., Yaung, J., Kim, Y. H., Barron, E., Ryan, S. J. & Hinton, D. R. 2008. Endoplasmic reticulum stress induced by oxidative stress in retinal pigment epithelial cells. *Graefes Arch Clin Exp Ophthalmol,* **246,** 677-83.

Hellen, C. U. & Sarnow, P. 2001. Internal ribosome entry sites in eukaryotic mRNA molecules. *Genes Dev,* **15,** 1593-612.

Hers, I., Vincent, E. E. & Tavare, J. M. 2011. Akt signalling in health and disease. *Cell Signal,* **23,** 1515-27.

Holtz, W. A., Turetzky, J. M., Jong, Y. J. & O'Malley, K. L. 2006. Oxidative stress-triggered unfolded protein response is upstream of intrinsic cell death evoked by parkinsonian mimetics. *J Neurochem,* **99,** 54-69.

Hotamisligil, G. S. 2010. Endoplasmic reticulum stress and the inflammatory basis of metabolic disease. *Cell,* **140,** 900-17.

Hou, N. S., Gutschmidt, A., Choi, D. Y., Pather, K., Shi, X., Watts, J. L., Hoppe, T. & Taubert, S. 2014. Activation of the endoplasmic reticulum unfolded protein response by lipid disequilibrium without disturbed proteostasis in vivo. *Proc Natl Acad Sci U S A,* **111,** E2271-80.

Hu, P., Han, Z., Couvillon, A. D., Kaufman, R. J. & Exton, J. H. 2006. Autocrine tumor necrosis factor alpha links endoplasmic reticulum stress to the membrane death receptor pathway through IRE1alpha-mediated NF-

kappaB activation and down-regulation of TRAF2 expression. *Mol Cell Biol,* **26,** 3071-84.

Huang, S., Rutkowsky, J. M., Snodgrass, R. G., Ono-Moore, K. D., Schneider, D. A., Newman, J. W., Adams, S. H. & Hwang, D. H. 2012. Saturated fatty acids activate TLR-mediated proinflammatory signaling pathways. *J Lipid Res,* **53,** 2002-13.

Hwang, C., Sinskey, A. J. & Lodish, H. F. 1992. Oxidized redox state of glutathione in the endoplasmic reticulum. *Science,* **257,** 1496-502.

Iwata, Y. & Koizumi, N. 2012. Plant transducers of the endoplasmic reticulum unfolded protein response. *Trends Plant Sci,* **17,** 720-7.

Iynedjian, P. B. 2005. Lack of evidence for a role of TRB3/NIPK as an inhibitor of PKB-mediated insulin signalling in primary hepatocytes. *Biochem J,* **386,** 113-8.

Jove, M., Planavila, A., Laguna, J. C. & Vazquez-Carrera, M. 2005. Palmitate-induced interleukin 6 production is mediated by protein kinase C and nuclear-factor kappaB activation and leads to glucose transporter 4 down-regulation in skeletal muscle cells. *Endocrinology,* **146,** 3087-95.

Kaisho, T. & Akira, S. 2006. Toll-like receptor function and signaling. *J Allergy Clin Immunol,* **117,** 979-87; quiz 988.

Karin, M. 1995. The regulation of AP-1 activity by mitogen-activated protein kinases. *J Biol Chem,* **270,** 16483-6.

Kaufman, R. J. 2004. Regulation of mRNA translation by protein folding in the endoplasmic reticulum. *Trends Biochem Sci,* **29,** 152-8.

Kaufman, R. J., Scheuner, D., Schroder, M., Shen, X., Lee, K., Liu, C. Y. & Arnold, S. M. 2002. The unfolded protein response in nutrient sensing and differentiation. *Nat Rev Mol Cell Biol,* **3,** 411-21.

Kawai, T. & Akira, S. 2010. The role of pattern-recognition receptors in innate immunity: update on Toll-like receptors. *Nat Immunol,* **11,** 373-84.

Kawai, T., Takeuchi, O., Fujita, T., Inoue, J., Muhlradt, P. F., Sato, S., Hoshino, K. & Akira, S. 2001. Lipopolysaccharide stimulates the MyD88-independent pathway and results in activation of IFN-regulatory factor 3 and the expression of a subset of lipopolysaccharide-inducible genes. *J Immunol,* **167,** 5887-94.

Kim, J. K., Fillmore, J. J., Sunshine, M. J., Albrecht, B., Higashimori, T., Kim, D. W., Liu, Z. X., Soos, T. J., Cline, G. W., O'Brien, W. R., Littman, D. R. & Shulman, G. I. 2004. PKC-theta knockout mice are protected from fat-induced insulin resistance. *J Clin Invest,* **114,** 823-7.

Kleniewska, P., Piechota, A., Skibska, B. & Goraca, A. 2012. The NADPH oxidase family and its inhibitors. *Arch Immunol Ther Exp (Warsz),* **60,** 277-94.

Klip, A., Sun, Y., Chiu, T. T. & Foley, K. P. 2014. Signal transduction meets vesicle traffic: the software and hardware of GLUT4 translocation. *Am J Physiol Cell Physiol,* **306,** C879-86.

Kobe, B. & Kajava, A. V. 2001. The leucine-rich repeat as a protein recognition motif. *Curr Opin Struct Biol,* **11,** 725-32.

Koh, H. J., Toyoda, T., Didesch, M. M., Lee, M. Y., Sleeman, M. W., Kulkarni, R. N., Musi, N., Hirshman, M. F. & Goodyear, L. J. 2013. Tribbles 3 mediates endoplasmic reticulum stress-induced insulin resistance in skeletal muscle. *Nat Commun,* **4,** 1871.

Kozlov, A. V., Duvigneau, J. C., Miller, I., Nurnberger, S., Gesslbauer, B., Kungl, A., Ohlinger, W., Hartl, R. T., Gille, L., Staniek, K., Gregor, W., Haindl, S. & Redl, H. 2009. Endotoxin causes functional endoplasmic reticulum failure, possibly mediated by mitochondria. *Biochim Biophys Acta,* **1792,** 521-30.

Kuribayashi, J. S., Bombardieri, C. R., Baracho, G. V., Aliberti, J., Machado, F. S., Kalil, J., Guilherme, L., Kokron, C. M., Rizzo, L. V. & de Camargo, M. M. 2008. Slower rescue of ER homeostasis by the unfolded protein response pathway associated with common variable immunodeficiency. *Mol Immunol,* **45,** 2990-7.

Lambertucci, R. H., Hirabara, S. M., Silveira Ldos, R., Levada-Pires, A. C., Curi, R. & Pithon-Curi, T. C. 2008. Palmitate increases superoxide production through mitochondrial electron transport chain and NADPH oxidase activity in skeletal muscle cells. *J Cell Physiol,* **216,** 796-804.

Lanner, J. T., Georgiou, D. K., Joshi, A. D. & Hamilton, S. L. 2010. Ryanodine receptors: structure, expression, molecular details, and function in calcium release. *Cold Spring Harb Perspect Biol,* **2,** a003996.

Lee, J. S., Pinnamaneni, S. K., Eo, S. J., Cho, I. H., Pyo, J. H., Kim, C. K., Sinclair, A. J., Febbraio, M. A. & Watt, M. J. 2006. Saturated, but not n-6 polyunsaturated, fatty acids induce insulin resistance: role of intramuscular accumulation of lipid metabolites. *J Appl Physiol,* **100,** 1467-74.

Lee, J. Y., Sohn, K. H., Rhee, S. H. & Hwang, D. 2001. Saturated fatty acids, but not unsaturated fatty acids, induce the expression of cyclooxygenase-2 mediated through Toll-like receptor 4. *J Biol Chem,* **276,** 16683-9.

Lemaitre, B., Nicolas, E., Michaut, L., Reichhart, J. M. & Hoffmann, J. A. 1996. The dorsoventral regulatory gene cassette spatzle/Toll/cactus controls the potent antifungal response in Drosophila adults. *Cell,* **86,** 973-83.

Lenaz, G. 1987. Lipid fluidity and membrane protein dynamics. *Biosci Rep,* **7,** 823-37.

Li, Y., Soos, T. J., Li, X., Wu, J., Degennaro, M., Sun, X., Littman, D. R., Birnbaum, M. J. & Polakiewicz, R. D. 2004. Protein kinase C Theta inhibits insulin signaling by phosphorylating IRS1 at Ser(1101). *J Biol Chem,* **279,** 45304-7.

Lievremont, J. P., Rizzuto, R., Hendershot, L. & Meldolesi, J. 1997. BiP, a major chaperone protein of the endoplasmic reticulum lumen, plays a direct and important role in the storage of the rapidly exchanging pool of Ca2+. *J Biol Chem,* **272,** 30873-9.

Liu, J., Wu, X., Franklin, J. L., Messina, J. L., Hill, H. S., Moellering, D. R., Walton, R. G., Martin, M. & Garvey, W. T. 2010. Mammalian Tribbles homolog 3 impairs insulin action in skeletal muscle: role in glucose-induced insulin resistance. *Am J Physiol Endocrinol Metab,* **298,** E565-76.

Lyn, R. K., Singaravelu, R., Kargman, S., O'Hara, S., Chan, H., Oballa, R., Huang, Z., Jones, D. M., Ridsdale, A., Russell, R. S., Partridge, A. W. & Pezacki, J. P. 2014. Stearoyl-CoA desaturase inhibition blocks formation of hepatitis C virus-induced specialized membranes. *Sci Rep,* **4,** 4549.

Malhotra, J. D. & Kaufman, R. J. 2007a. The endoplasmic reticulum and the unfolded protein response. *Semin Cell Dev Biol,* **18,** 716-31.

Malhotra, J. D. & Kaufman, R. J. 2007b. Endoplasmic reticulum stress and oxidative stress: a vicious cycle or a double-edged sword? *Antioxid Redox Signal,* **9,** 2277-93.

Mannella, C. A. 2000. Introduction: our changing views of mitochondria. *J Bioenerg Biomembr,* **32,** 1-4.

Martins, A. R., Nachbar, R. T., Gorjao, R., Vinolo, M. A., Festuccia, W. T., Lambertucci, R. H., Cury-Boaventura, M. F., Silveira, L. R., Curi, R. & Hirabara, S. M. 2012. Mechanisms underlying skeletal muscle insulin resistance induced by fatty acids: importance of the mitochondrial function. *Lipids Health Dis,* **11,** 30.

Mayumi-Matsuda, K., Kojima, S., Suzuki, H. & Sakata, T. 1999. Identification of a novel kinase-like gene induced during neuronal cell death. *Biochem Biophys Res Commun,* **258,** 260-4.

Medzhitov, R., Preston-Hurlburt, P. & Janeway, C. A., Jr. 1997. A human homologue of the Drosophila Toll protein signals activation of adaptive immunity. *Nature,* **388,** 394-7.

Miyake, K. 2006. Roles for accessory molecules in microbial recognition by Toll-like receptors. *J Endotoxin Res,* **12,** 195-204.

Morino, K., Petersen, K. F. & Shulman, G. I. 2006. Molecular mechanisms of insulin resistance in humans and their potential links with mitochondrial dysfunction. *Diabetes,* **55 Suppl 2,** S9-S15.

Munford, R. S. & Hall, C. L. 1986. Detoxification of bacterial lipopolysaccharides (endotoxins) by a human neutrophil enzyme. *Science,* **234,** 203-5.

Nagashima, Y., Mishiba, K., Suzuki, E., Shimada, Y., Iwata, Y. & Koizumi, N. 2011. Arabidopsis IRE1 catalyses unconventional splicing of bZIP60 mRNA to produce the active transcription factor. *Sci Rep,* **1,** 29.

Needham, P. G. & Brodsky, J. L. 2013. How early studies on secreted and membrane protein quality control gave rise to the ER associated degradation (ERAD) pathway: the early history of ERAD. *Biochim Biophys Acta,* **1833,** 2447-57.

Nisimoto, Y., Jackson, H. M., Ogawa, H., Kawahara, T. & Lambeth, J. D. 2010. Constitutive NADPH-dependent electron transferase activity of the Nox4 dehydrogenase domain. *Biochemistry,* **49,** 2433-42.

Novosyadlyy, R., Kurshan, N., Lann, D., Vijayakumar, A., Yakar, S. & LeRoith, D. 2008. Insulin-like growth factor-I protects cells from ER stress-induced apoptosis via enhancement of the adaptive capacity of endoplasmic reticulum. *Cell Death Differ,* **15,** 1304-17.

Ohoka, N., Yoshii, S., Hattori, T., Onozaki, K. & Hayashi, H. 2005. TRB3, a novel ER stress-inducible gene, is induced via ATF4-CHOP pathway and is involved in cell death. *Embo J,* **24,** 1243-55.

Ozcan, U., Cao, Q., Yilmaz, E., Lee, A. H., Iwakoshi, N. N., Ozdelen, E., Tuncman, G., Gorgun, C., Glimcher, L. H. & Hotamisligil, G. S. 2004. Endoplasmic reticulum stress links obesity, insulin action, and type 2 diabetes. *Science,* **306,** 457-61.

Ozcan, U., Yilmaz, E., Ozcan, L., Furuhashi, M., Vaillancourt, E., Smith, R. O., Gorgun, C. Z. & Hotamisligil, G. S. 2006. Chemical chaperones reduce ER stress and restore glucose homeostasis in a mouse model of type 2 diabetes. *Science,* **313,** 1137-40.

Paglialunga, S., van Bree, B., Bosma, M., Valdecantos, M. P., Amengual-Cladera, E., Jorgensen, J. A., van Beurden, D., den Hartog, G. J., Ouwens, D. M., Briede, J. J., Schrauwen, P. & Hoeks, J. 2012. Targeting of mitochondrial reactive oxygen species production does not avert lipid-induced insulin resistance in muscle tissue from mice. *Diabetologia,* **55,** 2759-68.

Pal, D., Dasgupta, S., Kundu, R., Maitra, S., Das, G., Mukhopadhyay, S., Ray, S., Majumdar, S. S. & Bhattacharya, S. 2012. Fetuin-A acts as an endogenous ligand of TLR4 to promote lipid-induced insulin resistance. *Nat Med,* **18,** 1279-85.

Pallepati, P. & Averill-Bates, D. A. 2011. Activation of ER stress and apoptosis by hydrogen peroxide in HeLa cells: protective role of mild heat preconditioning at 40 degrees C. *Biochim Biophys Acta,* **1813,** 1987-99.

Panzhinskiy, E., Hua, Y., Culver, B., Ren, J. & Nair, S. 2013. Endoplasmic reticulum stress upregulates protein tyrosine phosphatase 1B and impairs glucose uptake in cultured myotubes. *Diabetologia,* **56,** 598-607.

Park, B. S., Song, D. H., Kim, H. M., Choi, B. S., Lee, H. & Lee, J. O. 2009. The structural basis of lipopolysaccharide recognition by the TLR4-MD-2 complex. *Nature,* **458,** 1191-5.

Patel, H., Shaw, S. G., Shi-Wen, X., Abraham, D., Baker, D. M. & Tsui, J. C. 2012. Toll-like receptors in ischaemia and its potential role in the pathophysiology of muscle damage in critical limb ischaemia. *Cardiol Res Pract,* **2012,** 121237.

Peng, G., Li, L., Liu, Y., Pu, J., Zhang, S., Yu, J., Zhao, J. & Liu, P. 2011. Oleate Blocks Palmitate-Induced Abnormal Lipid Distribution, Endoplasmic Reticulum Expansion and Stress, and Insulin Resistance in Skeletal Muscle. *Endocrinology*.

Peter, A., Weigert, C., Staiger, H., Machicao, F., Schick, F., Machann, J., Stefan, N., Thamer, C., Haring, H. U. & Schleicher, E. 2009. Individual stearoyl-coa desaturase 1 expression modulates endoplasmic reticulum stress and inflammation in human myotubes and is associated with skeletal muscle lipid storage and insulin sensitivity in vivo. *Diabetes,* **58,** 1757-65.

Pickersgill, L., Litherland, G. J., Greenberg, A. S., Walker, M. & Yeaman, S. J. 2007. Key role for ceramides in mediating insulin resistance in human muscle cells. *J Biol Chem,* **282,** 12583-9.

Pillon, N. J., Arane, K., Bilan, P. J., Chiu, T. T. & Klip, A. 2012. Muscle cells challenged with saturated fatty acids mount an autonomous inflammatory response that activates macrophages. *Cell Commun Signal,* **10,** 30.

Poltorak, A., He, X., Smirnova, I., Liu, M. Y., Van Huffel, C., Du, X., Birdwell, D., Alejos, E., Silva, M., Galanos, C., Freudenberg, M., Ricciardi-Castagnoli, P., Layton, B. & Beutler, B. 1998. Defective LPS signaling in C3H/HeJ and C57BL/10ScCr mice: mutations in Tlr4 gene. *Science,* **282,** 2085-8.

Powers, S. K., Duarte, J., Kavazis, A. N. & Talbert, E. E. 2010. Reactive oxygen species are signalling molecules for skeletal muscle adaptation. *Exp Physiol,* **95,** 1-9.

Powers, S. K. & Jackson, M. J. 2008. Exercise-induced oxidative stress: cellular mechanisms and impact on muscle force production. *Physiol Rev,* **88,** 1243-76.

Raetz, C. R. 1990. Biochemistry of endotoxins. *Annu Rev Biochem,* **59,** 129-70.

Randle, P. J. 1998. Regulatory interactions between lipids and carbohydrates: the glucose fatty acid cycle after 35 years. *Diabetes Metab Rev,* **14,** 263-83.

Randle, P. J., Garland, P. B., Hales, C. N. & Newsholme, E. A. 1963. The glucose fatty-acid cycle. Its role in insulin sensitivity and the metabolic disturbances of diabetes mellitus. *Lancet,* **1,** 785-9.

Reyna, S. M., Ghosh, S., Tantiwong, P., Meka, C. S., Eagan, P., Jenkinson, C. P., Cersosimo, E., Defronzo, R. A., Coletta, D. K., Sriwijitkamol, A. & Musi, N. 2008. Elevated toll-like receptor 4 expression and signaling in muscle from insulin-resistant subjects. *Diabetes,* **57,** 2595-602.

Rieusset, J., Chauvin, M. A., Durand, A., Bravard, A., Laugerette, F., Michalski, M. C. & Vidal, H. 2012. Reduction of endoplasmic reticulum stress using chemical chaperones or Grp78 overexpression does not protect muscle cells from palmitate-induced insulin resistance. *Biochem Biophys Res Commun,* **417,** 439-45.

Roden, M., Krssak, M., Stingl, H., Gruber, S., Hofer, A., Furnsinn, C., Moser, E. & Waldhausl, W. 1999. Rapid impairment of skeletal muscle glucose transport/phosphorylation by free fatty acids in humans. *Diabetes,* **48,** 358-64.

Roden, M., Price, T. B., Perseghin, G., Petersen, K. F., Rothman, D. L., Cline, G. W. & Shulman, G. I. 1996. Mechanism of free fatty acid-induced insulin resistance in humans. *J Clin Invest,* **97,** 2859-65.

Rothman, D. L., Magnusson, I., Cline, G., Gerard, D., Kahn, C. R., Shulman, R. G. & Shulman, G. I. 1995. Decreased muscle glucose transport/phosphorylation is an early defect in the pathogenesis of non-insulin-dependent diabetes mellitus. *Proc Natl Acad Sci U S A,* **92,** 983-7.

Russell, A. P., Gastaldi, G., Bobbioni-Harsch, E., Arboit, P., Gobelet, C., Deriaz, O., Golay, A., Witztum, J. L. & Giacobino, J. P. 2003. Lipid peroxidation in skeletal muscle of obese as compared to endurance-trained humans: a case of good vs. bad lipids? *FEBS Lett,* **551,** 104-6.

Sakamoto, K. & Holman, G. D. 2008. Emerging role for AS160/TBC1D4 and TBC1D1 in the regulation of GLUT4 traffic. *Am J Physiol Endocrinol Metab,* **295,** E29-37.

Saloranta, C., Koivisto, V., Widen, E., Falholt, K., DeFronzo, R. A., Harkonen, M. & Groop, L. 1993. Contribution of muscle and liver to glucose-fatty acid cycle in humans. *Am J Physiol,* **264,** E599-605.

Schmitz-Peiffer, C., Browne, C. L., Oakes, N. D., Watkinson, A., Chisholm, D. J., Kraegen, E. W. & Biden, T. J. 1997. Alterations in the expression and cellular localization of protein kinase C isozymes epsilon and theta are associated with insulin resistance in skeletal muscle of the high-fat-fed rat. *Diabetes,* **46,** 169-78.

Schroder, M. & Kaufman, R. J. 2005. The mammalian unfolded protein response. *Annu Rev Biochem,* **74,** 739-89.

Sela, M., White, F. H., Jr. & Anfinsen, C. B. 1957. Reductive cleavage of disulfide bridges in ribonuclease. *Science,* **125,** 691-2.

Serra, C., Federici, M., Buongiorno, A., Senni, M. I., Morelli, S., Segratella, E., Pascuccio, M., Tiveron, C., Mattei, E., Tatangelo, L., Lauro, R., Molinaro, M., Giaccari, A. & Bouche, M. 2003. Transgenic mice with dominant negative PKC-theta in skeletal muscle: a new model of insulin resistance and obesity. *J Cell Physiol,* **196,** 89-97.

Sheikh-Ali, M., Sultan, S., Alamir, A. R., Haas, M. J. & Mooradian, A. D. 2010. Effects of antioxidants on glucose-induced oxidative stress and endoplasmic reticulum stress in endothelial cells. *Diabetes Res Clin Pract,* **87,** 161-6.

Shi, H., Kokoeva, M. V., Inouye, K., Tzameli, I., Yin, H. & Flier, J. S. 2006. TLR4 links innate immunity and fatty acid-induced insulin resistance. *J Clin Invest,* **116,** 3015-25.

Singer, S. J. & Nicolson, G. L. 1972. The fluid mosaic model of the structure of cell membranes. *Science,* **175,** 720-31.

Song, M. J., Kim, K. H., Yoon, J. M. & Kim, J. B. 2006. Activation of Toll-like receptor 4 is associated with insulin resistance in adipocytes. *Biochem Biophys Res Commun,* **346,** 739-45.

St-Pierre, J., Buckingham, J. A., Roebuck, S. J. & Brand, M. D. 2002. Topology of superoxide production from different sites in the mitochondrial electron transport chain. *J Biol Chem,* **277,** 44784-90.

Stevens, F. J. & Argon, Y. 1999. Protein folding in the ER. *Semin Cell Dev Biol,* **10,** 443-54.

Stockli, J., Fazakerley, D. J. & James, D. E. 2011. GLUT4 exocytosis. *J Cell Sci,* **124,** 4147-59.

Sudhakar, A., Ramachandran, A., Ghosh, S., Hasnain, S. E., Kaufman, R. J. & Ramaiah, K. V. 2000. Phosphorylation of serine 51 in initiation factor 2 alpha (eIF2 alpha) promotes complex formation between eIF2 alpha(P) and eIF2B and causes inhibition in the guanine nucleotide exchange activity of eIF2B. *Biochemistry,* **39,** 12929-38.

Sun, Q. A., Hess, D. T., Nogueira, L., Yong, S., Bowles, D. E., Eu, J., Laurita, K. R., Meissner, G. & Stamler, J. S. 2011. Oxygen-coupled redox regulation of the skeletal muscle ryanodine receptor-Ca2+ release channel by NADPH oxidase 4. *Proc Natl Acad Sci U S A,* **108,** 16098-103.

Takeda, K. & Akira, S. 2004. TLR signaling pathways. *Semin Immunol,* **16,** 3-9.

Timmers, S., de Vogel-van den Bosch, J., Hesselink, M. K., van Beurden, D., Schaart, G., Ferraz, M. J., Losen, M., Martinez-Martinez, P., De Baets, M. H., Aerts, J. M. & Schrauwen, P. 2011. Paradoxical increase in TAG and DAG content parallel the insulin sensitizing effect of unilateral DGAT1 overexpression in rat skeletal muscle. *PLoS One,* **6,** e14503.

Tsukumo, D. M., Carvalho-Filho, M. A., Carvalheira, J. B., Prada, P. O., Hirabara, S. M., Schenka, A. A., Araujo, E. P., Vassallo, J., Curi, R., Velloso, L. A. & Saad, M. J. 2007. Loss-of-function mutation in Toll-like receptor 4 prevents diet-induced obesity and insulin resistance. *Diabetes,* **56,** 1986-98.

Ussher, J. R., Koves, T. R., Cadete, V. J., Zhang, L., Jaswal, J. S., Swyrd, S. J., Lopaschuk, D. G., Proctor, S. D., Keung, W., Muoio, D. M. & Lopaschuk, G. D. 2010. Inhibition of de novo ceramide synthesis reverses diet-induced insulin resistance and enhances whole-body oxygen consumption. *Diabetes,* **59,** 2453-64.

Vance, J. E. 1990. Phospholipid synthesis in a membrane fraction associated with mitochondria. *J Biol Chem,* **265,** 7248-56.

Vattem, K. M. & Wek, R. C. 2004. Reinitiation involving upstream ORFs regulates ATF4 mRNA translation in mammalian cells. *Proc Natl Acad Sci U S A,* **101,** 11269-74.

Volmer, R., van der Ploeg, K. & Ron, D. 2013. Membrane lipid saturation activates endoplasmic reticulum unfolded protein response transducers through their transmembrane domains. *Proc Natl Acad Sci U S A,* **110,** 4628-33.

Walter, P. & Ron, D. 2011. The unfolded protein response: from stress pathway to homeostatic regulation. *Science,* **334,** 1081-6.

Wang, C., Deng, L., Hong, M., Akkaraju, G. R., Inoue, J. & Chen, Z. J. 2001. TAK1 is a ubiquitin-dependent kinase of MKK and IKK. *Nature,* **412,** 346-51.

Weber, J. M. 2011. Metabolic fuels: regulating fluxes to select mix. *J Exp Biol,* **214,** 286-94.

White, M. F. 2003. Insulin signaling in health and disease. *Science,* **302,** 1710-1.

White, M. F. & Kahn, C. R. 1994. The insulin signaling system. *J Biol Chem,* **269,** 1-4.

Xu, L., Eu, J. P., Meissner, G. & Stamler, J. S. 1998. Activation of the cardiac calcium release channel (ryanodine receptor) by poly-S-nitrosylation. *Science,* **279,** 234-7.

Xue, X., Piao, J. H., Nakajima, A., Sakon-Komazawa, S., Kojima, Y., Mori, K., Yagita, H., Okumura, K., Harding, H. & Nakano, H. 2005. Tumor necrosis factor alpha (TNFalpha) induces the unfolded protein response (UPR) in a reactive oxygen species (ROS)-dependent fashion, and the UPR counteracts ROS accumulation by TNFalpha. *J Biol Chem,* **280,** 33917-25.

Yoshida, H., Matsui, T., Yamamoto, A., Okada, T. & Mori, K. 2001. XBP1 mRNA is induced by ATF6 and spliced by IRE1 in response to ER stress to produce a highly active transcription factor. *Cell,* **107,** 881-91.

Yuzefovych, L., Wilson, G. & Rachek, L. 2010. Different effects of oleate vs. palmitate on mitochondrial function, apoptosis, and insulin signaling in L6 skeletal muscle cells: role of oxidative stress. *Am J Physiol Endocrinol Metab,* **299,** E1096-105.

Zbinden-Foncea, H., Deldicque, L., Pierre, N., Francaux, M. & Raymackers, J. M. 2012. TLR2 and TLR4 activation induces p38 MAPK-dependent phosphorylation of S6 kinase 1 in C2C12 myotubes. *Cell Biol Int,* **36,** 1107-13.

Zendzian-Piotrowska, M., Baranowski, M., Zabielski, P. & Gorski, J. 2006. Effects of pioglitazone and high-fat diet on ceramide metabolism in rat skeletal muscles. *J Physiol Pharmacol,* **57 Suppl 10,** 101-14.

Zhang, K. & Kaufman, R. J. 2008. From endoplasmic-reticulum stress to the inflammatory response. *Nature,* **454,** 455-62.

Zhang, K., Shen, X., Wu, J., Sakaki, K., Saunders, T., Rutkowski, D. T., Back, S. H. & Kaufman, R. J. 2006. Endoplasmic reticulum stress activates cleavage of CREBH to induce a systemic inflammatory response. *Cell,* **124,** 587-99.

Chapter 5: Toll-Like Receptor 4 Knockout Mice Are Protected Against Endoplasmic Reticulum Stress Induced by a High-Fat Diet

Nicolas Pierre[1], Louise Deldicque[2], Caroline Barbé[1], Damien Naslain[1], Patrice D. Cani[3], Marc Francaux[1]

[1]Institute of Neuroscience, Université catholique de Louvain, Louvain-la-Neuve, Belgium

[2]Department of Kinesiology, Exercise Physiology Research Group, KU Leuven, Belgium

[3]Louvain Drug Research Institute, Université catholique de Louvain, Brussels, Belgium

PLoS ONE. May 31, 2013

Abstract

The purpose of this study was to investigate whether toll-like receptor 4 (TLR4) is implicated in the development of endoplasmic reticulum stress (ER stress) observed after a high-fat diet (HFD) in liver, skeletal muscle and adipose tissue. $TLR4^{-/-}$ and C57BL/6J wild-type mice (WT) were fed with chow or HFD (45% calories from fat) during 18 weeks. An oral glucose tolerance-test was performed. The animals were sacrificed in a fasted state and the tissues were removed. TLR4 deletion protected from body weight gain and glucose intolerance induced by HFD whereas energy intake was higher in transgenic mice suggesting larger energy expenditure. HFD induced an ER stress in skeletal muscle, liver and adipose tissue of WT mice as assessed by BiP, CHOP, spliced and unspliced XBP1 and phospho-eIF2α. $TLR4^{-/-}$ mice were protected against HFD-induced ER stress. Then, we investigated the main signaling downstream of TLR4 namely the NF-κB pathway, expecting to identify the mechanism by which TLR4 is able to activate ER stress. The mRNA levels of cytokines regulated by NF-κB namely TNFα, IL-1β and IL-6, were not changed after HFD and phospho-IκB-α (ser 32) was not changed. Our results indicate that TLR4 is essential for the development of ER stress related to HFD. Nevertheless, the NFκ-B pathway does not seem to be directly implicated. The reduced fat storage in $TLR4^{-/-}$ mice could explain the absence of an ER stress after HFD.

Introduction

Obesity is often associated with a chronic low grade inflammatory state (Greenberg and Obin, 2006, Wellen and Hotamisligil, 2005), which in turn contributes to the development of various metabolic diseases such as insulin resistance (Kim et al., 2004, Yuan et al., 2001, Hirosumi et al., 2002, Hotamisligil et al., 1996). During the last decade, major advances were made for identifying the molecular mechanisms leading to lipotoxicity in various cell types (Schaffer, 2003). A high level of circulating non-esterified fatty acids (NEFA) is able to induce insulin resistance within a few hours in healthy volunteers suggesting that an alteration in intracellular lipid metabolism may impair insulin signaling (Roden et al., 1999, Roden et al., 1996). Ceramides and diacylglycerol (DAG) are lipid-derived toxic metabolites inhibiting insulin signal via dephosphorylation of protein kinase B (PKB) and phosphorylation of a serine residue on insulin receptor substrate (IRS) (Summers, 2006, Idris et al., 2001). However, one may not exclude that circulating NEFA *per se* are able to act on insulin sensitivity through binding to a membrane receptor and activating a downstream cascade of events that would crosstalk with insulin signaling. Indeed, previous observations suggest that circulating NEFA can bind a plasma membrane receptor, namely the toll-like receptor 4 (TLR4), and its co-receptors CD14 and MD-2 (Shi et al., 2006, Lee et al., 2001).

The TLR are members of the pattern-recognition receptor family that play a key role in the innate immune system (Kaisho and Akira, 2006). To date, thirteen mammalian TLR have been identified (Kaisho and Akira, 2006). TLR4, a subclass of TLR, is activated by the lipidic

domain of lipopolysaccharide (LPS), a gram-negative bacterial cell wall component (Miyake, 2004). Ablation of TLR4 in transgenic mice confers partial protection against insulin resistance induced by lipid infusion or high-fat diet (HFD) (Shi et al., 2006, Radin et al., 2008, Tsukumo et al., 2007, Kim et al., 2007, Davis et al., 2008, Poggi et al., 2007). Therefore, TLR4 could be the missing link between high circulating lipids and insulin resistance.

Lipid excess is known to cause another cell stress known as endoplasmic reticulum (ER) stress (Boden, 2009, Tsiotra and Tsigos, 2006, Zhang and Kaufman, 2008, Deldicque et al., 2010) which is the consequence of a disequilibrium between the folding capacity of ER and the amount of proteins to be folded. To cope with this stress, the cell triggers a series of signal transduction known as the unfolded protein response (UPR), which is initiated at the level of three ER stress sensors: inositol-requiring 1α (IRE1α), double-stranded RNA-dependent protein kinase (PKR)-like ER kinase (PERK) and activating transcription factor 6 (ATF6). Each of these sensors is associated with the protein chaperone immunoglobulin-heavy-chain-binding protein (BiP). Upon accumulation of unfolded proteins in the ER lumen, BiP is released from PERK, IRE1α and ATF6 leading to their activation and downstream signaling. These pathways initiate a homeostatic response via: 1) protein synthesis inhibition through the phosphorylation of eukaryotic translation-initiation factor 2α (eIF2α); 2) transcriptional up-regulation of genes involved in protein folding, transport and ER-associated protein degradation; 3) apoptosis mediated by C/EBP homologous (CHOP) (Zhang and Kaufman, 2008).

ER stress was observed in liver of ob/ob and high-fat fed mice and was proposed to be involved in the pathophysiology of insulin resistance through an interaction between UPR and inflammation signaling (Ozcan et al., 2004). Indeed, a growing body of evidence suggests that UPR and insulin resistance are interconnected through at least 2 mechanisms: 1) IRE1α pathway induces c-Jun N-terminal kinase (JNK) phosphorylation which inhibits IRS; 2) PERK and IRE1α pathway activate transcription factors such as nuclear factor-κB (NF-κB) and activator protein 1 (AP-1) which migrate to the nucleus and induce the transcription of cytokines known to contribute to the development of insulin resistance (Zhang and Kaufman, 2008, Urano et al., 2000, Ozcan et al., 2004).

ER stress and TLR4 signaling are both major players in the development of insulin resistance induced by lipid excess. Whether those two actors act independently or are causally linked is still unknown. In the present study, we hypothesized that TLR4 signaling would mediate lipid-induced ER stress via activation of the NF-κB pathway. To test this hypothesis, TLR4 knockout (TLR4$^{-/-}$) and wild-type (WT) mice were fed with a HFD and the activation of ER stress in liver, skeletal muscle and adipose tissue was measured. Our results show that ER stress is activated by a HFD in WT whereas it is not in TLR4$^{-/-}$ mice.

Materials and methods

Animal care and protocol

All protocols were approved by the ethical committee for animal use of the Université catholique de Louvain (Belgium) and the

housing conditions were as specified by the Belgian Law of April 6, 2010 on the protection of laboratory animals (agreement n° LA 1220548). 14-16-week-old male TLR4$^{-/-}$ (Hoshino et al., 1999)[1] and C57BL/6J wild-type mice (WT) were purchased from Transgenose Institute (CNRS, Orléans, France) and the Laboratory of Experimental Surgery (UCL, Woluwé, Belgium), respectively. TLR4$^{-/-}$ genotype was confirmed by PCR. Animals were housed in cages *per* 4-5 in a controlled environment (22-23 °C, 14/10 h light/dark cycle). Mice were fed *ad libitum* with one of the two experimental diets during 18 weeks: standard chow (chow) or high-fat diet (HFD). They were divided in four groups: WT mice fed with chow (n = 10) or HFD (n = 9), TLR4$^{-/-}$ mice fed with chow (n = 9) or HFD (n = 8). Standard chow (10% calories from fat[2], 4% calories from sucrose (Cani et al., 2004)) and HFD (45% calories from fat[2], 17% calories from sucrose) were purchased from SAFE (A04, Augy, France) and Research Diets (D12451, New Brunswick, USA), respectively. Food intake was recorded weekly during the 18 weeks of the nutritional intervention. At the end of the protocol, 6-h-fasted mice were anesthetized with an intraperitoneal injection of a solution (4 ml.kg^{-1}) containing ketamine (40 mg.ml^{-1}) and xylazine (4 mg.kg^{-1}) to preserve organ perfusion during dissection. The depth of anaesthesia was assessed by the absence of eyelid and pedal withdrawal reflexes.

[1]Generated by homologous recombination, the coding sequence of the transmembrane and cytoplasmic regions of TLR4 (amino acid residue 86-835) was replaced by a neomycin resistance gene.

[2]Lipids composition	HFD	Chow
% calories from saturated NEFA	17	2.1
% calories from monounsaturated NEFA	21	1.6
% calories from polyunsaturated NEFA	7	5.2

The right and left gastrocnemius muscles, the left lobe of the liver, the subcutaneous and visceral adipose tissues were rapidly removed and immediately frozen in liquid nitrogen. At the end of the procedure, mice were killed by cervical dislocation. Samples were stored at -80 °C until processed.

Non-esterified fatty acids measurement

Blood samples were taken from portal vein and frozen at -20 C°. NEFA were measured by colorimetric assay according to the manufacturer's guidelines (Diagnostic Systems, Holzheim, Germany).

Protein extraction and Western blotting

Liver (~50 mg), gastrocnemius (~50 mg) and subcutaneous adipose tissue (~100 mg) were ground using a mortar and a pestle (Bel-Art Products, Pequannock, NJ, USA). Liver and gastrocnemius were homogenised in ice-cold and pH 7.0 buffer [20 mM Tris, 270 mM sucrose, 5 mM EGTA, 1 mM EDTA, 1% Triton X-100, 1 mM sodium orthovanadate, 50 mM sodium β-glycerophosphate, 5 mM sodium pyrophosphate, 50 mM sodium fluoride, 1 mM 1,4-dithiothreitol (DTT), and 10% protease inhibitor cocktail 10X (Roche Applied Science, Vilvoorde, Belgium)]. Subcutaneous adipose tissue was homogenised in ice-cold pH 7.4 RIPA buffer [50 mM Tris-HCl, 150 mM NaCl, 1 mM EDTA, 1% NP-40, 0.25% deoxycholic acid, 2 mM sodium orthovanadate, 5 mM phenylmethylsulfonyl fluoride and a protease inhibitor cocktail (Roche Applied Science)]. Homogenates were centrifuged at 10,000 *g* for 10 min, at 4 °C. Supernatants were immediately stored at -80 °C. Protein concentration was determined

using the DC protein assay kit (Bio-Rad Laboratories, Nazareth, Belgium) with bovine serum albumin as a standard. Proteins lysates (40-60 µg) were combined with Laemmli buffer and separated by SDS-PAGE (10-12%) for 1 h at a constant intensity of 40 mA. Proteins were then transferred to PVDF membranes for 2-3 h at constant voltage of 80 V. Membranes were blocked for 1 h in Tris-buffered saline with 0.1% Tween 20 (TBST) containing 5% non-fat dried milk. Then, membranes were incubated overnight at 4 °C in TBST containing 1% bovine serum albumin and one of the following primary antibodies (1:500 or 1:1000 dilution): BiP, phosphorylated-eIF2α (p-eIF2α, Ser 51), phosphorylated-JNK (Thr183/Tyr185), phosphorylated ERK1/2 (Thr202/Tyr204), phosphorylated p-38 (Thr180/Tyr182), IκB-α, phosphorylated IκB-α (Ser 32) and eEF2 (eukaryotic elongation factor 2). All primary antibodies were obtained from Cell Signaling Technology (Leiden, The Netherlands). Membranes were washed three times with TBST then incubated 1 h at room temperature with a secondary antibody (1:10,000 or 1:5,000 diluted in 5% non-fat dry milk) conjugated to horseradish peroxidase (Sigma, Bornem, Belgium). After three additional washes, chemiluminescent detection was carried out using an ECL Western blotting kit (Amersham ECL Plus, GE Healthcare, Diegem, Belgium). Pictures were taken with a charge-coupled device (CCD) camera (Gbox, Syngene, The Netherlands). Signal quantification was determined by GeneTool software (Syngene). All results were normalized to eEF2 protein then expressed relative to the control group (WT mice fed with chow).

RNA extraction and quantitative Real-time PCR

Total RNA extraction from frozen gastrocnemius (~50 mg), liver (~30 mg) and subcutaneous adipose tissue (~70 mg) was done with Trizol® (Invitrogen, Vilvoorde, Belgium), according to the manufacturer's instructions. The RNA quality and quantity were assessed by 1.5% agarose gel electrophoresis and Nanodrop® spectrophotometry. Reverse transcription was performed with iScript cDNA synthesis kit (Bio-Rad) from 1 µg total RNA. Real time PCR experiments were done on a MyIQ2 thermocycler (Bio-Rad) using the following conditions: 3 min at 95 °C, followed by 35 cycles of 30 s at 95 °C, 30 s at 60 °C and 30 s at 72 °C. Samples were analyzed in duplicate in 10 µl reaction volume containing 4.8 µl IQSybrGreen SuperMix (Bio-Rad), 0.1 µl of each primer (100 nM final) and 5 µl cDNA. Primers sequences are reported in Table 5.1. Melting curves were systematically analyzed to ensure the specificity of the amplification process. Target genes were normalized using three reference genes according to geNorm analysis (Vandesompele et al., 2002) and finally expressed relatively to the control group. The references genes were ribosomal protein L19 (RPL19), cyclophilin (CPHN) and hypoxanthine phosphoribosyltransferase 1 (HPRT1).

Table 5.1. Sequences of primers (5'-3')

Genes	Forward	Reverse
XBP1s	TGAGAACCAGGAGTTAAGAACACGC	CCTGCACCTGCTGCGGAC
XBP1u	TGAGAACCAGGAGTTAAGAACACGC	CACATAGTCTGAGTGCTGCGG
CHOP	CCTGAGGAGAGAGTGTTCCAG	CTCCTGCAGATCCTCATACCA
RPL19	GAAGGTCAAAGGGAATGTGTTCA	CCTTGTCTGCCTTCAGCTTGT
CPHN	CGTCTCCTTCGAGCTGTTTG	CCACCCTGGCACATGAATC
HPRT1	AGGCCAGACTTTGTTGGATTT	CAGGACTCCTCGTATTTGCAG
IL-6	ACTTCCATCCAGTTGCCTTCT	GAATTGCCATTGCACAACTCT
IL-1β	GTCTGAAGCAGCTATGGCAAC	TTTGAAGCTGGATGCTCTCAT
TNFα	CCAGACCCTCACACTCAGATCA	CACTTGGTGGTTTGCTACGAC

XBP1s: X-box-binding protein 1 spliced, XBP1u: X-box-binding protein 1 unspliced, CHOP: C/EBP homologous, RPL19: Ribosomal protein L19, CPHN: Cyclophilin, HPRT1: Hypoxanthine phosphoribosyltransferase 1, IL-6: interleukin-6, IL-1β: interleukin-1β TNFα: tumor necrosis factor-α.

Oral glucose tolerance test

Seventeen weeks after the beginning of the protocol, 6-h-fasted mice were force-fed with a glucose solution (1 $g.kg^{-1}$ glucose, 40% glucose solution). Plasma glucose concentration was determined with a glucose meter (Roche Diagnostics) on 3.5 µl of blood collected from the tip of the tail vein, 30 min before and 0, 15, 30, 60, 90 and 120 min following glucose gavage. Areas under the curve (AUC) were calculated according to the trapeze method.

Statistical analysis

Results are presented as means ± SEM. Two-way ANOVA was used to assess statistical differences amongst means. When appropriate, the Bonferroni test was used as a post-hoc analysis. The significative threshold was set for a *P*-value < 0.05.

Results

TLR4 deficiency protects from obesity due to 18-weeks high-fat diet without reducing energy intake

In basal conditions, body weight of TLR4$^{-/-}$ was higher than WT mice (~2.5 g, $P < 0.001$). After 18-weeks chow, body weight was increased by 5.4 ± 0.3 g in WT and 5.4 ± 0.4 g in TLR4$^{-/-}$ mice (Figure 5.1A). This gain was 81% higher upon HFD in comparison with chow in WT ($P < 0.001$) but was not different in TLR4$^{-/-}$ mice (Figure 5.1A). Compared to chow, visceral and subcutaneous adipose tissues were larger after HFD in WT (79% and 160% respectively, $P < 0.001$) but not in TLR4$^{-/-}$ mice (Figure 5.1C and 5.1D). When fed *ad libitum* with chow, TLR4$^{-/-}$ mice ingested more energy than WT (12.6 kcal.week^{-1}, $P < 0.001$) (Figure 5.1B). Upon HFD, the increase in weekly energy intake was larger in TLR4$^{-/-}$ mice (26%) than in WT (15%, $P < 0.001$) (Figure 5.1B). All together these results suggest that the energy expenditure of TLR4$^{-/-}$ is higher than WT mice.

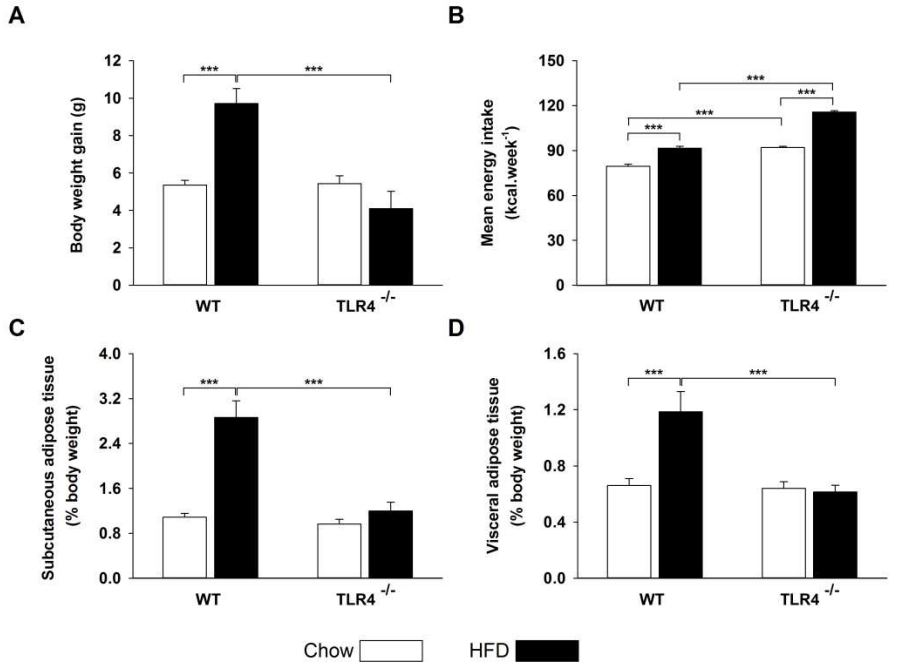

Figure 5.1. TLR4 deficiency protects from obesity without reducing energy intake. (A) Body weight gain calculated as the body weight difference between the end (18 weeks) and the beginning of the diet. (B) Mean energy intake expressed in kcal.week^{-1} (C) Subcutaneous adipose tissue weight expressed in percentage of body weight. (D) Visceral adipose tissue weight expressed in percentage of body weight. Values are expressed as means ± SEM (n = 8-10), * $P < 0.05$, ** $P < 0.01$, *** $P < 0.001$

TLR4 deficiency protects from ER stress induced by a high-fat diet

BiP expression increased in skeletal muscle (85%, $P = 0.002$), liver (150%, $P = 0.031$) and adipose tissue (188%, $P = 0.039$) of WT mice fed with a HFD, whereas TLR4$^{-/-}$ mice were completely resistant to HFD-induced BiP expression (Figure 5.2). The unspliced form of XBP1 mRNA (XBP1u) increased by 38% ($P = 0.041$) in skeletal muscle and by 48% ($P = 0.01$) in liver of WT mice upon HFD (Figure 5.3). Unexpectedly, XBP1u transcripts decreased (-47%, $P = 0.008$) in adipose tissue of WT mice upon HFD (Figure 5.3). The spliced form

of XBP1 mRNA (XBP1s) increased by 34% (P = 0.026) in skeletal muscle of WT mice upon HFD (Figure 5.3). CHOP transcripts were up-regulated by HFD in skeletal muscle (27%, P = 0.041), liver (29%, P = 0.016) and adipose tissue (56%, P = 0.006) of WT mice (Figure 3). HFD did not induce any change in ER stress markers in TLR4$^{-/-}$ mice (Figure 5.2 and Figure 5.3).

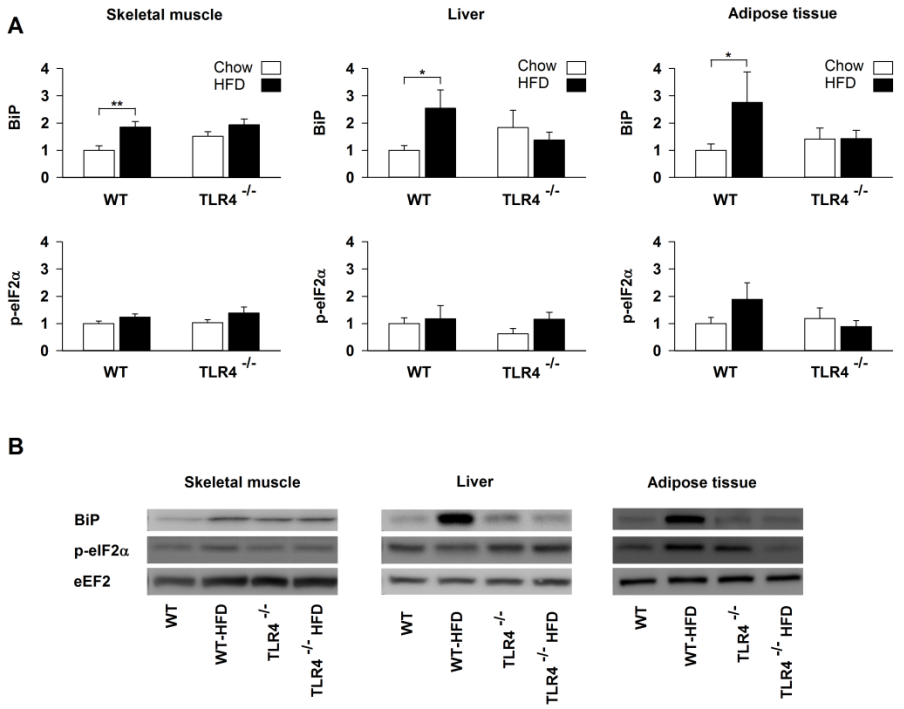

Figure 5.2. ER stress protein markers are not induced in TLR4$^{-/-}$ mice after a high-fat diet. (A) Protein expression of BiP and phosphorylated eIF2α in skeletal muscle, liver and subcutaneous adipose tissue of wild-type (WT) and TLR4 knockout (TLR4$^{-/-}$) mice fed with a standard (chow) or a high-fat diet (HFD). Results are presented as means ± SEM (n = 8-10), * P < 0.05, ** P < 0.01, *** P < 0.001. (B) Illustration of the data presented in panel A.

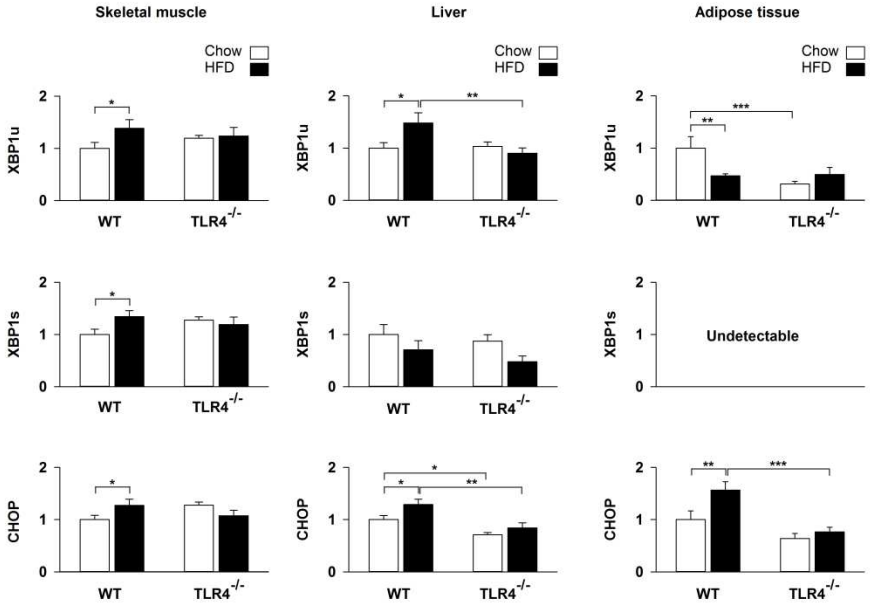

Figure 5.3. ER stress mRNA markers are not up-regulated in TLR4-/- mice after a high-fat diet. mRNA level of XBP1u (X-box-binding protein 1 unspliced), XBP1s (X-box-binding protein 1 spliced) and CHOP (C/EBP homologous) in skeletal muscle, liver and subcutaneous adipose tissue of wild-type (WT) and TLR4 knockout ($TLR4^{-/-}$) mice fed with a standard (chow) or a high-fat diet (HFD). Results are expressed as means ± SEM (n = 8-10), * $P < 0.05$, ** $P < 0.01$, *** $P < 0.001$

TLR4 downstream signaling after a high-fat diet

Since our results suggested that ER stress induced by a HFD is dependent upon TLR4, we decided to investigate the signaling downstream of TLR4 expecting to identify the mechanism by which TLR4 is able to activate ER stress. TLR4 leads to the activation of the NF-κB pathway, which regulates the transcription of cytokines such as IL-6, TNFα and IL-1β. Inflammation is known for inducing ER stress (Zhang and Kaufman, 2008). None of the cytokines that we measured was increased after HFD (Figure 5.4A). Furthermore, the HFD did not increase the phosphorylation state of IκB-α and did not decrease IκB-α protein level (Figure 5.4B). Nevertheless, in the adipose tissue, IκB-α was 70% higher in TLR4$^{-/-}$ than in WT mice as evidenced by the significant between-strain effect of the ANOVA design (P = 0.027). In the same tissue, the level of phospho-IκB-α was undetectable in all conditions.

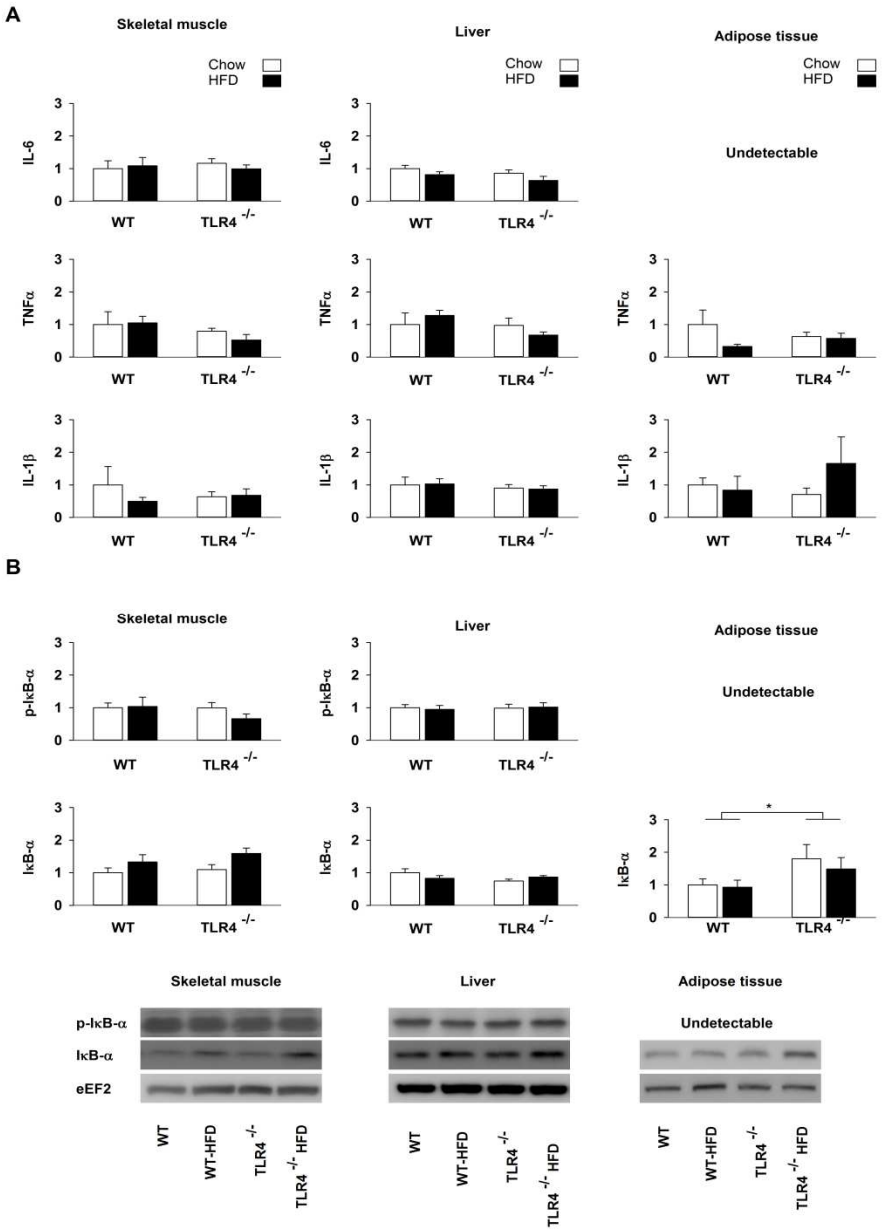

Figure 5.4. NFκB pathway is not implicated in HFD-induced ER stress. (A) mRNA level of IL-6 (interleukin-6), IL-1β (interleukin-1β), TNFα (tumor necrosis factor-α) are measured in skeletal muscle, liver and subcutaneous adipose tissue of wild-type (WT) and TLR4 knockout (TLR4$^{-/-}$) mice fed with a standard (chow) or a high-fat diet (HFD) (B) Phosphorylation state and expression of IκB-α in skeletal muscle, liver and subcutaneous adipose tissue of wild-type (WT) and TLR4 knockout (TLR4$^{-/-}$) mice fed with a standard (chow) or a high-fat diet (HFD). Results are presented as means ± SEM (n = 8-10), * $P < 0.05$, ** $P < 0.01$, *** $P < 0.001$

The phosphorylation state of the mitogen-activated protein kinases (MAPK) is under the control of the TLR4 pathway (Akira and Sato, 2003). HFD did not change the phosphorylation state of p-38 in all investigated organs (Figure 5.5). In skeletal muscle, the phosphorylation state of ERK1/2 was 44% lower in TLR4$^{-/-}$ than in WT mice (between-strain effect: P = 0.033). The phosphorylation state of ERK1/2 decreased in skeletal muscle (-51%, P = 0.016) and liver (-35%, P = 0.019) of WT mice upon HFD whereas it was not affected in TLR4$^{-/-}$ mice (Figure 5.5). After HFD, the phosphorylation state of ERK1/2 was 95% higher in adipose tissue of WT than TLR4$^{-/-}$ mice (P = 0.025) (Figure 5.5). The phosphorylation state of JNK did not change in skeletal muscle and liver, whereas it was dramatically increased by 169% in adipose tissue of WT mice upon HFD (P < 0.001) (Figure 5.5). The phosphorylation state of JNK remained unaffected in TLR4$^{-/-}$ mice (Figure 5.5). These results emphasize the fact that HFD regulates MAPK activity mainly at the level of the adipose tissue.

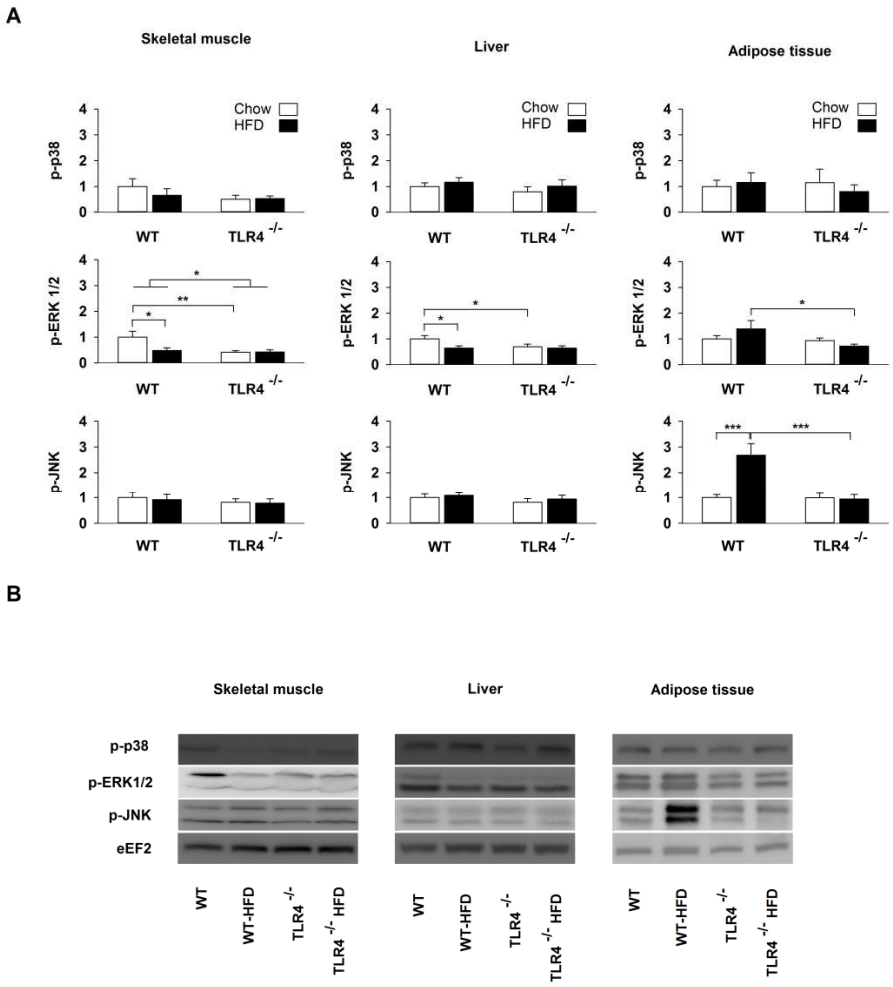

Figure 5.5. Changes in MAPK phosphorylation after a high-fat diet in wild-type and TLR4$^{-/-}$ mice. (A) Phosphorylation state of p38, JNK and ERK1/2 in skeletal muscle, liver and subcutaneous adipose tissue of wild-type (WT) and TLR4 knockout (TLR4$^{-/-}$) mice fed with a standard (chow) or a high-fat diet (HFD). Results are presented as means ± SEM (n = 8-10), * $P < 0.05$, ** $P < 0.01$, *** $P < 0.001$. (B) Illustration of the data presented in panel A.

Oral glucose tolerance test and plasma NEFA

To assess glucose tolerance, we performed an oral glucose tolerance test (OGTT). After 18-weeks chow, AUC was slightly but not significantly larger in TLR4$^{-/-}$ than in WT mice (Figure 5.6A). WT mice fed with HFD developed glucose intolerance as demonstrated by

a higher AUC (45%, P = 0.01), whereas no significant change was observed in TLR4$^{-/-}$ mice (Figure 5.6A). The circulating NEFA measured in a fasted state were not significantly lower in TLR4$^{-/-}$ mice and were not affected by the HFD (Figure 5.6B).

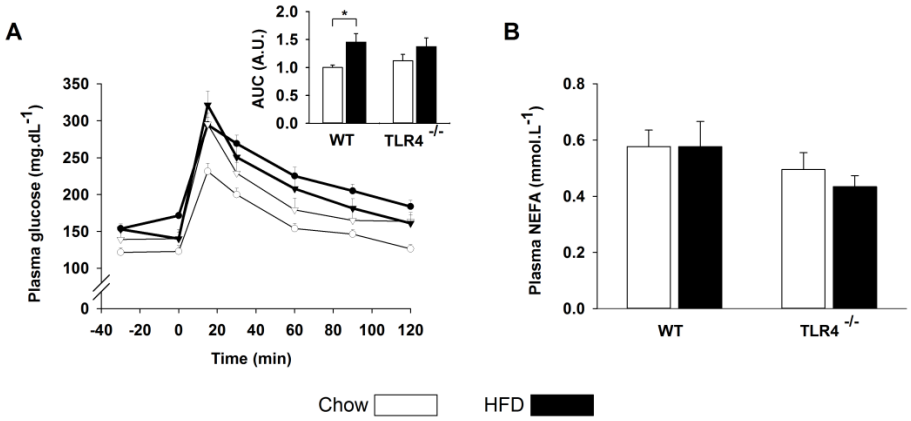

Figure 5.6. OGTT and circulating NEFA after a high-fat diet in wild-type and TLR4$^{-/-}$ mice. (A) Plasma glucose concentration following an oral glucose load. Wild-type mice upon chow (○), wild-type mice upon a high-fatd diet (●), TLR4 knockout mice upon chow (▽), TLR4 knockout mice upon a high-fat diet (▼). The *inset* represents the area under the curve (AUC) expressed in arbitrary units (A.U.). (B) Fasting NEFA concentrations expressed in mmol.L^{-1}.

Discussion

TLR4 deficiency protects against ER stress induced by a HFD

The main finding of the present study is that TLR4 deficiency protects against ER stress induced by a HFD. BiP is a chaperone that plays a key role in activating cell response to ER stress and its expression is highly regulated by the UPR (Lee, 2001). In WT mice, BiP was increased during HFD in skeletal muscle, liver and adipose tissues whereas TLR4$^{-/-}$ mice did not show any change. The three branches of the UPR are able to regulate BiP, which is therefore considered as the endpoint marker of the UPR whatever the activated

signaling cascade. Consequently, our results confirm the presence of an ER stress in skeletal muscle, liver and adipose tissues of WT mice after a HFD (Deldicque et al., 2010, Ozcan et al., 2004). BiP was unaffected in TLR4$^{-/-}$ mice fed with a HFD suggesting that this receptor contributes to the development of ER stress induced by lipid excess.

CHOP is another well-recognized ER stress marker, which is coordinately regulated with BiP (Wang et al., 1996). CHOP is a family member of the ER stress-inducible genes, the transcription of which is regulated both by ATF6 and ATF4, the latter being a downstream effector of the PERK/eIF2α pathway (Zhang and Kaufman, 2008). In WT, CHOP mRNA was increased after a HFD in the three organs analysed in the present study. No changes were observed in TLR4$^{-/-}$ mice supporting the results obtained on BiP.

XBP1u is also a member of the ER stress-inducible gene family, which is regulated by ATF6 (Yoshida et al., 2001, Lee et al., 2002). In skeletal muscle and liver, XBP1u mRNA was increased in WT after HFD whereas this change was completely abolished in TLR4$^{-/-}$ mice. These results suggest that the ATF6 pathway was not activated in skeletal muscle and liver of TLR4$^{-/-}$ mice while it was in WT mice. XBP1u seems regulated differently in adipose tissue. Upon chow, XPB1u mRNA was lower in TLR4$^{-/-}$ than in WT mice. It decreased in WT after HFD and remained unchanged in TLR4$^{-/-}$ mice. This clearly indicates that the regulation of the UPR by a HFD is tissue-specific.

XBP1s was undetectable in adipose tissue. In all conditions, the values of cycle threshold (Ct) were higher than 35 and therefore, were not accurate enough for interpretation (Nolan et al., 2006). This was

not the case in skeletal muscle wherein XBP1s was increased in WT upon HFD, but not in TLR4$^{-/-}$ mice. This indicates that the IRE1α pathway was likely activated in WT and that this activation was lacking in TLR4$^{-/-}$ mice. No changes were observed in XPBls mRNA in liver of WT and TLR4$^{-/-}$ mice. This provides an additional argument for a tissue-specific regulation of the UPR by a HFD (Ye et al., 2010).

We measured the phosphorylation state of eIF2α as a marker of the PERK pathway activation. In our experimental conditions, phospho-eIF2α was affected neither by the mice strain, nor by the diet.

In WT mice fed with HFD, several ER stress markers were increased while others did not change. A distinction must be made in the interpretation of ER stress marker changes. On one hand, the phosphorylation of eIF2α and the splicing of XBP1 are direct markers of UPR activation (Malhotra and Kaufman, 2007). On the other hand, BiP, CHOP and unspliced XBP1 are called ER stress-inducible genes, meaning that they are the consequence of UPR. They represent a long term adaptation to a stress condition and may be continuously overexpressed to cope with ER stress. On the contrary, XBP1 splicing and eIF2α phosphorylation seem to be transiently activated. For example, the activation of the PERK pathway is dependent on the acute nutritional status (Oyadomari et al., 2008). Oyadomari *et al.* (2008) shown that the phosphorylation of eIF2α is barely detectable in the liver of fasted animals and increased 4 hours after feeding standard diet; this effect was higher in animals fed with HFD. Since the animals used in the present experiment were sacrificed after a fasted period of 6 hours, it is possible that we missed transient changes in the

phosphorylation state of eIF2α. Furthermore, caution must be taken when interpreting result from eIF2α phosphorylation as a consequence of ER stress. Beside the control of PERK, eIF2α can also be phosphorylated by three other kinases, namely PKR (protein kinase R), GCN2 (general control nonrepressed 2), HRI (Heme-regulated inhibitor kinase) and dephosphorylated by GADD34 (Protein phosphatase 1 regulatory subunit 15A) (Novoa et al., 2001, Williams, 1999, Berlanga et al., 1999).

NFκB pathway is not implicated in HFD-induced ER stress

The results of the present study support the presence of interdependency between TLR4 and ER stress. We tried to further understand how the absence of TLR4 could down-regulate ER stress. Our first hypothesis was based on a reduced activation of the NF-κB pathway in TLR4$^{-/-}$ mice after a HFD, which would reduce the inflammatory state and consequently ER stress. This hypothesis was not corroborated as the NF-κB pathway was not activated after a HFD in WT and TLR4$^{-/-}$ mice in our conditions. The mRNA level of cytokines regulated by NF-κB, namely TNFα, IL-1β and IL-6 (Zhang and Kaufman, 2008), was not changed and IκB-α, an inhibitory protein of NF-κB, was not decreased after HFD and it phosphorylation state was not affected.

It has been reported that circulating LPS, the main TLR4 ligand, was increased after a HFD likely because of a more leaky gut (Cani et al., 2007, Cani et al., 2008, Kim et al., 2012). Studies showed that LPS induced ER stress in lung (Endo et al., 2006), human B cells (Kuribayashi et al., 2008) and liver (Kozlov et al., 2009). Plasma LPS

was not measured in the present study. Therefore, we may not rule out that circulating LPS induced ER stress in WT and not in TLR4$^{-/-}$ mice. Nevertheless, this hypothesis seems unlikely because of the lack of NF-κB activation in TLR4$^{-/-}$ and WT mice.

In vitro and *in vivo* studies suggest that TLR4 recognizes NEFA in addition to LPS (Shi et al., 2006, Lee et al., 2001). Like others (Garbow et al., 2011, Gao et al., 2010), we did not observe any difference in plasma NEFA concentration after a HFD arguing against a NEFA-dependent activation of TLR4 during a HFD. Nevertheless, the blood samples were taken in a fasted state and therefore, we may not exclude a transitory increase of circulating NEFA during the postprandial phase.

TLR4 deficiency protect against body weight gain and adipose tissue extension induced by a HFD

In addition to the protection from ER stress, others and we observed that the deletion of the gene coding for TLR4 provides also a protection against obesity (Radin et al., 2008, Tsukumo et al., 2007, Saberi et al., 2009), probably because of a more favorable energy balance. In parallel to body weight gain, we and others showed that TLR4 deficiency protects from visceral and subcutaneous adipose tissue expansion induced by a HFD (Tsukumo et al., 2007, Davis et al., 2008, Radin et al., 2008). Upon chow, the energy intake was higher in TLR4$^{-/-}$ than in WT mice whereas the body weight gains were similar. Upon HFD, both genotypes increased energy intake, which was the largest in TLR4$^{-/-}$ mice as previously reported (Tsukumo et al., 2007, Davis et al., 2008). Since the body weight gain

was lower in TLR4$^{-/-}$ than in WT mice, it is likely that fat absorption and/or energy expenditure were altered. To the best of our knowledge, no results have been reported regarding an impaired fat absorption in TLR4 deficient mice submitted to a HFD. Indirect calorimetry measurements demonstrated that energy expenditure and fatty acids utilization were increased upon a HFD in mice with a loss of function mutation of the gene coding for TLR4 (C3H/HeJ) (Tsukumo et al., 2007). Frisard *et al*. (2010) showed that the skeletal muscle of C3H/HeJ mice exhibits an increased fatty acid oxidation, citrate synthase activity and beta-hydroxyacyl CoA dehydrogenase activity (Frisard et al., 2010). Therefore, the metabolic consequences related to fat storage could explain the presence of an ER stress in WT after a HFD without a direct implication of the NF-κB pathway. In TLR4$^{-/-}$ mice, the metabolic changes towards greater energy expenditure and reduced body fat content would be protective.

TLR4 deficiency protects from glucose intolerance induced by a HFD

Recent findings showed that high glucose level induces ER stress, probably via the glucosamine pathway (Srinivasan et al., 2009, Buse, 2006). Indeed, an elevated glucose level causes ER stress in primary cardiomyocytes (Younce et al., 2010), endothelial cells (Sheikh-Ali et al., 2010), liver (Beriault et al., 2011) and adipocytes (Alhusaini et al., 2010). Glucose level was slightly increased in the fasted state after HFD, but the concentrations were not different between WT and TLR4$^{-/-}$ mice. In the present study, glucose tolerance was assessed by an OGTT test. In the chow condition, there was no statistical

difference between WT and TLR4$^{-/-}$. After having received a HFD, WT mice became glucose intolerant whereas no difference was observed in TLR4$^{-/-}$ mice. This confirms other studies showing that TLR4 deficient mice are protected from insulin resistance induced by lipid infusion or a HFD (Shi et al., 2006, Radin et al., 2008, Tsukumo et al., 2007, Kim et al., 2007, Davis et al., 2008, Poggi et al., 2007). High sucrose diet has also been linked to insulin resistance (Dutta et al., 2001, Pagliassotti et al., 1994). In the HFD used in the present experiment, the sucrose content was higher than in chow (17 kcal% *vs* 4 kcal%), but far from the 60-70 kcal% usually used in the high sucrose diets (Omar et al., 2012, Dutta et al., 2001). Therefore, it is likely that ER stress and insulin resistance observed in WT and not in TLR4$^{-/-}$ mice after HFD is mostly due the fat content of the diet even if we may not rule out a partial indirect contribution of sucrose.

In human, TLR4 is more expressed in skeletal muscle of obese type 2 diabetic patients than lean healthy subjects (Reyna et al., 2008). These results are associated with a positive correlation between TLR4 protein content and insulin resistance, suggesting that TLR4 might be an actor of the process linking inflammation and insulin resistance in mice as well as in human. A broad spectrum of evidence suggests that TLR4 controls its own expression. For example, incubation of human primary myotubes with palmitate or lipid A, the LPS-binding domain of TLR4, increases its expression (Reyna et al., 2008). On the contrary, TLR4 mRNA is reduced in skeletal muscle of frail obese elderly patients after 12 weeks exercise training (Lambert et al., 2008). Endoplasmic reticulum dysfunction due to lipid excess is also known to disrupt insulin signal in mice (Ozcan et al., 2004). In human,

ER stress was observed in liver and adipose tissue of obese patients (Puri et al., 2008, Boden et al., 2008) and it was reduced after weight loss (Gregor et al., 2009). All together these results and those reported in the present paper suggest that a down-regulation of TLR4 or a reduced stimulation of this receptor by nutritional, pharmacological and/or exercise interventions could reveal a novel strategy for reducing low grade inflammation and ER stress-induced insulin resistance.

TLR4 deficiency protects from HFD-induced JNK activation in adipose tissue

TLR4 appears to mediate the signal linking obesity to insulin resistance. However, the underlying mechanisms are unclear and seem to be organ-dependent (Kim and Sears, 2010). In the present study, we found that TLR4 was essential for inducing ER stress in the insulin-sensitive tissues during a HFD. ER stress is now recognized as a central mechanism responsible for insulin resistance (Zhang and Kaufman, 2008). Indeed, activated IRE1α recruits TRAF2 (tumour-necrosis factor-α-receptor-associated factor 2) and triggers JNK phosphorylation (Urano et al., 2000). The phosphorylation of JNK mediates in turn the phosphorylation of IRS1 (insulin-receptor substrate 1) on serine residues which is known to inhibit phosphorylation of IRS1 on tyrosine residues causing insulin resistance (Hirosumi et al., 2002). In our study, the phosphorylation state of JNK was only affected in adipose tissue of WT mice after HFD whereas this effect was completely abolished in $TLR4^{-/-}$. Consequently, it is likely that TLR4 contributes to JNK

phosphorylation through ER stress in adipose tissue. This result supports the idea that the mechanism by which TLR4 mediates insulin resistance is organ-dependent. XBP1s mRNA was undetectable in adipose tissue and therefore we have no direct measurement of the activation of IRE1α in this tissue.

Independently of the UPR, ER stress induces an increase of lipid droplets (Zhang and Zhang, 2012). The intracellular lipid accumulation is known to disrupt insulin pathway through the generation of lipid-derived toxic metabolites such ceramides and DAG (Summers, 2006, Idris et al., 2001). Intracellular lipids were not measured in this study. Consequently, we may not rule out an implication of intracellular lipids in the link between TLR4 dependent-ER stress and insulin resistance.

Conclusion

TLR4 deficiency protects from obesity and glucose intolerance induced by a HFD as well as from ER stress in the main organs for glucose and lipid metabolism (skeletal muscle, liver and adipose tissue). Contrary to our hypothesis this phenomenon is not directly regulated by the NF-κB pathway but seems rather to be the indirect consequence of metabolic changes in TLR4$^{-/-}$ mice which lead to less fat accumulation.

References

Akira, S. & Sato, S. 2003. Toll-like receptors and their signaling mechanisms. *Scand J Infect Dis,* **35,** 555-62.

Alhusaini, S., McGee, K., Schisano, B., Harte, A., McTernan, P., Kumar, S. & Tripathi, G. 2010. Lipopolysaccharide, high glucose and saturated fatty acids induce endoplasmic reticulum stress in cultured primary human adipocytes: Salicylate alleviates this stress. *Biochem Biophys Res Commun,* **397,** 472-8.

Beriault, D. R., Sharma, S., Shi, Y., Khan, M. I. & Werstuck, G. H. 2011. Glucosamine-supplementation promotes endoplasmic reticulum stress, hepatic steatosis and accelerated atherogenesis in apoE-/- mice. *Atherosclerosis*.

Berlanga, J. J., Santoyo, J. & De Haro, C. 1999. Characterization of a mammalian homolog of the GCN2 eukaryotic initiation factor 2alpha kinase. *Eur J Biochem,* **265,** 754-62.

Boden, G. 2009. Endoplasmic reticulum stress: another link between obesity and insulin resistance/inflammation? *Diabetes,* **58,** 518-9.

Boden, G., Duan, X., Homko, C., Molina, E. J., Song, W., Perez, O., Cheung, P. & Merali, S. 2008. Increase in endoplasmic reticulum stress-related proteins and genes in adipose tissue of obese, insulin-resistant individuals. *Diabetes,* **57,** 2438-44.

Buse, M. G. 2006. Hexosamines, insulin resistance, and the complications of diabetes: current status. *Am J Physiol Endocrinol Metab,* **290,** E1-E8.

Cani, P. D., Amar, J., Iglesias, M. A., Poggi, M., Knauf, C., Bastelica, D., Neyrinck, A. M., Fava, F., Tuohy, K. M., Chabo, C., Waget, A., Delmee, E., Cousin, B., Sulpice, T., Chamontin, B., Ferrieres, J., *et al.* 2007. Metabolic endotoxemia initiates obesity and insulin resistance. *Diabetes,* **56,** 1761-72.

Cani, P. D., Bibiloni, R., Knauf, C., Waget, A., Neyrinck, A. M., Delzenne, N. M. & Burcelin, R. 2008. Changes in gut microbiota control metabolic endotoxemia-induced inflammation in high-fat diet-induced obesity and diabetes in mice. *Diabetes,* **57,** 1470-81.

Cani, P. D., Dewever, C. & Delzenne, N. M. 2004. Inulin-type fructans modulate gastrointestinal peptides involved in appetite regulation (glucagon-like peptide-1 and ghrelin) in rats. *Br J Nutr,* **92,** 521-6.

Davis, J. E., Gabler, N. K., Walker-Daniels, J. & Spurlock, M. E. 2008. Tlr-4 deficiency selectively protects against obesity induced by diets high in saturated fat. *Obesity (Silver Spring),* **16,** 1248-55.

Deldicque, L., Cani, P. D., Philp, A., Raymackers, J. M., Meakin, P. J., Ashford, M. L., Delzenne, N. M., Francaux, M. & Baar, K. 2010. The unfolded protein response is activated in skeletal muscle by high-fat feeding: potential role in the downregulation of protein synthesis. *Am J Physiol Endocrinol Metab,* **299,** E695-705.

Dutta, K., Podolin, D. A., Davidson, M. B. & Davidoff, A. J. 2001. Cardiomyocyte dysfunction in sucrose-fed rats is associated with insulin resistance. *Diabetes,* **50,** 1186-92.

Endo, M., Mori, M., Akira, S. & Gotoh, T. 2006. C/EBP homologous protein (CHOP) is crucial for the induction of caspase-11 and the pathogenesis of lipopolysaccharide-induced inflammation. *J Immunol,* **176,** 6245-53.

Frisard, M. I., McMillan, R. P., Marchand, J., Wahlberg, K. A., Wu, Y., Voelker, K. A., Heilbronn, L., Haynie, K., Muoio, B., Li, L. & Hulver, M. W. 2010. Toll-like receptor 4 modulates skeletal muscle substrate metabolism. *Am J Physiol Endocrinol Metab,* **298,** E988-98.

Gao, S., He, L., Ding, Y. & Liu, G. 2010. Mechanisms underlying different responses of plasma triglyceride to high-fat diets in hamsters and mice: roles of hepatic MTP and triglyceride secretion. *Biochem Biophys Res Commun,* **398,** 619-26.

Garbow, J. R., Doherty, J. M., Schugar, R. C., Travers, S., Weber, M. L., Wentz, A. E., Ezenwajiaku, N., Cotter, D. G., Brunt, E. M. & Crawford, P. A. 2011. Hepatic steatosis, inflammation, and ER stress in mice maintained long term on a very low-carbohydrate ketogenic diet. *Am J Physiol Gastrointest Liver Physiol,* **300,** G956-67.

Greenberg, A. S. & Obin, M. S. 2006. Obesity and the role of adipose tissue in inflammation and metabolism. *Am J Clin Nutr,* **83,** 461S-465S.

Gregor, M. F., Yang, L., Fabbrini, E., Mohammed, B. S., Eagon, J. C., Hotamisligil, G. S. & Klein, S. 2009. Endoplasmic reticulum stress is reduced in tissues of obese subjects after weight loss. *Diabetes,* **58,** 693-700.

Hirosumi, J., Tuncman, G., Chang, L., Gorgun, C. Z., Uysal, K. T., Maeda, K., Karin, M. & Hotamisligil, G. S. 2002. A central role for JNK in obesity and insulin resistance. *Nature,* **420,** 333-6.

Hoshino, K., Takeuchi, O., Kawai, T., Sanjo, H., Ogawa, T., Takeda, Y., Takeda, K. & Akira, S. 1999. Cutting edge: Toll-like receptor 4 (TLR4)-deficient mice are hyporesponsive to lipopolysaccharide: evidence for TLR4 as the Lps gene product. *J Immunol,* **162,** 3749-52.

Hotamisligil, G. S., Peraldi, P., Budavari, A., Ellis, R., White, M. F. & Spiegelman, B. M. 1996. IRS-1-mediated inhibition of insulin receptor tyrosine kinase activity in TNF-alpha- and obesity-induced insulin resistance. *Science,* **271,** 665-8.

Idris, I., Gray, S. & Donnelly, R. 2001. Protein kinase C activation: isozyme-specific effects on metabolism and cardiovascular complications in diabetes. *Diabetologia,* **44,** 659-73.

Kaisho, T. & Akira, S. 2006. Toll-like receptor function and signaling. *J Allergy Clin Immunol,* **117,** 979-87; quiz 988.

Kim, F., Pham, M., Luttrell, I., Bannerman, D. D., Tupper, J., Thaler, J., Hawn, T. R., Raines, E. W. & Schwartz, M. W. 2007. Toll-like receptor-4 mediates vascular inflammation and insulin resistance in diet-induced obesity. *Circ Res,* **100,** 1589-96.

Kim, J. J. & Sears, D. D. 2010. TLR4 and Insulin Resistance. *Gastroenterol Res Pract,* **2010**.

Kim, J. K., Fillmore, J. J., Sunshine, M. J., Albrecht, B., Higashimori, T., Kim, D. W., Liu, Z. X., Soos, T. J., Cline, G. W., O'Brien, W. R., Littman, D. R. & Shulman, G. I. 2004. PKC-theta knockout mice are protected from fat-induced insulin resistance. *J Clin Invest,* **114,** 823-7.

Kim, K. A., Gu, W., Lee, I. A., Joh, E. H. & Kim, D. H. 2012. High Fat Diet-Induced Gut Microbiota Exacerbates Inflammation and Obesity in Mice via the TLR4 Signaling Pathway. *PLoS One,* **7,** e47713.

Kozlov, A. V., Duvigneau, J. C., Miller, I., Nurnberger, S., Gesslbauer, B., Kungl, A., Ohlinger, W., Hartl, R. T., Gille, L., Staniek, K., Gregor, W., Haindl, S.

& Redl, H. 2009. Endotoxin causes functional endoplasmic reticulum failure, possibly mediated by mitochondria. *Biochim Biophys Acta,* **1792,** 521-30.

Kuribayashi, J. S., Bombardieri, C. R., Baracho, G. V., Aliberti, J., Machado, F. S., Kalil, J., Guilherme, L., Kokron, C. M., Rizzo, L. V. & de Camargo, M. M. 2008. Slower rescue of ER homeostasis by the unfolded protein response pathway associated with common variable immunodeficiency. *Mol Immunol,* **45,** 2990-7.

Lambert, C. P., Wright, N. R., Finck, B. N. & Villareal, D. T. 2008. Exercise but not diet-induced weight loss decreases skeletal muscle inflammatory gene expression in frail obese elderly persons. *J Appl Physiol,* **105,** 473-8.

Lee, A. S. 2001. The glucose-regulated proteins: stress induction and clinical applications. *Trends Biochem Sci,* **26,** 504-10.

Lee, J. Y., Sohn, K. H., Rhee, S. H. & Hwang, D. 2001. Saturated fatty acids, but not unsaturated fatty acids, induce the expression of cyclooxygenase-2 mediated through Toll-like receptor 4. *J Biol Chem,* **276,** 16683-9.

Lee, K., Tirasophon, W., Shen, X., Michalak, M., Prywes, R., Okada, T., Yoshida, H., Mori, K. & Kaufman, R. J. 2002. IRE1-mediated unconventional mRNA splicing and S2P-mediated ATF6 cleavage merge to regulate XBP1 in signaling the unfolded protein response. *Genes Dev,* **16,** 452-66.

Malhotra, J. D. & Kaufman, R. J. 2007. The endoplasmic reticulum and the unfolded protein response. *Semin Cell Dev Biol,* **18,** 716-31.

Miyake, K. 2004. Endotoxin recognition molecules, Toll-like receptor 4-MD-2. *Semin Immunol,* **16,** 11-6.

Nolan, T., Hands, R. E. & Bustin, S. A. 2006. Quantification of mRNA using real-time RT-PCR. *Nat Protoc,* **1,** 1559-82.

Novoa, I., Zeng, H., Harding, H. P. & Ron, D. 2001. Feedback inhibition of the unfolded protein response by GADD34-mediated dephosphorylation of eIF2alpha. *J Cell Biol,* **153,** 1011-22.

Omar, B., Pacini, G. & Ahren, B. 2012. Differential development of glucose intolerance and pancreatic islet adaptation in multiple diet induced obesity models. *Nutrients,* **4,** 1367-81.

Oyadomari, S., Harding, H. P., Zhang, Y., Oyadomari, M. & Ron, D. 2008. Dephosphorylation of translation initiation factor 2alpha enhances glucose tolerance and attenuates hepatosteatosis in mice. *Cell Metab,* **7,** 520-32.

Ozcan, U., Cao, Q., Yilmaz, E., Lee, A. H., Iwakoshi, N. N., Ozdelen, E., Tuncman, G., Gorgun, C., Glimcher, L. H. & Hotamisligil, G. S. 2004. Endoplasmic reticulum stress links obesity, insulin action, and type 2 diabetes. *Science,* **306,** 457-61.

Pagliassotti, M. J., Shahrokhi, K. A. & Moscarello, M. 1994. Involvement of liver and skeletal muscle in sucrose-induced insulin resistance: dose-response studies. *Am J Physiol,* **266,** R1637-44.

Poggi, M., Bastelica, D., Gual, P., Iglesias, M. A., Gremeaux, T., Knauf, C., Peiretti, F., Verdier, M., Juhan-Vague, I., Tanti, J. F., Burcelin, R. & Alessi, M. C. 2007. C3H/HeJ mice carrying a toll-like receptor 4 mutation are protected against the development of insulin resistance in white adipose tissue in response to a high-fat diet. *Diabetologia,* **50,** 1267-76.

Puri, P., Mirshahi, F., Cheung, O., Natarajan, R., Maher, J. W., Kellum, J. M. & Sanyal, A. J. 2008. Activation and dysregulation of the unfolded protein response in nonalcoholic fatty liver disease. *Gastroenterology,* **134,** 568-76.

Radin, M. S., Sinha, S., Bhatt, B. A., Dedousis, N. & O'Doherty, R. M. 2008. Inhibition or deletion of the lipopolysaccharide receptor Toll-like receptor-4 confers partial protection against lipid-induced insulin resistance in rodent skeletal muscle. *Diabetologia,* **51,** 336-46.

Reyna, S. M., Ghosh, S., Tantiwong, P., Meka, C. S., Eagan, P., Jenkinson, C. P., Cersosimo, E., Defronzo, R. A., Coletta, D. K., Sriwijitkamol, A. & Musi, N. 2008. Elevated toll-like receptor 4 expression and signaling in muscle from insulin-resistant subjects. *Diabetes,* **57,** 2595-602.

Roden, M., Krssak, M., Stingl, H., Gruber, S., Hofer, A., Furnsinn, C., Moser, E. & Waldhausl, W. 1999. Rapid impairment of skeletal muscle glucose transport/phosphorylation by free fatty acids in humans. *Diabetes,* **48,** 358-64.

Roden, M., Price, T. B., Perseghin, G., Petersen, K. F., Rothman, D. L., Cline, G. W. & Shulman, G. I. 1996. Mechanism of free fatty acid-induced insulin resistance in humans. *J Clin Invest,* **97,** 2859-65.

Saberi, M., Woods, N. B., de Luca, C., Schenk, S., Lu, J. C., Bandyopadhyay, G., Verma, I. M. & Olefsky, J. M. 2009. Hematopoietic cell-specific deletion of toll-like receptor 4 ameliorates hepatic and adipose tissue insulin resistance in high-fat-fed mice. *Cell Metab,* **10,** 419-29.

Schaffer, J. E. 2003. Lipotoxicity: when tissues overeat. *Curr Opin Lipidol,* **14,** 281-7.

Sheikh-Ali, M., Sultan, S., Alamir, A. R., Haas, M. J. & Mooradian, A. D. 2010. Hyperglycemia-induced endoplasmic reticulum stress in endothelial cells. *Nutrition,* **26,** 1146-50.

Shi, H., Kokoeva, M. V., Inouye, K., Tzameli, I., Yin, H. & Flier, J. S. 2006. TLR4 links innate immunity and fatty acid-induced insulin resistance. *J Clin Invest,* **116,** 3015-25.

Srinivasan, V., Tatu, U., Mohan, V. & Balasubramanyam, M. 2009. Molecular convergence of hexosamine biosynthetic pathway and ER stress leading to insulin resistance in L6 skeletal muscle cells. *Mol Cell Biochem,* **328,** 217-24.

Summers, S. A. 2006. Ceramides in insulin resistance and lipotoxicity. *Prog Lipid Res,* **45,** 42-72.

Tsiotra, P. C. & Tsigos, C. 2006. Stress, the endoplasmic reticulum, and insulin resistance. *Ann N Y Acad Sci,* **1083,** 63-76.

Tsukumo, D. M., Carvalho-Filho, M. A., Carvalheira, J. B., Prada, P. O., Hirabara, S. M., Schenka, A. A., Araujo, E. P., Vassallo, J., Curi, R., Velloso, L. A. & Saad, M. J. 2007. Loss-of-function mutation in Toll-like receptor 4 prevents diet-induced obesity and insulin resistance. *Diabetes,* **56,** 1986-98.

Urano, F., Wang, X., Bertolotti, A., Zhang, Y., Chung, P., Harding, H. P. & Ron, D. 2000. Coupling of stress in the ER to activation of JNK protein kinases by transmembrane protein kinase IRE1. *Science,* **287,** 664-6.

Vandesompele, J., De Preter, K., Pattyn, F., Poppe, B., Van Roy, N., De Paepe, A. & Speleman, F. 2002. Accurate normalization of real-time quantitative RT-PCR data by geometric averaging of multiple internal control genes. *Genome Biol,* **3,** RESEARCH0034.

Wang, X. Z., Lawson, B., Brewer, J. W., Zinszner, H., Sanjay, A., Mi, L. J., Boorstein, R., Kreibich, G., Hendershot, L. M. & Ron, D. 1996. Signals from the stressed endoplasmic reticulum induce C/EBP-homologous protein (CHOP/GADD153). *Mol Cell Biol,* **16,** 4273-80.

Wellen, K. E. & Hotamisligil, G. S. 2005. Inflammation, stress, and diabetes. *J Clin Invest,* **115,** 1111-9.

Williams, B. R. 1999. PKR; a sentinel kinase for cellular stress. *Oncogene,* **18,** 6112-20.

Ye, R., Jung, D. Y., Jun, J. Y., Li, J., Luo, S., Ko, H. J., Kim, J. K. & Lee, A. S. 2010. Grp78 heterozygosity promotes adaptive unfolded protein response and attenuates diet-induced obesity and insulin resistance. *Diabetes,* **59,** 6-16.

Yoshida, H., Matsui, T., Yamamoto, A., Okada, T. & Mori, K. 2001. XBP1 mRNA is induced by ATF6 and spliced by IRE1 in response to ER stress to produce a highly active transcription factor. *Cell,* **107,** 881-91.

Younce, C. W., Wang, K. & Kolattukudy, P. E. 2010. Hyperglycaemia-induced cardiomyocyte death is mediated via MCP-1 production and induction of a novel zinc-finger protein MCPIP. *Cardiovasc Res,* **87,** 665-74.

Yuan, M., Konstantopoulos, N., Lee, J., Hansen, L., Li, Z. W., Karin, M. & Shoelson, S. E. 2001. Reversal of obesity- and diet-induced insulin resistance with salicylates or targeted disruption of Ikkbeta. *Science,* **293,** 1673-7.

Zhang, K. & Kaufman, R. J. 2008. From endoplasmic-reticulum stress to the inflammatory response. *Nature,* **454,** 455-62.

Zhang, X. & Zhang, K. 2012. Endoplasmic Reticulum Stress-Associated Lipid Droplet Formation and Type II Diabetes. *Biochem Res Int,* **2012,** 247275.

Chapter 6: Activation of ER stress by hydrogen peroxide in C2C12 myotubes

Nicolas Pierre[a], Caroline Barbé[a], Hélène Gilson[a], Louise Deldicque[b], Jean-Marc Raymackers[a], Marc Francaux[a]

[a]Institute of Neuroscience, Université catholique de Louvain, Louvain-la-Neuve, Belgium

[b]Department of Kinesiology, Exercise Physiology Research Group, KU Leuven, Belgium

Biochemical and Biophysical Research Communications. July 18, 2014; 450: 459-463

Abstract

The purpose of this study was to examine the link between oxidative stress and endoplasmic reticulum (ER) stress in myogenic cells. C2C12 myotubes were incubated with hydrogen peroxide (H_2O_2, 200 µM) and harvested 4 h or 17 h after the induction of this oxidative stress. A massive upregulation of binding immunoglobulin protein (BiP) was found, indicating the presence of ER stress. Nevertheless, the three branches of the unfolded protein response (UPR) were not activated to the same extent. The double-stranded RNA-dependent protein kinase (PKR)-like ER kinase (PERK) branch was the most activated as shown by the increase of phospho-eukaryotic translation-initiation factor 2α (eIF2α, Ser51) and the mRNA levels of activating transcription factor 4 (ATF4), C/EBP homologous (CHOP) and tribbles homolog 3 (TRB3). The slight increase in the spliced form of X-box binding protein 1 (XBP1s) together with the decrease of the unspliced form (XBP1u) indicated a higher endoribonuclease activity of inositol-requiring 1α (IRE1α). The transcriptional activity of activating transcription factor 6 (ATF6) remained unchanged after incubation with H_2O_2. The mechanisms by which the three branches of UPR can be specifically regulated by oxidative stress are currently unresolved and need further investigations.

Keywords

Unfolded protein response (UPR), oxidative stress, binding immunoglobulin protein (BiP), activating transcription factor 6 (ATF6), X-box binding protein 1 spliced (XBP1s), eukaryotic translation-initiation factor 2α (eIF2α)

Introduction

Oxidative stress is due to an imbalance between free radical production and antioxidant capacity of the cell. Mitochondria produce reactive oxygen species (ROS) like superoxide, which is converted into hydrogen peroxide (H_2O_2) by the reaction catalysed by superoxide dismutase (SOD). ROS are recognized as signaling molecules regulating physiological and pathological events (Veal et al., 2007). Nowadays, endoplasmic reticulum (ER) appears to be a key player in the integration and sensing oxidative signals (Malhotra and Kaufman, 2007b).

ER is a vast membranous network surrounding the nucleus. This organelle provides an oxidizing and high calcium environment where most secreted and membrane proteins are folded (Zhang and Kaufman, 2008). Increasing protein load relative to the folding capacity of the ER leads to accumulation of unfolded proteins, a condition known as ER stress. To cope with this stress, eukaryotic cells have developed an adaptive response called the unfolded protein response (UPR). Unfolded proteins are sensed by three ER transmembrane proteins: inositol-requiring 1α (IRE1α), double-stranded RNA-dependent protein kinase (PKR)-like ER kinase (PERK) and activating transcription factor 6 (ATF6). Under unstressed conditions, each of these ER stress sensors is maintained in an inactive state through binding with the protein chaperone binding immunoglobulin protein (BiP). Upon ER stress, BiP is released, leading to activation of the three sensors and downstream signaling. UPR pathways rapidly inhibit protein synthesis through the phosphorylation of eukaryotic translation-initiation factor 2α (eIF2α).

This step is followed by a transcriptional upregulation of specific genes coding for proteins implicated in folding, transport and ER-associated degradation (ERAD). If these adaptive responses fail to restore ER homeostasis, an apoptotic response mediated by C/EBP homologous (CHOP) is induced (Zhang and Kaufman, 2008).

High concentrations in lipids activate ER stress in various organs like pancreas, liver and adipose tissue (Ozcan et al., 2004, Laybutt et al., 2007), but also in C2C12 myogenic cells and skeletal muscle of mice (Pierre et al., 2013, Deldicque et al., 2010). In human muscle, ER stress has been observed in sporadic inclusion body myositis, polymyositis, and type 2 diabetes (Vattemi et al., 2004, Koh et al., 2013). The mechanisms triggering ER stress in muscle cells are still incompletely resolved. Recent studies have shown physical and biochemical interactions between mitochondria and ER (Csordas and Hajnoczky, 2009). On the one hand, ER and mitochondria are physically associated at the level of a sub-compartment called mitochondria-associated ER membrane (MAM). On the other hand, calcium and ROS are key molecules involved in the communication between mitochondria and ER. For example, mitochondrial ROS can target ER-based calcium channels leading to calcium release from the ER to the cytosol. The perturbation of ER calcium homeostasis disrupts protein folding and induces ER stress (Csordas and Hajnoczky, 2009). It has been shown that oxidative stress induces ER stress in murine fibrosarcoma cells (L929), murine mesencephalic cells (MN9D), human retinal pigment epithelium (RPE) cells, Chinese hamster ovary (CHO) cells, HeLa cells and heart cells (H9c2) (Xue et al., 2005, Holtz et al., 2006, He et al., 2008, Borradaile et al., 2006,

Pallepati and Averill-Bates, 2011). However, the pattern of UPR activation seems dependent on cell types. In HeLa cells, H_2O_2 activates the three UPR pathways (Pallepati and Averill-Bates, 2011) whereas in L929 cells, H_2O_2 activates the PERK pathway but not the IRE1 pathway (Xue et al., 2005).

Because muscle cells are great ROS providers (Barbieri and Sestili, 2012), oxidative stress is a potential regulator of ER stress in these cells. Therefore, the purpose of this study was to investigate whether oxidative stress could induce ER stress in the C2C12 myogenic cell line and to identify which signaling pathways of UPR are specifically activated.

Materials and Methods

Cell culture

C2C12 mouse myoblasts (ATCC, USA) were cultured at 37 °C in a humidified incubator containing 5% CO_2. Cells were seeded in 8.8 cm^2 culture dishes (Nunc, Belgium) and grown in a high glucose (4.5 g/L) Dulbeccos's Modified Eagle Medium (DMEM, Life Technologies, USA) supplemented with 10% (v/v) foetal bovine serum, 100 U/ml penicillin and 100 µg/ml streptomycin (Life Technologies). When cells reached confluence (48 h), medium was replaced by a differentiation medium containing DMEM, 2% (v/v) horse serum (Lonza, Belgium), 100 U/ml penicillin and 100 µg/ml streptomycin. After 96 h of differentiation, 200 µM hydrogen peroxide (Sigma-Aldrich, Belgium) or 1 µM thapsigargin (Tocris Bioscience, UK) or appropriate solvent in control condition (i.e.,

water for hydrogen peroxide and DMSO for thapsigargin) was added to the dishes. Cells were harvested after 4 or 17 h.

Western blotting

Cells were lysed in ice-cold and pH 7.0 lysis buffer containing 20 mM Tris, 270 mM sucrose, 5 mM EGTA, 1 mM EDTA, 1 mM sodium orthovanadate, 50 mM β-glycerophosphate, 5 mM sodium pyrophosphate, 50 mM sodium fluoride, 1 mM DTT (1,4-dithiothreitol), 0.1% (v/v) Triton X-100 and 10% protease inhibitor cocktail (Roche Applied Science, Belgium). The homogenates were then centrifuged at 10,000 *g* for 10 min, at 4 °C. Protein concentration was determined using the Detergent Compatible (DC) protein assay kit (Bio-Rad Laboratories, Belgium). Cell lysates were separated by SDS/PAGE and transferred to polyvinylidene fluoride (PVDF) membrane (GE Healthcare, Belgium). Membranes were blocked for 1 h in a Blotto solution containing Tris-buffered saline with 0.1% (v/v) Tween 20 (TBST) with 5% (w/v) non-fat dried milk. Then, membranes were incubated overnight at 4 °C with the following primary antibodies: eukaryotic elongation factor 2 (eEF2), BiP, IRE1α, protein disulfide isomerase (PDI), phosphorylated-eIF2α (Ser51), phosphorylated-JNK (Thr183/Tyr185). All primary antibodies were from Cell Signaling Technology (The Netherlands). Then membranes were incubated for 1 h at room temperature with a secondary antibody. Proteins were finally detected using Enhanced Chemiluminescence (ECL) Western blotting Detection System Plus (GE Healthcare). The films were then scanned on an ImageScanner using the Labscan software and quantified with the Image Master 1D

Image Analysis Software (GE Healthcare). All results were normalized to eEF2 protein and finally expressed relatively to the control condition.

RNA extraction and quantitative Real-Time PCR

Total RNA extraction from cells was done with Trizol (Life Technologies), according to the manufacturer's instructions. The RNA quality was assessed by 1.5% (w/v) agarose gel electrophoresis, while the quantity and purity were measured by NanoDrop® spectrophotometer (Isogen Life Science, Belgium). Reverse transcription was performed with iScript cDNA synthesis kit (Bio-Rad) from 1 µg total RNA. Real time PCR experiments were done on a MyIQ2 thermocycler (Bio-Rad). Samples were analyzed in duplicate in 10 µl reaction volume containing 4.8 µl IQSybrGreen SuperMix (Bio-Rad), 0.1 µl of each primer (100 nM final concentration) and 5 µl of cDNA. Primers sequences are reported in Table 6.1. Melting curves were systematically analyzed to ensure the specificity of the amplification process. Relative quantities were calculated with the standard curve method. Target genes were normalized using three reference genes according to the geNorm analysis (Vandesompele et al., 2002) and finally expressed relatively to the control group. The reference genes were cyclophilin (CPHN), glyceraldehyde-3-phosphate dehydrogenase (GAPDH) and beta-2-microglobulin (B2M3).

Table 6.1. Sequences of primers (5'-3')

Primers	Forward	Reverse
BiP	CTATTCCTGCGTCGGTGTGT	GCAAGAACTTGATGTCCTGCT
CHOP	CCTGAGGAGAGAGTGTTCCAG	CTCCTGCAGATCCTCATACCA
XBP1u	TGAGAACCAGGAGTTAAGAACACGC	CACATAGTCTGAGTGCTGCGG
XBP1s	TGAGAACCAGGAGTTAAGAACACGC	CCTGCACCTGCTGCGGAC
ATF4	GAGCTTCCTGAACAGCGAAGTG	TGGCCACCTCCAGATAGTCATC
TRB3	TGTGAGAGGACGAAGCTGGTG	TCGTGGAATGGGTATCTGCC
CPHN	CGTCTCCTTCGAGCTGTTTG	CCACCCTGGCACATGAATC
GAPDH	TGGAAAGCTGTGGCGTGAT	TGCTTCACCACCTTCTTGAT
B2M3	AAGCCGAACATACTGAACTGC	CGTCTACTGGGATCGAGACAT

BiP: binding immunoglobulin protein, CHOP: C/EBP homologous, XBP1u: X-box-binding protein 1 unspliced, XBP1s: X-box-binding protein 1 spliced, ATF4: activating transcription factor 4, TRB3: Tribbles homolog 3, CPHN: Cyclophilin, GAPDH: Glyceraldehyde-3-phosphate dehydrogenase, B2M3: Beta-2-microglobulin.

Plasmids and cell transfection

ATF6 transcriptional activity has been detected with Luciferase reporter genes. p5xATF6-GL3 plasmid (Addgene plasmid 11976) contains five repeats of the ATF6 binding site cloned into a minimal promoter preceding the firefly luciferase gene (Wang et al., 2000). *Renilla* plasmid was used to normalize transfection efficiency. Plasmids were amplified in XL1-Blue (Stratagene, USA) and purified with the NucleoBond Xtra Maxi Plus Kit (Macherey-Nagel, Belgium). C2C12 myoblasts were co-transfected (Amaxa Nucleofector™ Technology, Lonza) at 50-60% confluence according to the manufacturer's instructions. C2C12 myoblasts (1.10^6) were suspended in 100 µl of mouse neuron Nucleofector solution (Lonza) with 2.5 µg of p5xATF6-GL3 and 2.5 µg of *Renilla* plasmid. Then, cells were nucleofected and cultivated as described above. After appropriate treatment, cells were lysed with Passive Lysis Buffer (Promega, The Netherlands) and assayed for firefly and *Renilla* luciferase activities

using the Dual Luciferase Reporter Assay System (Promega). Firefly luciferase activity was reported to *Renilla* luciferase activity.

Statistical analysis

All results were expressed relatively to the control group and are presented as means ± SEM. Three independent cultures were used. In each culture, the results were generated in duplicate or triplicate. Student test or one-way ANOVA was used to assess statistical differences amongst means. When appropriate, the Dunnett's method was used as a post-hoc analysis. The significance threshold was set for a *P*-value < 0.05. Statistical significance is indicated in figures with * ($P < 0.05$) and ** ($P < 0.01$).

Results

H_2O_2 increases the transcription of UPR-inducible genes

Transcripts coding for several proteins involved in UPR were regulated upon H_2O_2 in C2C12 myotubes. Four hours after H_2O_2 exposure, the spliced form of X-box binding protein 1 (XBP1s) increased by 64% ($P < 0.01$) whereas the unspliced form (XBP1u) decreased by 23% ($P = 0.021$) (Figure 6.1A). The two forms of XBP1 were not modified 17 h after H_2O_2 exposure (Figure 6.1B). Short- (4 h) and long-term (17 h) response to H_2O_2 exposure increased the transcript coding for the chaperone BiP (65%, $P < 0.01$ and 98%, $P = 0.014$; respectively) (Figure 6.1). Four hours after H_2O_2 treatment, activating transcription factor 4 (ATF4), CHOP and tribbles homolog 3 (TRB3) mRNA increased by 82% ($P < 0.01$), 331% ($P < 0.01$) and 165% ($P < 0.01$) respectively (Figure 6.1A). A longer period (17 h)

induced a higher increase of ATF4 (141% $P = 0.011$) CHOP (17-fold, $P < 0.01$) and TRB3 (34-fold, $P < 0.01$) mRNA (Figure 6.1B).

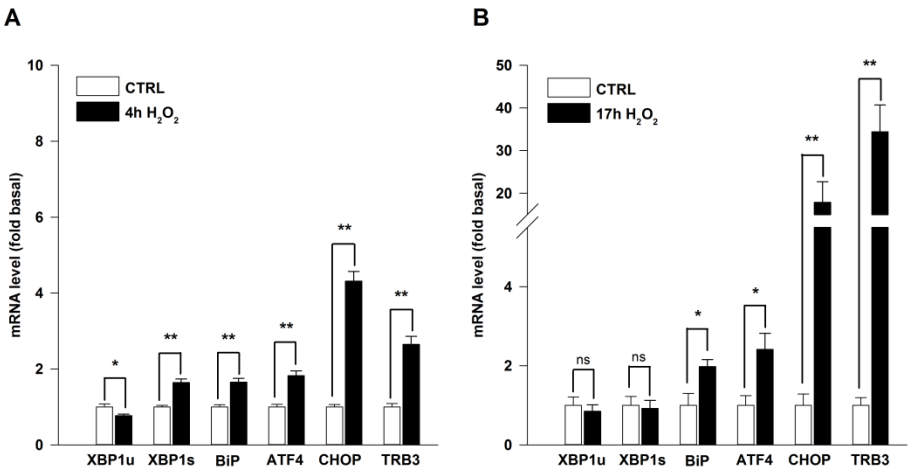

Figure 6.1. mRNA levels of XBP1u, XBP1s, BiP, ATF4, CHOP and TRB3 measured in C2C12 myotubes after 4 h (A) or 17 h (B) of H_2O_2 exposure. Results are expressed as means ± SEM (n = 3); ns, not-significant ($P \geq 0.05$); * $P < 0.05$; ** $P < 0.01$.

H_2O_2 increases the expression of ER stress protein markers

The protein chaperone BiP was increased 4 h (683%, $P < 0.01$) and 17 h after H_2O_2 exposure (674% $P < 0.01$) (Figure 6.2). These results confirm those obtained by mRNA analysis (Figure 6.1). The phosphorylation state of eIF2α increased 5-fold ($P = 0.02$) 4 h after H_2O_2 exposure and was maintained until 17 h (336%, $P < 0.01$). The protein expression of IRE1α did not change 4 h after H_2O_2 exposure whereas it increased by almost 8-fold ($P < 0.01$) after 17 h. Finally, PDI protein and the phosphorylation state of JNK were not modified by H_2O_2 (Figure 6.2).

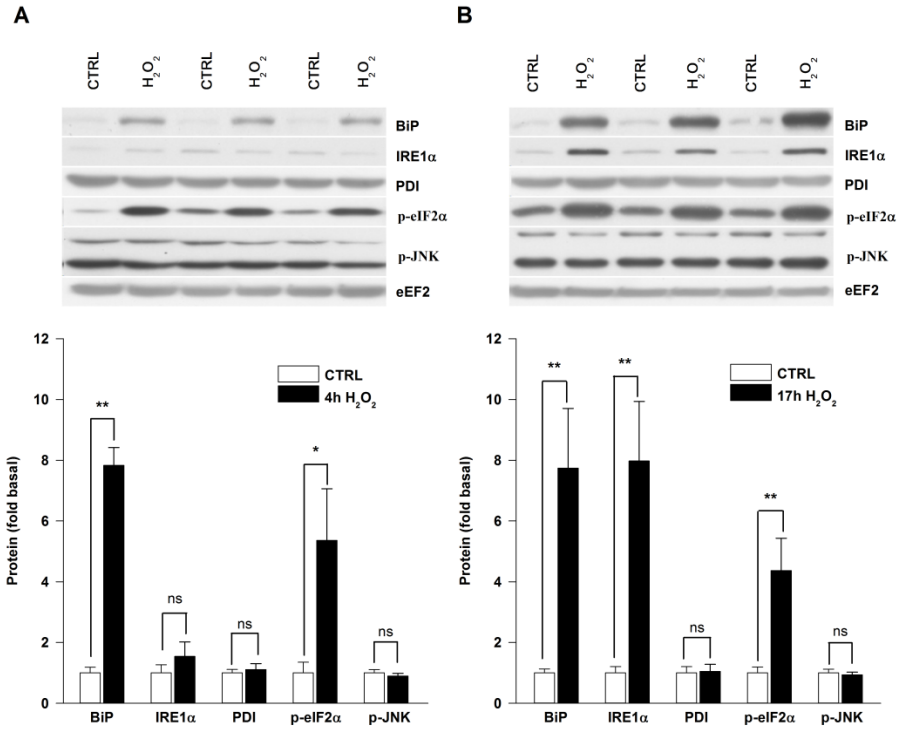

Figure 6.2. Protein expression of BiP, IRE1α, PDI, phosphorylation state of eIF2α and JNK measured in C2C12 myotubes after 4 h or 17 h of H_2O_2 exposure. Results are expressed as means ± SEM (n = 3); ns, not-significant ($P \geq 0.05$); * $P < 0.05$; ** $P < 0.01$.

H_2O_2 does not activate the ATF6 pathway

The activation of the ATF6 branch of UPR was assessed by measuring the transcriptional activity of this protein. Four hours and 17 h after H_2O_2 exposure, the transcriptional activity of ATF6 did not change (Figure 6.3). In contrast, it was increased by 2-fold ($P < 0.01$) after 4 h thapsigargin treatment and by 24-fold ($P < 0.01$) after 17 h (Figure 6.3A and 6.3B).

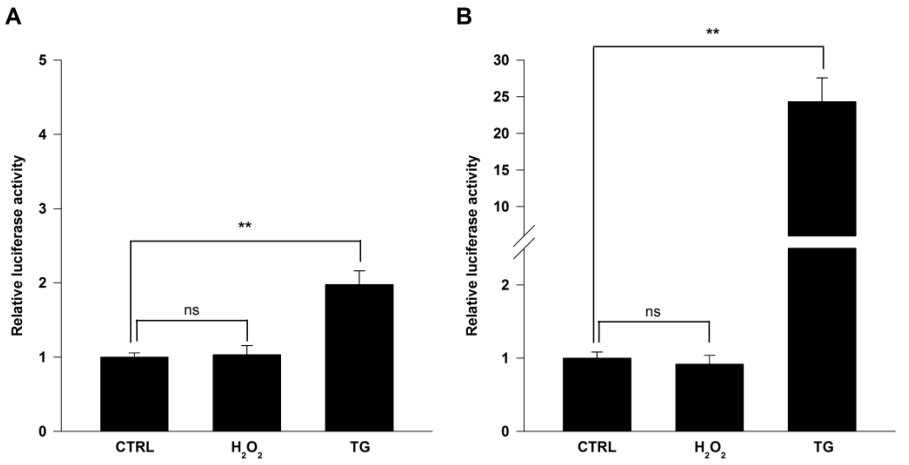

Figure 6.3. Relative ATF6 activity measured by the p5xATF6-GL3 plasmid luciferase activity normalized to the *Renilla* luciferase activity in C2C12 myotubes after 4 h (A) or 17 h (B) of H_2O_2 exposure. Results are expressed as means ± SEM (n = 3); ns, not-significant ($P \geq 0.05$); * $P < 0.05$; ** $P < 0.01$.

Discussion

Muscle cells are highly exposed to oxidant molecules. In this context, detection and response to oxidative stress is critical for cell survival. In this study, we show that ER of C2C12 myotubes senses and responds to oxidative stress. Indeed, H_2O_2 treatment activates UPR and increases the level of BiP, a well-recognized marker of ER stress (Lee, 2005). Due to its diffusion capacity across cell membranes, H_2O_2 has been widely used as a model of oxidative stress (Veal et al., 2007). Nevertheless, the highly reactive nature of ROS implicates a rapid disappearance of the stress inducer. Gülden et al. (2010) showed that H_2O_2 (200 µM) was almost completely eliminated from the culture medium of C6 glioma cells after 1 h (Gulden et al., 2010). In this study, we decided to investigate a short- (4 h) and a long-term (17 h) response after an oxidative stress induced by 200 µM H_2O_2. Preliminary experiments (data not shown) and results from the

literature (Nishida et al., 2007) led us to choose this concentration because it was the best compromise between cell survival and activation of the UPR.

IRE1 pathway is the only common branch of UPR between lower eukaryotes and metazoans (Walter and Ron, 2011). When unfolded proteins accumulate into ER, BiP dissociates from IRE1α leading to its homodimerization and trans-autophosphorylation that in turn, activates its kinase and endoribonuclease (RNAse) domains. IRE1 RNAse cleaves an intron from XBP1 mRNA, which induces a translational frame shift. The isoform resulting from XBP1s mRNA translation is a potent transcription factor that binds to the consensus mammalian ER stress response element (ERSE) (Zhang and Kaufman, 2008). Consequently, the spliced form of XBP1 mRNA (XBP1s) is a proximal and specific marker of the IRE1 pathway. Our results showed an increase of XBP1s after H_2O_2 exposure as well as a decrease of the unspliced form giving arguments for an activation of the IRE1 branch of UPR.

Our results confirm a recent study showing an activation of IRE1 by H_2O_2 in HeLa cells (Pallepati and Averill-Bates, 2011) but not those reported by Xue et al. (2005) who did not observe any change of XBP1s upon H_2O_2 treatment (1 mM for 1-8 h) in L929 fibroblasts (Holtz et al., 2006). In the latter study, XBP1s mRNA was measured by Northern blot, a technique possibly not sensitive enough to detect the slight (64%), but significant increase that we observed.

In response to ER stress, activated IRE1α recruits TRAF2 (tumor-necrosis factor-α-receptor-associated factor 2). This complex induces the phosphorylation of JNK linking ER stress to inflammation

pathways (Urano et al., 2000). In our study, we showed an activation of the IRE1α pathway but no change was observed in the phosphorylation state of JNK. This inconsistent result could be explained by three hypotheses: 1) we missed a rapid and transient phosphorylation of JNK that could occur before 4 h; 2) the activation of the IRE1 pathway is too weak to induce JNK phosphorylation. Indeed, XBP1s, a direct marker of IRE1 pathway, increased slightly in comparison to others UPR markers; 3) IRE1 mediated-JNK activation is not present in C2C12 myotubes. To the best of our knowledge, this pathway has not been demonstrated in muscle cells.

The most immediate response to ER stress is the translational inhibition of protein synthesis. Upon ER stress, PERK homodimerizes to promote its trans-autophosphorylation. The activation of PERK induces the phosphorylation of eIF2α, which inhibits global translation while activating selective translation (Lu et al., 2004). In agreement with previous results obtained in other cell types (Xue et al., 2005, Holtz et al., 2006), we observed that H_2O_2 induced eIF2α phosphorylation in C2C12 myotubes. However, we may not exclude that eIF2α could be phosphorylated independently of PERK upon oxidative stress. Four different kinases are known to phosphorylate eIF2α: PERK, general control non repressed 2 kinase (GCN2), heme-regulated inhibitor kinase (HRI) and interferon-induced double-stranded RNA-dependent protein kinase (PKR). The kinase that phosphorylates eIF2α under oxidative stress is still under debate. Some authors suggested the existence of another eIF2α-kinase specifically induced by oxidative stress (Ron, 2002, Harding et al., 2003). Recently, a higher phosphorylation state of PERK was reported

upon H_2O_2 exposure in HeLa cells but on the opposite, in L929 fibroblasts, other authors reported, no change in PERK phosphorylation state while the phosphorylation state of eIF2α was increased (Xue et al., 2005, Pallepati and Averill-Bates, 2011). Consequently, eIF2α phosphorylation induced by H_2O_2 is possibly mediated by PERK but we may not exclude a contribution of another kinase.

ATF4 transcript is the most investigated UPR downstream effector translated under eIF2α phosphorylation. This transcription factor upregulates CHOP, the main mediator of ER-mediated apoptosis (Wu and Kaufman, 2006). Furthermore, ATF4 cooperates with CHOP to induce the transcription of TRB3 (Ohoka et al., 2005). Consistently with the activation of the PERK branch of UPR, we showed that the mRNA levels of ATF4, CHOP and TRB3 increased after H_2O_2 exposure in C2C12 myotubes.

The ER lumen provides an oxidizing environment, which allows the formation of disulfide bonds. At the end of these oxidation reactions, the electrons are finally transferred to oxygen to form H_2O_2 inside ER. Therefore, a higher folding rate increases the production of H_2O_2 (Zhang and Kaufman, 2008), which subsequently can activate ER stress and UPR as shown in the present study. On the opposite, ER stress also regulates antioxidant defences (Harding et al., 2003). For example, the PERK pathway activates the transcription of glutathione S-transferase subunits favouring the redox buffer capacity of ER (Malhotra and Kaufman, 2007a). The activation of the PERK branch after H_2O_2 exposure that we observed is compatible with the idea that

ER has the capacity of sensing oxidative environment and to trigger antioxidant response.

The third branch of UPR is initiated by the translocation of ATF6 to the Golgi apparatus where it is cleaved by two proteases. The proteolysis releases a fragment containing a basic region and leucine zipper (bZIP) domain, which migrates to the nucleus, binds to ERSE and induces the transcription of UPR-inducible genes (Zhang and Kaufman, 2008). Activation of ATF6 can be assessed by measuring BiP dissociation, ATF6 translocation, ATF6 cleavage or ATF6 transcriptional activity. The last strategy, used in our experiments, is recognized as a very sensitive method (Shen and Prywes, 2005). The lack of changes in the ATF6 transcriptional activity reported in the present study provides evidence against the activation of the ATF6 branch of UPR by H_2O_2 in C2C12 myotubes. This is an apparent contradiction with the upregulation of the cleavage of ATF6 found in HeLa cells after H_2O_2 exposure (Pallepati and Averill-Bates, 2011). Therefore, in our study, we may not rule out a cleavage of ATF6 without changing its transcriptional activity.

In conclusion, ER of C2C12 myotubes appears to be able to sense and respond to oxidative stress. Nevertheless, H_2O_2-induced oxidative stress does not activate the three branches of UPR to the same extent. The downstream effectors of PERK i.e. eIF2α, ATF4, CHOP and TRB3 are highly responsive to oxidative stress. The IRE1 pathway is slightly activated whereas the transcriptional activity of ATF6 pathway is not modified. The mechanisms by which branches of UPR can be specifically activated by oxidative stress are currently unresolved and need further investigations.

References

Barbieri, E. & Sestili, P. 2012. Reactive oxygen species in skeletal muscle signaling. *J Signal Transduct,* **2012,** 982794.

Borradaile, N. M., Buhman, K. K., Listenberger, L. L., Magee, C. J., Morimoto, E. T., Ory, D. S. & Schaffer, J. E. 2006. A critical role for eukaryotic elongation factor 1A-1 in lipotoxic cell death. *Mol Biol Cell,* **17,** 770-8.

Csordas, G. & Hajnoczky, G. 2009. SR/ER-mitochondrial local communication: calcium and ROS. *Biochim Biophys Acta,* **1787,** 1352-62.

Deldicque, L., Cani, P. D., Philp, A., Raymackers, J. M., Meakin, P. J., Ashford, M. L., Delzenne, N. M., Francaux, M. & Baar, K. 2010. The unfolded protein response is activated in skeletal muscle by high-fat feeding: potential role in the downregulation of protein synthesis. *Am J Physiol Endocrinol Metab,* **299,** E695-705.

Gulden, M., Jess, A., Kammann, J., Maser, E. & Seibert, H. 2010. Cytotoxic potency of H2O2 in cell cultures: impact of cell concentration and exposure time. *Free Radic Biol Med,* **49,** 1298-305.

Harding, H. P., Zhang, Y., Zeng, H., Novoa, I., Lu, P. D., Calfon, M., Sadri, N., Yun, C., Popko, B., Paules, R., Stojdl, D. F., Bell, J. C., Hettmann, T., Leiden, J. M. & Ron, D. 2003. An integrated stress response regulates amino acid metabolism and resistance to oxidative stress. *Mol Cell,* **11,** 619-33.

He, S., Yaung, J., Kim, Y. H., Barron, E., Ryan, S. J. & Hinton, D. R. 2008. Endoplasmic reticulum stress induced by oxidative stress in retinal pigment epithelial cells. *Graefes Arch Clin Exp Ophthalmol,* **246,** 677-83.

Holtz, W. A., Turetzky, J. M., Jong, Y. J. & O'Malley, K. L. 2006. Oxidative stress-triggered unfolded protein response is upstream of intrinsic cell death evoked by parkinsonian mimetics. *J Neurochem,* **99,** 54-69.

Koh, H. J., Toyoda, T., Didesch, M. M., Lee, M. Y., Sleeman, M. W., Kulkarni, R. N., Musi, N., Hirshman, M. F. & Goodyear, L. J. 2013. Tribbles 3 mediates endoplasmic reticulum stress-induced insulin resistance in skeletal muscle. *Nat Commun,* **4,** 1871.

Laybutt, D. R., Preston, A. M., Akerfeldt, M. C., Kench, J. G., Busch, A. K., Biankin, A. V. & Biden, T. J. 2007. Endoplasmic reticulum stress contributes to beta cell apoptosis in type 2 diabetes. *Diabetologia,* **50,** 752-63.

Lee, A. S. 2005. The ER chaperone and signaling regulator GRP78/BiP as a monitor of endoplasmic reticulum stress. *Methods,* **35,** 373-81.

Lu, P. D., Harding, H. P. & Ron, D. 2004. Translation reinitiation at alternative open reading frames regulates gene expression in an integrated stress response. *J Cell Biol,* **167,** 27-33.

Malhotra, J. D. & Kaufman, R. J. 2007a. The endoplasmic reticulum and the unfolded protein response. *Semin Cell Dev Biol,* **18,** 716-31.

Malhotra, J. D. & Kaufman, R. J. 2007b. Endoplasmic reticulum stress and oxidative stress: a vicious cycle or a double-edged sword? *Antioxid Redox Signal,* **9,** 2277-93.

Nishida, H., Ichikawa, H. & Konishi, T. 2007. Shengmai-san enhances antioxidant potential in C2C12 myoblasts through the induction of intracellular glutathione peroxidase. *J Pharmacol Sci,* **105,** 342-52.

Ohoka, N., Yoshii, S., Hattori, T., Onozaki, K. & Hayashi, H. 2005. TRB3, a novel ER stress-inducible gene, is induced via ATF4-CHOP pathway and is involved in cell death. *Embo J,* **24,** 1243-55.

Ozcan, U., Cao, Q., Yilmaz, E., Lee, A. H., Iwakoshi, N. N., Ozdelen, E., Tuncman, G., Gorgun, C., Glimcher, L. H. & Hotamisligil, G. S. 2004. Endoplasmic reticulum stress links obesity, insulin action, and type 2 diabetes. *Science,* **306,** 457-61.

Pallepati, P. & Averill-Bates, D. A. 2011. Activation of ER stress and apoptosis by hydrogen peroxide in HeLa cells: protective role of mild heat preconditioning at 40 degrees C. *Biochim Biophys Acta,* **1813,** 1987-99.

Pierre, N., Deldicque, L., Barbe, C., Naslain, D., Cani, P. D. & Francaux, M. 2013. Toll-like receptor 4 knockout mice are protected against endoplasmic reticulum stress induced by a high-fat diet. *PLoS One,* **8,** e65061.

Ron, D. 2002. Translational control in the endoplasmic reticulum stress response. *J Clin Invest,* **110,** 1383-8.

Shen, J. & Prywes, R. 2005. ER stress signaling by regulated proteolysis of ATF6. *Methods,* **35,** 382-9.

Urano, F., Wang, X., Bertolotti, A., Zhang, Y., Chung, P., Harding, H. P. & Ron, D. 2000. Coupling of stress in the ER to activation of JNK protein kinases by transmembrane protein kinase IRE1. *Science,* **287,** 664-6.

Vandesompele, J., De Preter, K., Pattyn, F., Poppe, B., Van Roy, N., De Paepe, A. & Speleman, F. 2002. Accurate normalization of real-time quantitative RT-PCR data by geometric averaging of multiple internal control genes. *Genome Biol,* **3,** RESEARCH0034.

Vattemi, G., Engel, W. K., McFerrin, J. & Askanas, V. 2004. Endoplasmic reticulum stress and unfolded protein response in inclusion body myositis muscle. *Am J Pathol,* **164,** 1-7.

Veal, E. A., Day, A. M. & Morgan, B. A. 2007. Hydrogen peroxide sensing and signaling. *Mol Cell,* **26,** 1-14.

Walter, P. & Ron, D. 2011. The unfolded protein response: from stress pathway to homeostatic regulation. *Science,* **334,** 1081-6.

Wang, Y., Shen, J., Arenzana, N., Tirasophon, W., Kaufman, R. J. & Prywes, R. 2000. Activation of ATF6 and an ATF6 DNA binding site by the endoplasmic reticulum stress response. *J Biol Chem,* **275,** 27013-20.

Wu, J. & Kaufman, R. J. 2006. From acute ER stress to physiological roles of the Unfolded Protein Response. *Cell Death Differ,* **13,** 374-84.

Xue, X., Piao, J. H., Nakajima, A., Sakon-Komazawa, S., Kojima, Y., Mori, K., Yagita, H., Okumura, K., Harding, H. & Nakano, H. 2005. Tumor necrosis factor alpha (TNFalpha) induces the unfolded protein response (UPR) in a reactive oxygen species (ROS)-dependent fashion, and the UPR counteracts ROS accumulation by TNFalpha. *J Biol Chem,* **280,** 33917-25.

Zhang, K. & Kaufman, R. J. 2008. From endoplasmic-reticulum stress to the inflammatory response. *Nature,* **454,** 455-62.

Chapter 8: Discussion, limitations and conclusion

8.1. Discussion

8.1.1. Regulation of endoplasmic reticulum stress, body mass, and insulin sensitivity by toll-like receptor 4

TLR4 and ER stress

High concentrations in lipids induce ER stress in many cell types including myocytes, hepatocytes and adipocytes (Flamment et al., 2012). In those cells, disruption of ER homeostasis has been causally linked to insulin resistance physiopathology (Ozcan et al., 2006). However, little is known about the mechanism by which lipids act on ER. In the study presented in chapter 5, we hypothesized that TLR4 mediates circulating NEFA-induced ER stress. To test this hypothesis, WT and $TLR4^{-/-}$ mice were fed with chow or HFD. Our results indicated that $TLR4^{-/-}$ mice were protected against ER stress in skeletal muscle, liver and adipose tissue. To investigate how TLR4 regulates ER stress, we measured the TLR4 downstream effectors. Surprisingly, neither NF-κB nor MAPK pathways were activated by HFD. Except for the phosphorylation state of JNK in adipose tissue, none of the markers of the TLR4 pathway were upregulated by HFD in WT and $TLR4^{-/-}$ mice. Furthermore, no change was observed in circulating NEFA concentrations after HFD. These results argue against a direct regulation of ER stress by TLR4 signaling. However, we cannot exclude that 1) NF-κB and MAPK pathways were transiently activated after an acute elevation of circulating NEFA

concentrations caused by a high-fat meal, so we missed these changes because tissue and blood samples were taken in a fasted state; 2) our markers were not sensitive enough to detect an activation of the TLR4 downstream effectors.

In C2C12 myotubes, we clearly found a disconnection between TLR4 activation and ER stress (data not shown). TLR4 knockdown by siRNA failed to reduce ER stress induced by palmitate. On the other hand, in a time-course experiment (0-24 h), LPS (1 µg/ml) did not increase the mRNA levels of ATF4, CHOP, TRB3, XBP1s and BiP. On the contrary, LPS drastically increased the cytokines IL-6 (160-fold) and monocyte chemotactic protein 1 (MCP1) (187-fold). In our experiment, the activation of TLR4 induced by LPS does not seem comparable with physiological conditions. For instance, IL-6 mRNA is upregulated no more than 3-fold in the *vastus lateralis* from obese subjects (Reyna et al., 2008), as well as in skeletal muscle of HFD-fed mice (Cani et al., 2007). This suggests that even if LPS and/or circulating NEFA activate TLR4, this regulation is probably not sufficient to trigger ER stress in muscle cells. Consequently, we propose that TLR4 does not act directly on ER homeostasis in muscle cells. This observation is probably cell-type specific. Indeed, LPS does induce ER stress in numerous cell types (chapter 2). More generally, cells with high secretory activity could be more sensitive to ER stress than those that are not specialized in protein secretion such as muscle cells. In most eukaryotic cells, about one-third of the proteins are synthetized in the ER (Hetz, 2012). However, the ER folding machinery of specialized secretory cells (e.g., hepatocytes, B

lymphocytes, pancreatic β cells, macrophages) faces additional challenges due to the high protein demand (Hetz, 2012). For instance, ~80% of the proteins synthetized in pancreatic β cells are exported (Kramer and Poort, 1972) and, liver cells secrete millions proteins *per* minute (Hotamisligil, 2010). Consequently, we can imagine a threshold of ER stress adapted to cell functions.

In our study, a direct relationship between TLR4 and ER stress seems unlikely. However, TLR4 is associated with ER stress as demonstrated by the use of knockout mice. Like others, we found that TLR4 deficiency protects against HFD-induced obesity (Tsukumo et al., 2007, Radin et al., 2008). Therefore, the protective effect observed on ER stress could be related to leanness rather than a direct TLR4 signaling. Obesity is associated with numerous disorders that can alter ER homeostasis (e.g., inflammation, oxidative stress, mitochondrial dysfunction, lipotoxicity and glucotoxicity). In our study, obesity is a confounding factor that makes the results difficult to interpret.

When lipids accumulate in the cytosol, more proteins are needed to store fat in lipid droplets (Hotamisligil, 2006). Consequently, ER stress could be due to an increase of protein synthesis. Alternatively, lipotoxicity can disrupt the folding capacity. Lipid excess is associated with ROS production in muscle cells, and it has been proposed, in other cell types, that oxidative stress induces ER stress (chapter 2). In the study reported in the chapter 6, we tested whether oxidative stress *per se* could induce ER stress in C2C12 myotubes. Interestingly, we showed that H_2O_2 triggers ER stress in C2C12 myotubes. We can

suppose that, like thapsigargin, oxidative stress alters calcium homeostasis by targeting ER-based calcium channel (chapter 2). However, we did not measure the calcium release from ER, thus we may not exclude the presence of another mechanism. For instance, the folding capacity and the ERAD system could be overwhelmed by the presence of proteins damaged by ROS. Whatever the mechanisms, our results provide an argument for the involvement of ROS in lipid-induced ER stress in muscle cells. Recently, N-acetylcysteine and ebselen antioxidant molecules alleviated ER stress induced by NEFA in 3T3-L1 adipocytes (Kawasaki et al., 2012). However, using the natural antioxidant tetramethylpyrazine, we were unable to block palmitate-induced ER stress in C2C12 myotubes (data not shown). At the present time, we cannot propose that ROS are the intermediates by which lipids disrupt ER homeostasis in muscle cells. More research is required to test other antioxidant agents, and probably specific molecules targeting mitochondrial ROS could be helpful. Indeed, lipid-stimulated ROS production seems to be related to mitochondrial dysfunction (chapter 2). In different cell-types, the use of antioxidant agents enabled to reduce ER stress induced by various conditions (chapter 2), suggesting that oxidative stress could be a common mediator by which metabolic factors are sensed by ER.

Modulation of energetic metabolism by TLR4

The protective effect of TLR4 deficiency on obesity seems to be related to a higher energy expenditure rather than a decrease of energy intake. However, a reduction of fat absorption cannot be excluded in TLR4 deficient mice. To the best of our knowledge, this has not been

investigated yet. In agreement with Tsukumo et al. (2007), we found that energy intake increased in WT as well as TLR4$^{-/-}$ mice submitted to HFD (Tsukumo et al., 2007). On the other hand, measurements of oxygen consumption showed that, upon HFD, energy expenditure increases in TLR4 deficient compared to control mice (Tsukumo et al., 2007). Consequently, TLR4 is probably not involved in the regulation of appetite and satiety. Nevertheless, contrasting results have been reported. In HFD-fed mice, TLR4 or MyD88 knockdown reduced the caloric intake, suggesting that TLR4 regulates appetite (Galbo et al., 2013). These conflicting results remain difficult to explain.

Interestingly, regulation of energetic metabolism emerges as a new function of TLR4 (Pang et al., 2010). Upon HFD, fatty acid oxidation increases in TLR4 deficient mice as shown by the reduction in the respiratory exchange ratio; this is not the case in the WT mice (Tsukumo et al., 2007). According to this finding, TLR4 deficient mice could adapt energetic substrate to diet composition. In line with Tsukumo et al. (2007), it has been reported a higher fatty acid oxidation capacity, beta-hydroxyacyl CoA dehydrogenase and citrate synthase activity in the skeletal muscle of TLR4 deficient mice (Frisard et al., 2010). Intraperitoneal injection of LPS in WT mice produced both an increase of glucose oxidation and a reduction of fatty acid oxidation in skeletal muscle (Frisard et al., 2010). In C2C12 myotubes, IKK inhibitor prevented the shift in energetic substrate induced by low dose of LPS (50 pg/ml), suggesting an implication of NF-κB (Frisard et al., 2010). More investigations are needed to better

understand how TLR4 regulates energetic metabolism.

In the context of HFD, not all studies found an implication of TLR4 in body weight gain. The reason of this discrepancy is unclear but a sex-dependent effect has been proposed since Shi et al. (2006) reported that, upon HFD, female TLR4$^{-/-}$ mice gain more weight than female WT mice (Shi et al., 2006). However, in another study, male TLR4$^{-/-}$ mice were not protected from body weight gain induced by HFD, suggesting no sex-dependent effect (Kim et al., 2007).

Some authors proposed that the different genetic alterations existing in the TLR4 deficient mice could explain the divergent results obtained concerning obesity (Saberi et al., 2009, Tsukumo et al., 2007). Three models of TLR4 deficient mice are available. Two of them are natural loss-of-function mutation (C3H/HeJ) or natural deletion (C57BL/10ScN). The third one, TLR4$^{-/-}$ mice, used in our study, have been generated by homologous recombination (Hoshino et al., 1999). The hypothesis of a specific adaptation related to the different genetic alterations might also be ruled out. In our study, male TLR4$^{-/-}$ mice were protected against body weight gain induced by HFD, whereas another study did not find such effect (Kim et al., 2007). Similarly, conflicting results are present in the literature regarding C3H/HeJ mice (Tsukumo et al., 2007, Poggi et al., 2007) and C57BL/10ScN mice (Radin et al., 2008, Davis et al., 2008). It is currently difficult to explain such contradictory results, but differences in circulating LPS could be involved. Interestingly, HFD increases circulating LPS, and chronic infusion of LPS induces obesity in mice (Cani et al., 2007). As a consequence, LPS could be responsible of the

pathological adaptation discussed above. We can speculate that circulating LPS concentrations depend on HFD composition and period, inducing thereby differences in body weight gain. In the studies described in this paragraph, the percentage of calories from fat ranged from 45 to 60%, and the HFD period ranged from 7 to 36 weeks. Complementary to this hypothesis, the source of fat could also be critical. Indeed, saturated NEFA, unlike unsaturated NEFA, are known to activate TLR4 (chapter 2). Thus, HFD composition could influence the concentration of circulating saturated NEFA, which in turn might regulate TLR4-induced obesity. In connection with this hypothesis, high-fat palmitate, unlike HFD control, upregulates IL-6 and TNFα in mice adipose tissue (Davis et al., 2008). Unfortunately, the origin of fat is rarely indicated in the studies.

Regulation of insulin sensitivity by TLR4

In the last decade, TLR4 emerged as a candidate linking dietary fat intake to insulin resistance. However, results from the literature remain unclear. In HFD-fed mice, two studies reported a protective role of TLR4 deficiency on insulin resistance (Shi et al., 2006, Tsukumo et al., 2007), whereas two others did not find such effect (Poggi et al., 2007, Radin et al., 2008). These conflicting results could be explained by differences in HFD composition and period (see above), and/or techniques used to evaluate insulin sensitivity. Indeed, OGTT (Tsukumo et al., 2007), ITT (Shi et al., 2006, Radin et al., 2008) or euglycemic-hyperinsulinemic clamp (Poggi et al., 2007) has been performed. In our study, we found that $TLR4^{-/-}$ mice are slightly less glucose intolerant than their WT counterparts after HFD. This is

in agreement with Tsukumo et al. (2007) although the effect on glucose tolerance was much more pronounced in that study. However, it is hazardous to compare our results with those obtained in that report due to differences in the HFD models. For instance, after only 8 weeks on HFD, the body weight of WT mice increased by ~50% compared to control mice. In our study, 8 weeks of HFD did not change body weight (data not shown), this highlights major differences in HFD models.

Inflammation seems to be the obvious mechanism by which TLR4 mediates insulin resistance. In line with this hypothesis, TLR4 deficient mice were protected against HFD-induced insulin resistance and inflammation in skeletal muscle, liver and adipose tissue (Shi et al., 2006, Tsukumo et al., 2007). However, in our study the inflammation markers were not upregulated by HFD. This discrepancy could be due to the severity of HFD-induced obesity. As mentioned above, body weight was drastically increased after HFD in the study of Tsukumo et al. (2007). Likewise, in the study of Shi et al. (2006) body weight increased by 60-70% in WT mice after HFD. In our experiment, body weight was increased by 18% in WT mice after HFD (data not shown). In another study, increase of body mass was limited to ~10% after HFD and, no change was observed in the mRNA levels of TNFα, MCP1 and IL-6 cytokines in the adipose tissue (Davis et al., 2008). Altogether, this suggests that only extreme models of HFD are associated with obesity-induced inflammation in mice. The link between TLR4, inflammation and insulin resistance remains to be demonstrated in more physiological conditions.

ER stress could also mediate the action of TLR4 on insulin sensitivity. As described in chapter 3, ER stress is recognized as a central mechanism of insulin resistance physiopathology. Interestingly, we found that TLR4$^{-/-}$ mice were protected against ER stress induced by HFD in the main organs for glucose metabolism. However, the results obtained do not allow to establish a link between ER stress and insulin resistance. Firstly, insulin resistance has not been demonstrated since insulin concentration during OGTT was not measured, and ITT was not performed. Secondly, the main intermediate of ER stress-induced insulin resistance, i.e., JNK (chapter 3), was not activated by HFD except in the adipose tissue. In this tissue, the other markers of TLR4 signaling were not upregulated, supporting the idea of an ER stress-dependent activation of JNK. Regarding liver, ER stress stimulates lipogenesis through activation of the transcription factor sterol regulatory element binding protein 1c (Kammoun et al., 2009). This mechanism has been causally associated with liver insulin resistance (Kammoun et al., 2009). In our study, liver ER stress could potentially participate to glucose intolerance induced by HFD. The role of ER stress in skeletal muscle insulin resistance is particularly unclear. It will be discussed in the next subpart.

Alternatively, ceramides could account for TLR4-induced insulin resistance. Until recently, it was well accepted that saturated NEFA induced *de novo* ceramides synthesis by providing a substrate for SPT, the rate limiting enzyme of ceramide synthesis. A paper published in The Journal of Clinical Investigation demonstrated that saturated lipids also promote *de novo* ceramide synthesis through TLR4

(Holland et al., 2011). The authors provide evidences that can be summarized as follows: 1) LPS time-dependently increased ceramides content in isolated rat *soleus*; 2) In *soleus*, TLR4 deficient mice were protected against accumulation of ceramides induced by lard oil infusion or palmitate treatment; 3) LPS as well as palmitate upregulated enzymes driving ceramide biosynthesis such as SPT2, ceramide synthase 1 (CerS1), CerS2 and CerS6 in C2C12 myotubes. As mentioned in chapter 3, ceramides are mediators of lipid-induced insulin resistance. Collectively, these observations suggest the existence of another mechanism by which TLR4 could act on insulin sensitivity.

The use of global deficiency in TLR4 leads to difficulties when interpreting the results: 1) confounding effect obesity; 2) identification of the tissue responsible for the protective effect observed. A well-designed study tried to overcome these drawbacks (Jia et al., 2014). Liver-specific TLR4 null mice ($TLR4^{LKO}$) were generated thanks to a Cre-LoxP system. Under HFD, $TLR4^{LKO}$ mice became obese as WT mice, suppressing *de facto* the confounding factor of obesity. Interestingly, HFD-induced insulin resistance was attenuated in $TLR4^{LKO}$. Consequently, liver seems a key organ in which TLR4 exerts its deleterious effects on insulin signaling. However, contradictory results were reported (Galbo et al., 2013). Indeed, in this study, TLR4 deficient mice were not protected against liver insulin resistance induced by HFD. This suggests major differences in the physiopathology of insulin resistance between global and liver-specific TLR4 knockout.

Macrophage infiltration is well known to play a central role in the development of insulin resistance (Shoelson et al., 2006). In the context of obesity, proinflammatory cytokines can be mainly produced by the infiltrated macrophages. For instance, TNFα is essentially synthetized by macrophages in adipose tissue from ob/ob mice (Weisberg et al., 2003). Given that macrophages highly express TLR4 and contribute to insulin resistance, myeloid-specific TLR4 null mice ($TLR4^{\Delta m\phi}$) were generated (Jia et al., 2014). Unexpectedly, after HFD, $TLR4^{\Delta m\phi}$ were not protected against insulin resistance and, circulating inflammatory cytokines were elevated. In mice, hematopoietic cell-specific deletion of TLR4 provided divergent results (Saberi et al., 2009). According to this observation, TLR4 from lymphoid-derived cells rather than from macrophages could be involved in the physiopathology of insulin resistance.

In response to high level of circulating NEFA, metabolic tissues trigger an inflammatory response which in turn disrupts insulin signaling. Interestingly, a plasma membrane receptor of the innate immune system, TLR4, induces inflammation in response to saturated NEFA. In the wake of this discovery, studies demonstrated the implication of TLR4 in the development insulin resistance. However, it remains to unravel the tissues and cells contributing to this mechanism.

8.1.2. Insulin resistance induced by endoplasmic reticulum stress in muscle cells: what is wrong?

UPR, inflammation and insulin resistance

In the context of obesity, extracellular and intracellular lipids appear to initiate the development of metainflammation, i.e., inflammation induced by metabolic factors. This abnormal inflammation, also called low-grade inflammation, must be distinguished from the normal response to pathogen infection. In type 2 diabetes, the development of insulin resistance is intimately linked to metainflammation (Hotamisligil, 2005), this causal relationship has been discovered for over a hundred years. Indeed, in 1876 Ebstein observed that sodium salicylate reduced glycosuria in diabetic subjects (Shoelson et al., 2006). However, the mechanisms by which metabolic signals are transduced into inflammatory response remain unclear and belong to the emerging field of immunometabolism. Recently, it has been proposed that ER could be an integration center, which senses metabolic stress and triggers an inflammatory signal (Hotamisligil, 2010, Hotamisligil, 2006). More precisely, UPR signaling is coupled with the NF-κB and MAPK inflammatory pathways (Zhang and Kaufman, 2008). In the next paragraphs, we will focus on the experiments that revealed this mechanism.

Urano et al. (2000) treated rat pancreatic AR42J cells with tunicamycin and thapsigargin (Urano et al., 2000). They observed that JNK activity was drastically increased by both chemical ER stress inducers. Upon ER stress, IRE1α recruits the adapter protein TRAF2,

the complex IRE1α-TRAF2 activates JNK. This was the first time that ER stress was connected to JNK. These findings were extended to fibroblasts and liver cells (Ozcan et al., 2004). IRE1α$^{-/-}$ fibroblasts were protected against JNK activation induced by tunicamycin. Because JNK is well known to phosphorylate IRS-1 on an inhibitory serine residue (Ser^{307}), insulin pathway was also investigated. In Fao liver cells, tunicamycin disrupts insulin signaling as shown by the increase of phospho-IRS-1 (Ser^{307}), and the reduction of both phospho-Akt and phosphotyrosine-IRS-1 levels. Addition of a JNK inhibitor, SP600125, to tunicamycin restored insulin signaling. In wild-type fibroblasts, tunicamycin blocked insulin-induced IRS-1 phosphorylation on tyrosine residue, whereas such effect was not found in IRE1α$^{-/-}$ fibroblasts. All together, these results have established the principal mechanistic basis by which UPR disrupts insulin signaling, a pathway that we can called IRE1α-TRAF2-JNK-IRS-1.

In addition to JNK, UPR has been connected to NF-κB pathway (Hu et al., 2006). Similar to the mechanism described above, IRE1α activation leads to the formation of a complex IRE1α-TRAF2-IKK, resulting in the activation of IKK, another inflammatory kinase well known to impair insulin signaling through IRS-1 serine phosphorylation (chapter 3). In different cancer cell lines, tunicamycin as well as thapsigargin activate IKK as shown by the increase of phospho-IκBα and the decrease of IκBα levels. IRE1α knockdown protected against IKK activation, demonstrating that IRE1α is upstream of IKK.

JNK and IKK are at the interface between UPR and insulin

signaling. However, activation of JNK and IKK by IRE1α has been demonstrated only with non-physiological ER stress inducers. Furthermore, such connection has not been explored in skeletal muscle, a major site of insulin resistance.

In our study, ER stress was induced by palmitate and we used C2C12 myotubes as a model of muscle cells. In C2C12 and L6 myotubes, numerous studies demonstrated that palmitate inhibits insulin signaling, glucose uptake and glycogen synthesis (Hage Hassan et al., 2012, Yuzefovych et al., 2010, Chavez et al., 2003, Chavez and Summers, 2003, Lee et al., 2006). On the other hand, results from our lab and others demonstrated that palmitate induces ER stress in C2C12 myotubes (Deldicque et al., 2010, Salvado et al., 2013, Hage Hassan et al., 2012). Our experiment confirms these findings. In addition, palmitate activated the IRE1α-JNK pathway in C2C12 myotubes. Indeed, palmitate increased the phosphorylation state of the JNK downstream target c-Jun and, IRE1α knockdown prevented this effect. However, palmitate did not modify phospho-JNK level. This apparent discrepancy seems related to differences in the duration of the phosphorylation states. For instance, JNK phosphorylation induced by interleukin 1β is transient (30 min), whereas the phosphorylation state of c-Jun persists after 2 h in smooth muscle (Zhang et al., 2012). Although IRE1α knockdown protected against JNK activation, it did not prevent the inhibitory effect of palmitate on Akt. This suggests that JNK do not act on insulin pathway in C2C12 myotubes. As a consequence, the IRE1α-JNK-IRS-1 pathway probably does not exist in muscle cells.

Early studies on JNK and metabolism pointed out the central role of this kinase in the physiopathology of insulin resistance (Hirosumi et al., 2002, Hotamisligil, 2005). Remarkably, inflammation, ER stress and oxidative stress converge toward JNK. JNK activity is drastically increased in liver, adipose tissue and skeletal muscle of obese mice (Hirosumi et al., 2002). JNK1 knockout ob/ob mice do not develop insulin resistance. However, those mice are also protected against body weight gain, probably via effects on energy expenditure (Hirosumi et al., 2002). Once again, the confounding factor of obesity makes difficult to identify the mechanism by which JNK1 acts on insulin signaling. Interestingly, in HFD-fed mice, activation of JNK in skeletal muscle was less clear than in adipose tissue and liver (Hirosumi et al., 2002). Furthermore, phospho-JNK level was not upregulated in skeletal muscle of type 2 diabetic subjects and HFD-fed mice (Koh et al., 2013). In relation with these observations, the role of JNK in skeletal muscle insulin resistance has been recently challenged (Pal et al., 2013). Indeed, muscle-specific overactivation of JNK failed to disrupt insulin signaling and to modify the OGTT response in mice. On the other hand, muscle-specific JNK1 deficient mice were not protected against HFD-induced insulin resistance as shown by OGTT, ITT and insulin-stimulated Akt phosphorylation in skeletal muscle. However, in a similar experiment, contradictory results have been reported (Sabio et al., 2010). Consequently, the contribution of JNK to skeletal muscle insulin resistance is not clear at the moment.

In the study from Hage Hassan et al. (2012), the authors suggested that only non-physiologic ER stress can disrupt insulin signaling in muscle cells. Indeed, chemical chaperone prevented insulin resistance induced by tunicamycin but not by palmitate. To support this finding, they showed that both IRE1α and JNK phosphorylation states increased much more with tunicamycin than palmitate (Hage Hassan et al., 2012). To test whether non-physiologic ER stress could activate IRE1α-JNK pathway in a higher extent, we used thapsigargin (data not shown). It has been showed in our lab that thapsigargin (17 h, 200 nM) induces a higher level of ER stress than palmitate (17 h, 1 mM) in C2C12 myotubes (Deldicque et al., 2010). In our experiment, 1 µM thapsigargin for 17 h increased 2-fold more XBP1s than palmitate. Although short (1-4 h) and long period (17 h) of incubation with thapsigargin produced a massive ER stress, JNK was not activated. Indeed, the phosphorylation state of JNK was not modified, whereas phospho-c-Jun level was drastically reduced mainly because of a decrease of its total form. As shown by the use of siRNA, the effect of thapsigargin on phospho-c-Jun was independent of IRE1α. Consequently, insulin resistance induced by thapsigargin is unlikely related to IRE1α-JNK pathway. Nevertheless, tunicamycin for 16 h or 24 h increased the phosphorylation state of JNK in C2C12 myotubes (Hage Hassan et al., 2012, Panzhinskiy et al., 2013). According to these observations, two different chemical ER stress inducers regulate JNK in an opposite way. Although difficult to explain, these results indicate that ER stress response would greatly depend on the stressor agent.

In the study presented in chapter 7, we have also evaluated the connection between IRE1α and NF-κB pathway (data not shown). In order to test the causal relationship between IRE1α and IKK in C2C12 myotubes, we measured two downstream target of IKK, IκBα and the p65 subunit of NF-κB (data not shown). Upon IKK activation, IκBα is degraded and the p65 subunit of NF-κB is phosphorylated on Ser^{536} (Sakurai et al., 2003). Although 17 h thapsigargin decreased IκBα level, IRE1α knockdown did not modify this effect. Furthermore, the phosphorylation state of NF-κB p65 was not changed by 1-4 h and 17 h incubation with thapsigargin. Collectively, our results suggest no link between IRE1α and NF-κB pathway in C2C12 myotubes. However, we did not measure other markers of the NF-κB pathway such as phospho-IκBα, phospho-IKKα/β and NF-κB DNA binding activity. Therefore, we cannot definitively conclude that the NF-κB pathway is not under the control of IRE1α. Further researches are needed to describe more clearly the relationship between IRE1α and the NF-κB pathway in muscle cells.

TRB3 and insulin resistance

Alternatively to the hypothesis tested above, ER stress can disrupt insulin signaling through the upregulation of TRB3 (chapter 3). In our experiment, we observed an inverted relation between TRB3 mRNA level and insulin signaling under palmitate treatment. Consequently, we decided to downregulate TRB3 to evaluate its role in palmitate-induced insulin resistance. TRB3 siRNA did not restore Akt inhibition, suggesting no link between TRB3 expression and Akt phosphorylation state in C2C12 myotubes treated with palmitate. This

finding is in disagreement with those reported elsewhere. The interaction between TRB3 and Akt has been confirmed in mice skeletal muscles (Koh et al., 2006). Furthermore, in mice *tibialis anterior*, TRB3 overexpression inhibited the insulin pathway (Koh et al., 2013). However, the results obtained in that study are not totally convincing. In Figure 2d, the reduction of phospho-Akt (Thr^{308}) level induced by TRB3 overexpression is only a trend. In supplementary Figure S3, TRB3 overexpression did not reduce phospho-Akt (Ser^{473}) level after insulin stimulation. In the same study, the authors showed that TRB3 siRNA restored the inhibitory effect of tunicamycin on insulin-induced glucose uptake in C2C12 myotubes. However, the action of TRB3 siRNA on Akt phosphorylation sate was not shown despite the fact that TRB3 is known to inhibit the latter. The authors demonstrated a new inhibitory interaction of TRB3 with IRS-1. Consequently, the mechanism by which TRB3 reduced glucose uptake upon tunicamycin treatment could be due to IRS-1 and/or Akt inhibition. In our study, we did not measure insulin signaling at the level of IRS-1, so we cannot know whether TRB3 acts on IRS-1. However, given that IRS-1 is upstream of Akt, we can suppose that TRB3 did not inhibit IRS-1 in our model.

Strikingly, one year after the report from Koh et al. (2013), the same laboratory published a paper showing contradictory results (An et al., 2014). In this study, TRB3 was overexpressed specifically in skeletal muscles of mice. Surprisingly, those mice were not insulin-resistant as shown by OGTT, ITT, and insulin-stimulated Akt and IRS-1 tyrosine phosphorylation in skeletal muscle. According to the authors, these conflicting results could be explained by a chronic vs

acute adaptation to TRB3 overexpression.

Although some conflicting results appear in the literature, TRB3 overexpression inhibits insulin-stimulated Akt phosphorylation and glucose uptake in muscle cell lines (Liu et al., 2010, Koh et al., 2006). Furthermore, as noticed above, TRB3 siRNA reversed tunicamycin-induced insulin resistance (Koh et al., 2013). These findings are not in agreement with our study. However, differences in the level of TRB3 induction could explain such conflicting results. Indeed, in C2C12 myotubes, TRB3 mRNA was much more increased with tunicamycin than palmitate (Hage Hassan et al., 2012). On the other hand, overexpression techniques produce a drastic upregulation of TRB3 protein (Liu et al., 2010, Koh et al., 2006). According to western blot detection, Akt is much more expressed than TRB3 in C2C12 myotubes. Indeed, TRB3, unlike Akt, is never detected in the control condition (Koh et al., 2013). Consequently, we can imagine that only a massive induction of TRB3 is able to block Akt. Although TRB3 increases with palmitate, Akt expression could remain in a large excess compared to TRB3. In this unfavorable stoichiometry, TRB3 might not be able to inhibit Akt.

We cannot exclude that TRB3 do not interact with Akt. Indeed, a study published in the Biochemical Journal casts a doubt (Iynedjian, 2005). In hepatocytes, TRB3 was overexpressed with a molar excess of ~25-fold over Akt. This drastic increase of TRB3 did not affect insulin-stimulated Akt phosphorylation (Thr^{308} and Ser^{473}). These results are in opposition with those reported by Du et al. (2003) who were the first to show an interaction between TRB3 and Akt (Du et al., 2003). It remains difficult to explain such a discrepancy.

In our experiment, the results obtained are incomplete since we were unable to detect the protein level of TRB3. TRB3 was undetectable despite the use of three commercial antibodies (Santa Cruz, Calbiochem and Atlas). We tested them with positive (thapsigargin, palmitate and tunicamycin) and negative (TRB3 siRNA) controls without success. As a consequence, TRB3 protein knockdown is maybe too weak to restore insulin signaling.

In addition, conclusions of our study are limited by the absence of physiological measures such as glucose uptake or glycogen synthesis. We measured glucose uptake, but the effect of insulin was weak (~40%) (data not shown). When we added palmitate and siRNA, intra- and inter-variability were increased and the results were not interpretable. As already reported, insulin slightly increases glucose uptake in C2C12 myotubes, maybe because these cells do not have the complete machinery for glucose transport (Chavez and Summers, 2003).

ER stress and insulin resistance

Our study supports recent results demonstrating no link between physiological ER stress and insulin resistance in muscle cells. Indeed, insulin resistance induced by palmitate is not prevented by PBA, TUDCA, or BiP overexpression in C2C12 myotubes (Hage Hassan et al., 2012, Rieusset et al., 2012). This is not in line with *in vivo* data. In ob/ob mice, chemical chaperones increased glucose uptake in skeletal muscle (Ozcan et al., 2006). A systemic effect could reconcile *in vitro* and *in vivo* data. Indeed, chemical chaperones reduce glycaemia,

insulinemia and maybe inflammatory cytokines. This might affect skeletal muscle insulin sensitivity independently of ER stress. Furthermore, in the study from Ozcan et al. (2006), ER stress was not assessed in skeletal muscle. Consequently, it is not possible to associate glucose uptake to ER stress in this tissue.

Contrary to physiological ER stress, chemically-induced ER stress is well known to impair insulin action in muscle cells. Indeed, TUDCA reduced insulin signaling impairment induced by tunicamycin in C2C12 myotubes (Hage Hassan et al., 2012). According to these findings, the authors proposed that only a massive ER stress induces insulin resistance in muscle cells. Importantly, these observations challenge the conclusions drawn in previous studies using chemical ER stress inducers. What is the physiological relevance of the results obtained with these agents? As already noticed in this chapter and the chapter 3, *in vitro*, the link between UPR, inflammation, and insulin signaling is based on experiments using tunicamycin or thapsigargin. The conclusions from these studies should be carefully compared to physiological mechanisms. Although Hotamisligil is probably the author who contributed the most to establish the relationship between UPR and insulin signaling, he recently wrote: "*Notably, the extreme level of ER stress induced by tunicamycin is not physiological and is beyond what the liver experiences during metabolic fluctuations or even in most disease states*", further: "*We may be able to better understand the metabolic impact of ER stress by distinguishing between a physiological setting for the UPR (high glucose, dietary exposure, or lactation) and an extreme, death-inducing UPR (for example, liver cells treated with*

tunicamycin)" (Hotamisligil, 2010). In line with these recommendations, chemical ER stress inducers should be used as a positive control and not as a model of physiological ER stress.

Independently of ER stress, intramuscular ceramides have been proposed to mediate saturated NEFA-induced insulin resistance in muscle cells (Hage Hassan et al., 2012, Schmitz-Peiffer et al., 1999). Upon saturated NEFA exposure, ceramides content increases through *de novo* synthesis and maybe through an indirect regulation mediated by TLR4 (see 8.1.1). In muscle cells, ceramides are known to inhibit insulin signaling at the level of Akt (chapter 3). In addition to intramuscular ceramides, recent findings suggested a role of circulating ceramides in skeletal muscle insulin resistance. Circulating ceramides are elevated in type 2 diabetic patient (Boon et al., 2013). In lean mice, infusion of low density lipoproteins associated with ceramides induced insulin resistance specifically in the skeletal muscle (Boon et al., 2013). However, transport, regulation and action mechanism of circulating ceramides remain poorly understood.

8.1.3. Immunometabolism: an evolutionary point of view

Host defense and metabolism have been historically seen as two distinct disciplines. In education, this separation is used for didactic purposes, but this hides a highly integrated system. The research field of immunometabolism studies the mechanism by which immune system influences metabolism and vice versa. Immune and metabolic responses share numerous signaling pathways. For instance, TLR4 is expressed in non-immune cells and recognizes exogenous as well as endogenous ligands. In addition to inflammatory response, TLR4

engagement leads to metabolic changes in these cells (see above). Some proinflammatory cytokines possesses their own receptor in non-immune cells, for instance, the tumor necrosis factor receptor (TNFR) for TNFα. TNFR activation induces insulin resistance through JNK/IKK (Hotamisligil, 2005). Furthermore, metabolic tissues are infiltrated by numerous immune cells. In liver, 5% of total cells are the resident macrophages Kupffer cells (Shoelson et al., 2006). Macrophage infiltration in adipose tissue seems to initiate inflammation-induced insulin resistance (Shoelson et al., 2006). Finally, ER appears as a key integrator, which transduces metabolic signal into inflammatory signal (Hotamisligil, 2006).

Strikingly, in this work we found two examples showing no relationship between immune and metabolic systems in muscle cells. First, ER stress was not present after LPS treatment. Second, IRE1-JNK pathway does not seem related to insulin resistance. In hepatocytes and adipocytes these two mechanisms have been shown (Alhusaini et al., 2010, Zhang et al., 2006, Ozcan et al., 2004). Why does it not work in muscle cells? To speculate on this question, it could be interesting to take into account the evolution of species. Sensing nutrients as well as defense against pathogen appear the most fundamental requirements for living organisms. In lower species both systems are integrated. For instance, adipose tissue from *Drosophilia* contains immune cells and the equivalent of mammalian liver (Hotamisligil, 2006). This structure is known as “fat body”. In more evolved species, liver and adipose tissue are independent organs, whereas immune cells are ubiquitous. Thus, we can imagine a close relation between immune system and metabolism in liver as well as in

adipose tissue. This interaction could be less important in skeletal muscle. In the literature some observations support such idea, but this remains hypothetical. In mice, hematopoietic cell-specific deletion of TLR4 protected against insulin resistance in liver and adipose tissue, but not in skeletal muscle (Saberi et al., 2009). This suggests that interactions between immune cells and muscle cells are not a main component of insulin resistance in this tissue. In line with this result, skeletal muscle is less infiltrated by macrophages than liver and adipose tissue (Saberi et al., 2009). Interestingly, the key proteins linking inflammation to insulin resistance (IKKβ, NF-κB, PKCθ and JNK) were specifically altered in skeletal muscle by genetic manipulation. Contrary to heterozygous IKKβ mice, muscle-specific knockout mice for IKKβ were not protected against obesity-induced insulin resistance (Rohl et al., 2004, Yuan et al., 2001). In mice, muscle-specific inhibition of NF-κB did not prevent insulin resistance induced by HFD. Furthermore, overactivation of NF-κB in skeletal muscle does not lead to insulin resistance (Cai et al., 2004). As noticed in chapter 3, mice expressing a muscle-specific dominant-negative of PKCθ are obese and insulin-resistant. Finally, JNK muscle-specific deficiency furnished controversial results (see 8.1.2). Taken together, these observations suggest that skeletal muscle inflammation is not a major component of insulin resistance physiopathology.

It would be interesting to compare immunometabolism network in each cell types in order to better understand insulin resistance. It will probably lead to unravel many distinct types of insulin resistance.

8.2. Limitations

In almost all the studies found in the literature, including those presented herein, UPR is used as marker of ER stress. Consequently, we make the hypothesis that UPR or ER stress evaluation leads to the same result. This assumption can be formulated as follows: ER stress activates UPR and, accordingly, ER homeostasis can be assessed by measuring UPR. Is it always true? The question deserves to be asked and a preliminary answer will be exposed in the next paragraphs.

The main mechanism of UPR activation is based on the release of BiP from the ER stress sensors (PERK, IRE1α and ATF6) when unfolded proteins accumulate inside the ER (chapter 1). This is clearly an oversimplification and additional mechanisms have been proposed (Hotamisligil, 2010). Nevertheless, BiP detachment actives the three ER stress sensors. Consequently, if ER stress is present, the three UPR pathways should be activated. However, some studies reported a selective activation of UPR branches, suggesting thereby a disconnection between ER stress and UPR, and/or additional sensing mechanisms of ER stress.

In macrophages, TLR4 or TLR2 activation induced the splicing of XBP1 independently of ER stress as shown by the absence of effect on phospho-PERK, cleaved ATF6 protein levels and BiP, PDI, CHOP mRNA levels (Martinon et al., 2010). In L929 fibroblasts, H_2O_2 or arsenite induces the phosphorylation of eIF2α, whereas no change was observed in the phosphorylation state of PERK and the spliced form of XBP1 (Xue et al., 2005). Collectively, these findings suggest that, in particular conditions, UPR could be activated independently of ER stress.

Furthermore, UPR signaling is subject to regulation. eIF2α and ATF6 activations can be uncoupled from ER stress. In addition to PERK, three kinases are upstream of eIF2α: GCN2, HRI and PKR. HRI function is restricted to erythroid cells, whereas GCN2 is activated by amino acid deprivation and UV irradiation (Dey et al., 2010). In addition to double-strand RNA, PKR responds to ER stress, inflammatory mediators and nutrients (Nakamura et al., 2010, Hotamisligil, 2010). Consequently, this kinase integrates multiple signals and can activate eIF2α independently of ER stress. Regarding ATF6, it has been reported that p38 phosphorylates the cleaved form of ATF6 and enhances its transcriptional activity in HEK-293 cells and primary ventricular myocytes (Luo and Lee, 2002, Thuerauf et al., 1998). It has also been reported that peroxisome proliferators-activator receptor gamma coactivator-1 alpha (PGC-1α) modulates UPR through coactivation of ATF6 transcriptional activity in mice skeletal muscle (Wu et al., 2011). More generally, ATF4/ATF6/XBP1 form dimers with numerous partners, which are either activators or repressors (Schroder and Kaufman, 2005). According to these observations, two limitations appear when UPR is used to monitor ER stress: 1) phosphorylation of eIF2α is not specific to PERK activation; 2) UPR-inducible genes can be regulated independently of ER stress. Therefore, care must be taken when interpreting UPR as a marker of ER stress. Nevertheless, the spliced form of XBP1 seems to be the more specific marker of ER stress, except in macrophages (see above).

In the study presented in chapter 6, the pattern of UPR activation deserves a particular attention. To the best of our knowledge, the splicing of XBP1 by IRE1α is specifically dependent on ER stress in

muscle cells. Consequently, we supposed that H_2O_2 induced ER stress in C2C12 myotubes. However, we found a partial and unequal activation of UPR, the PERK signaling was much more activated than the IRE1α branch, while the AT6 pathway was probably unaffected by H_2O_2. In a general view, sensing and responding to ROS at the level of ER is a well-adapted mechanism to manage oxidative stress induced by protein folding reactions (chapter 1). According to our results, the PERK branch is probably specialized in the detection of oxidative stress. This is consistent with the antioxidant response triggered by this pathway (chapter 1). In our study, we supposed that PERK is activated by ER stress, and in turn phosphorylates eIF2α. Because we were not able to measure phospho-PERK despite using positive control (data not shown), we cannot rule out the involvement of other kinases. Results from the literature can give some clues. No evidences indicate an activation of GCN2 by oxidative stress. Although PKR does not seem activated by oxidative stress, one study reported that H_2O_2 upregulates its expression at the transcriptional level in human T lymphocyte cells (Pyo et al., 2008). Thus, instead or in addition to PERK this kinase could be involved in H_2O_2-induced eIF2α phosphorylation. A fifth kinase of eIF2α, specifically activated by oxidative stress, has been proposed by David Ron (Ron, 2002). This kinase has currently not been identified. PERK is probably activated under oxidative stress, but this remains controversial. In fibroblast cells, H_2O_2 induced eIF2α phosphorylation without PERK activation (Xue et al., 2005). However, PERK is phosphorylated after H_2O_2 treatment in HeLa cells (Pallepati and Averill-Bates, 2011). The mechanism by which ER senses oxidative stress is still unclear. In our

study, the pattern of UPR activation suggests that ER possesses a specific mechanism to detect oxidative stress. However, the absence of data on PERK and PKR is clearly a limitation for our study.

It should be interesting to compare *in situ* ER homeostasis to UPR signaling under various stresses. Interestingly, researchers used the secreted alkaline phosphatase (SEAP) system to monitor ER stress *in situ* (Hiramatsu et al., 2006). Cells were transfected with a reporter gene coding for a truncated form of the human placental alkaline phosphatase. This protein is secreted due to the removal of the membrane anchoring domain. Then, the activity of alkaline phosphatase is measured by chemiluminescence directly in the medium. SEAP activity is dose-dependently reduced by chemical ER stress inducers. Alternatively, morphological modification of ER has already been used to estimate ER stress in parallel with UPR markers. Indeed, ER is dilated when unfolded proteins accumulate inside it. For instance, TNFα as well as tunicamycin induce ER dilatation as shown by electron microscopy (Xue et al., 2005). To extend our knowledge on ER stress, it will be interesting to develop new strategies allowing to monitor the amount of unfolded proteins.

Another limitation of this work is the use of palmitate in non-physiological conditions (chapter 7). Palmitate is the most abundant saturated NEFA in the blood (Chavez and Summers, 2003). In human, the plasmatic concentration of palmitate ranges from ~100 µM (healthy subjects) to ~200 µM (obese subjects) (Yi et al., 2007). Although these values are subject to large interindividual variability,

the concentration of palmitate used in our study (1 mM) exceeds the physiological range.

Furthermore, interaction between saturated and unsaturated NEFA metabolism regulates their effect on insulin pathway. In C2C12 myotubes, palmitate alone induces insulin resistance, whereas this deleterious effect is prevented by addition of oleate (Salvado et al., 2013, Coll et al., 2008). Interestingly, palmitate incorporation into lipid-derived toxic metabolites, such as ceramides and DAG, decreases when it is co-supplemented with unsaturated NEFA. In human myoblast exposed to palmitate, addition of oleate preventes ceramides and DAG increase, two well-known mediators of lipid-induced insulin resistance (chapter 3) (Pickersgill et al., 2007). Consequently, the use of palmitate without unsaturated NEFA is far to mimic perfectly the real physiological conditions.

8.3. Conclusion

In the context of obesity, extracellular and intracellular lipids exert dramatic effects on cellular processes. Here, we investigated the mechanism by which lipids disrupt ER homeostasis. We show that a receptor of the innate immune system, TLR4, could indirectly mediate lipid-induced ER stress in skeletal muscle, liver and adipose tissue. In addition, our work highlights that ER stress is activated by oxidative stress in muscle cells. This provides an argument to propose ROS as common intermediates by which metabolic factors alter ER homeostasis.

In muscle cells challenged with lipid, we were interested by the consequence of ER stress on insulin signaling. Although ER homeostasis plays a central role in insulin resistance physiopathology, results from the literature are particularly conflicting in muscle cells. We show that, contrary to other cell types, muscle cells do not seem to possess the signaling mechanism linking UPR to insulin resistance.

References

Alhusaini, S., McGee, K., Schisano, B., Harte, A., McTernan, P., Kumar, S. & Tripathi, G. 2010. Lipopolysaccharide, high glucose and saturated fatty acids induce endoplasmic reticulum stress in cultured primary human adipocytes: Salicylate alleviates this stress. *Biochem Biophys Res Commun,* 397, 472-8.

An, D., Lessard, S. J., Toyoda, T., Lee, M. Y., Koh, H. J., Qi, L., Hirshman, M. F. & Goodyear, L. J. 2014. Overexpression of TRB3 in Muscle Alters Muscle Fiber Type and Improves Exercise Capacity in Mice. *Am J Physiol Regul Integr Comp Physiol*.

Boon, J., Hoy, A. J., Stark, R., Brown, R. D., Meex, R. C., Henstridge, D. C., Schenk, S., Meikle, P. J., Horowitz, J. F., Kingwell, B. A., Bruce, C. R. & Watt, M. J. 2013. Ceramides contained in LDL are elevated in type 2 diabetes and promote inflammation and skeletal muscle insulin resistance. *Diabetes,* 62, 401-10.

Cai, D., Frantz, J. D., Tawa, N. E., Jr., Melendez, P. A., Oh, B. C., Lidov, H. G., Hasselgren, P. O., Frontera, W. R., Lee, J., Glass, D. J. & Shoelson, S. E. 2004. IKKbeta/NF-kappaB activation causes severe muscle wasting in mice. *Cell,* 119, 285-98.

Cani, P. D., Amar, J., Iglesias, M. A., Poggi, M., Knauf, C., Bastelica, D., Neyrinck, A. M., Fava, F., Tuohy, K. M., Chabo, C., Waget, A., Delmee, E., Cousin, B., Sulpice, T., Chamontin, B., Ferrieres, J., *et al.* 2007. Metabolic endotoxemia initiates obesity and insulin resistance. *Diabetes,* 56, 1761-72.

Chavez, J. A., Knotts, T. A., Wang, L. P., Li, G., Dobrowsky, R. T., Florant, G. L. & Summers, S. A. 2003. A role for ceramide, but not diacylglycerol, in the antagonism of insulin signal transduction by saturated fatty acids. *J Biol Chem,* 278, 10297-303.

Chavez, J. A. & Summers, S. A. 2003. Characterizing the effects of saturated fatty acids on insulin signaling and ceramide and diacylglycerol accumulation in 3T3-L1 adipocytes and C2C12 myotubes. *Arch Biochem Biophys,* 419, 101-9.

Coll, T., Eyre, E., Rodriguez-Calvo, R., Palomer, X., Sanchez, R. M., Merlos, M., Laguna, J. C. & Vazquez-Carrera, M. 2008. Oleate reverses palmitate-induced insulin resistance and inflammation in skeletal muscle cells. *J Biol Chem,* 283, 11107-16.

Davis, J. E., Gabler, N. K., Walker-Daniels, J. & Spurlock, M. E. 2008. Tlr-4 deficiency selectively protects against obesity induced by diets high in saturated fat. *Obesity (Silver Spring),* 16, 1248-55.

Deldicque, L., Cani, P. D., Philp, A., Raymackers, J. M., Meakin, P. J., Ashford, M. L., Delzenne, N. M., Francaux, M. & Baar, K. 2010. The unfolded protein response is activated in skeletal muscle by high-fat feeding: potential role in the downregulation of protein synthesis. *Am J Physiol Endocrinol Metab,* 299, E695-705.

Dey, S., Baird, T. D., Zhou, D., Palam, L. R., Spandau, D. F. & Wek, R. C. 2010. Both transcriptional regulation and translational control of ATF4 are central to the integrated stress response. *J Biol Chem,* 285, 33165-74.

Du, K., Herzig, S., Kulkarni, R. N. & Montminy, M. 2003. TRB3: a tribbles homolog that inhibits Akt/PKB activation by insulin in liver. *Science,* 300, 1574-7.

Flamment, M., Hajduch, E., Ferre, P. & Foufelle, F. 2012. New insights into ER stress-induced insulin resistance. *Trends Endocrinol Metab,* 23, 381-90.

Frisard, M. I., McMillan, R. P., Marchand, J., Wahlberg, K. A., Wu, Y., Voelker, K. A., Heilbronn, L., Haynie, K., Muoio, B., Li, L. & Hulver, M. W. 2010. Toll-like receptor 4 modulates skeletal muscle substrate metabolism. *Am J Physiol Endocrinol Metab,* 298, E988-98.

Galbo, T., Perry, R. J., Jurczak, M. J., Camporez, J. P., Alves, T. C., Kahn, M., Guigni, B. A., Serr, J., Zhang, D., Bhanot, S., Samuel, V. T. & Shulman, G. I. 2013. Saturated and unsaturated fat induce hepatic insulin resistance independently of TLR-4 signaling and ceramide synthesis in vivo. *Proc Natl Acad Sci U S A,* 110, 12780-5.

Hage Hassan, R., Hainault, I., Vilquin, J. T., Samama, C., Lasnier, F., Ferre, P., Foufelle, F. & Hajduch, E. 2012. Endoplasmic reticulum stress does not mediate palmitate-induced insulin resistance in mouse and human muscle cells. *Diabetologia,* 55, 204-14.

Hetz, C. 2012. The unfolded protein response: controlling cell fate decisions under ER stress and beyond. *Nat Rev Mol Cell Biol,* 13, 89-102.

Hiramatsu, N., Kasai, A., Hayakawa, K., Yao, J. & Kitamura, M. 2006. Real-time detection and continuous monitoring of ER stress in vitro and in vivo by ES-TRAP: evidence for systemic, transient ER stress during endotoxemia. *Nucleic Acids Res,* 34, e93.

Hirosumi, J., Tuncman, G., Chang, L., Gorgun, C. Z., Uysal, K. T., Maeda, K., Karin, M. & Hotamisligil, G. S. 2002. A central role for JNK in obesity and insulin resistance. *Nature,* 420, 333-6.

Holland, W. L., Bikman, B. T., Wang, L. P., Yuguang, G., Sargent, K. M., Bulchand, S., Knotts, T. A., Shui, G., Clegg, D. J., Wenk, M. R., Pagliassotti, M. J., Scherer, P. E. & Summers, S. A. 2011. Lipid-induced insulin resistance mediated by the proinflammatory receptor TLR4 requires saturated fatty acid-induced ceramide biosynthesis in mice. *J Clin Invest,* 121, 1858-70.

Hoshino, K., Takeuchi, O., Kawai, T., Sanjo, H., Ogawa, T., Takeda, Y., Takeda, K. & Akira, S. 1999. Cutting edge: Toll-like receptor 4 (TLR4)-deficient mice are hyporesponsive to lipopolysaccharide: evidence for TLR4 as the Lps gene product. *J Immunol,* 162, 3749-52.

Hotamisligil, G. S. 2005. Role of endoplasmic reticulum stress and c-Jun NH2-terminal kinase pathways in inflammation and origin of obesity and diabetes. *Diabetes,* 54 Suppl 2, S73-8.

Hotamisligil, G. S. 2006. Inflammation and metabolic disorders. *Nature,* 444, 860-7.

Hotamisligil, G. S. 2010. Endoplasmic reticulum stress and the inflammatory basis of metabolic disease. *Cell,* 140, 900-17.

Hu, P., Han, Z., Couvillon, A. D., Kaufman, R. J. & Exton, J. H. 2006. Autocrine tumor necrosis factor alpha links endoplasmic reticulum stress to the membrane death receptor pathway through IRE1alpha-mediated NF-kappaB activation and down-regulation of TRAF2 expression. *Mol Cell Biol,* 26, 3071-84.

Iynedjian, P. B. 2005. Lack of evidence for a role of TRB3/NIPK as an inhibitor of

PKB-mediated insulin signalling in primary hepatocytes. *Biochem J*, 386, 113-8.

Jia, L., Vianna, C. R., Fukuda, M., Berglund, E. D., Liu, C., Tao, C., Sun, K., Liu, T., Harper, M. J., Lee, C. E., Lee, S., Scherer, P. E. & Elmquist, J. K. 2014. Hepatocyte Toll-like receptor 4 regulates obesity-induced inflammation and insulin resistance. *Nat Commun*, 5, 3878.

Kammoun, H. L., Chabanon, H., Hainault, I., Luquet, S., Magnan, C., Koike, T., Ferre, P. & Foufelle, F. 2009. GRP78 expression inhibits insulin and ER stress-induced SREBP-1c activation and reduces hepatic steatosis in mice. *J Clin Invest*, 119, 1201-15.

Kawasaki, N., Asada, R., Saito, A., Kanemoto, S. & Imaizumi, K. 2012. Obesity-induced endoplasmic reticulum stress causes chronic inflammation in adipose tissue. *Sci Rep*, 2, 799.

Kim, F., Pham, M., Luttrell, I., Bannerman, D. D., Tupper, J., Thaler, J., Hawn, T. R., Raines, E. W. & Schwartz, M. W. 2007. Toll-like receptor-4 mediates vascular inflammation and insulin resistance in diet-induced obesity. *Circ Res*, 100, 1589-96.

Koh, H. J., Arnolds, D. E., Fujii, N., Tran, T. T., Rogers, M. J., Jessen, N., Li, Y., Liew, C. W., Ho, R. C., Hirshman, M. F., Kulkarni, R. N., Kahn, C. R. & Goodyear, L. J. 2006. Skeletal muscle-selective knockout of LKB1 increases insulin sensitivity, improves glucose homeostasis, and decreases TRB3. *Mol Cell Biol*, 26, 8217-27.

Koh, H. J., Toyoda, T., Didesch, M. M., Lee, M. Y., Sleeman, M. W., Kulkarni, R. N., Musi, N., Hirshman, M. F. & Goodyear, L. J. 2013. Tribbles 3 mediates endoplasmic reticulum stress-induced insulin resistance in skeletal muscle. *Nat Commun*, 4, 1871.

Kramer, M. F. & Poort, C. 1972. Unstimulated secretion of protein from rat exocrine pancreas cells. *J Cell Biol*, 52, 147-58.

Lee, J. S., Pinnamaneni, S. K., Eo, S. J., Cho, I. H., Pyo, J. H., Kim, C. K., Sinclair, A. J., Febbraio, M. A. & Watt, M. J. 2006. Saturated, but not n-6 polyunsaturated, fatty acids induce insulin resistance: role of intramuscular accumulation of lipid metabolites. *J Appl Physiol*, 100, 1467-74.

Liu, J., Wu, X., Franklin, J. L., Messina, J. L., Hill, H. S., Moellering, D. R., Walton, R. G., Martin, M. & Garvey, W. T. 2010. Mammalian Tribbles homolog 3 impairs insulin action in skeletal muscle: role in glucose-induced insulin resistance. *Am J Physiol Endocrinol Metab*, 298, E565-76.

Luo, S. & Lee, A. S. 2002. Requirement of the p38 mitogen-activated protein kinase signalling pathway for the induction of the 78 kDa glucose-regulated protein/immunoglobulin heavy-chain binding protein by azetidine stress: activating transcription factor 6 as a target for stress-induced phosphorylation. *Biochem J*, 366, 787-95.

Martinon, F., Chen, X., Lee, A. H. & Glimcher, L. H. 2010. TLR activation of the transcription factor XBP1 regulates innate immune responses in macrophages. *Nat Immunol*, 11, 411-8.

Nakamura, T., Furuhashi, M., Li, P., Cao, H., Tuncman, G., Sonenberg, N., Gorgun, C. Z. & Hotamisligil, G. S. 2010. Double-stranded RNA-dependent protein kinase links pathogen sensing with stress and metabolic homeostasis. *Cell*, 140, 338-48.

Ozcan, U., Cao, Q., Yilmaz, E., Lee, A. H., Iwakoshi, N. N., Ozdelen, E., Tuncman,

G., Gorgun, C., Glimcher, L. H. & Hotamisligil, G. S. 2004. Endoplasmic reticulum stress links obesity, insulin action, and type 2 diabetes. *Science*, 306, 457-61.

Ozcan, U., Yilmaz, E., Ozcan, L., Furuhashi, M., Vaillancourt, E., Smith, R. O., Gorgun, C. Z. & Hotamisligil, G. S. 2006. Chemical chaperones reduce ER stress and restore glucose homeostasis in a mouse model of type 2 diabetes. *Science*, 313, 1137-40.

Pal, M., Wunderlich, C. M., Spohn, G., Bronneke, H. S., Schmidt-Supprian, M. & Wunderlich, F. T. 2013. Alteration of JNK-1 signaling in skeletal muscle fails to affect glucose homeostasis and obesity-associated insulin resistance in mice. *PLoS One*, 8, e54247.

Pallepati, P. & Averill-Bates, D. A. 2011. Activation of ER stress and apoptosis by hydrogen peroxide in HeLa cells: protective role of mild heat preconditioning at 40 degrees C. *Biochim Biophys Acta*, 1813, 1987-99.

Pang, S., Tang, H., Zhuo, S., Zang, Y. Q. & Le, Y. 2010. Regulation of fasting fuel metabolism by toll-like receptor 4. *Diabetes*, 59, 3041-8.

Panzhinskiy, E., Hua, Y., Culver, B., Ren, J. & Nair, S. 2013. Endoplasmic reticulum stress upregulates protein tyrosine phosphatase 1B and impairs glucose uptake in cultured myotubes. *Diabetologia*, 56, 598-607.

Pickersgill, L., Litherland, G. J., Greenberg, A. S., Walker, M. & Yeaman, S. J. 2007. Key role for ceramides in mediating insulin resistance in human muscle cells. *J Biol Chem*, 282, 12583-9.

Poggi, M., Bastelica, D., Gual, P., Iglesias, M. A., Gremeaux, T., Knauf, C., Peiretti, F., Verdier, M., Juhan-Vague, I., Tanti, J. F., Burcelin, R. & Alessi, M. C. 2007. C3H/HeJ mice carrying a toll-like receptor 4 mutation are protected against the development of insulin resistance in white adipose tissue in response to a high-fat diet. *Diabetologia*, 50, 1267-76.

Pyo, C. W., Lee, S. H. & Choi, S. Y. 2008. Oxidative stress induces PKR-dependent apoptosis via IFN-gamma activation signaling in Jurkat T cells. *Biochem Biophys Res Commun*, 377, 1001-6.

Radin, M. S., Sinha, S., Bhatt, B. A., Dedousis, N. & O'Doherty, R. M. 2008. Inhibition or deletion of the lipopolysaccharide receptor Toll-like receptor-4 confers partial protection against lipid-induced insulin resistance in rodent skeletal muscle. *Diabetologia*, 51, 336-46.

Reyna, S. M., Ghosh, S., Tantiwong, P., Meka, C. S., Eagan, P., Jenkinson, C. P., Cersosimo, E., Defronzo, R. A., Coletta, D. K., Sriwijitkamol, A. & Musi, N. 2008. Elevated toll-like receptor 4 expression and signaling in muscle from insulin-resistant subjects. *Diabetes*, 57, 2595-602.

Rieusset, J., Chauvin, M. A., Durand, A., Bravard, A., Laugerette, F., Michalski, M. C. & Vidal, H. 2012. Reduction of endoplasmic reticulum stress using chemical chaperones or Grp78 overexpression does not protect muscle cells from palmitate-induced insulin resistance. *Biochem Biophys Res Commun*, 417, 439-45.

Rohl, M., Pasparakis, M., Baudler, S., Baumgartl, J., Gautam, D., Huth, M., De Lorenzi, R., Krone, W., Rajewsky, K. & Bruning, J. C. 2004. Conditional disruption of IkappaB kinase 2 fails to prevent obesity-induced insulin resistance. *J Clin Invest*, 113, 474-81.

Ron, D. 2002. Translational control in the endoplasmic reticulum stress response. *J Clin Invest*, 110, 1383-8.

Saberi, M., Woods, N. B., de Luca, C., Schenk, S., Lu, J. C., Bandyopadhyay, G., Verma, I. M. & Olefsky, J. M. 2009. Hematopoietic cell-specific deletion of toll-like receptor 4 ameliorates hepatic and adipose tissue insulin resistance in high-fat-fed mice. *Cell Metab*, 10, 419-29.

Sabio, G., Kennedy, N. J., Cavanagh-Kyros, J., Jung, D. Y., Ko, H. J., Ong, H., Barrett, T., Kim, J. K. & Davis, R. J. 2010. Role of muscle c-Jun NH2-terminal kinase 1 in obesity-induced insulin resistance. *Mol Cell Biol*, 30, 106-15.

Sakurai, H., Suzuki, S., Kawasaki, N., Nakano, H., Okazaki, T., Chino, A., Doi, T. & Saiki, I. 2003. Tumor necrosis factor-alpha-induced IKK phosphorylation of NF-kappaB p65 on serine 536 is mediated through the TRAF2, TRAF5, and TAK1 signaling pathway. *J Biol Chem*, 278, 36916-23.

Salvado, L., Coll, T., Gomez-Foix, A. M., Salmeron, E., Barroso, E., Palomer, X. & Vazquez-Carrera, M. 2013. Oleate prevents saturated-fatty-acid-induced ER stress, inflammation and insulin resistance in skeletal muscle cells through an AMPK-dependent mechanism. *Diabetologia*, 56, 1372-82.

Schmitz-Peiffer, C., Craig, D. L. & Biden, T. J. 1999. Ceramide generation is sufficient to account for the inhibition of the insulin-stimulated PKB pathway in C2C12 skeletal muscle cells pretreated with palmitate. *J Biol Chem*, 274, 24202-10.

Schroder, M. & Kaufman, R. J. 2005. The mammalian unfolded protein response. *Annu Rev Biochem*, 74, 739-89.

Shi, H., Kokoeva, M. V., Inouye, K., Tzameli, I., Yin, H. & Flier, J. S. 2006. TLR4 links innate immunity and fatty acid-induced insulin resistance. *J Clin Invest*, 116, 3015-25.

Shoelson, S. E., Lee, J. & Goldfine, A. B. 2006. Inflammation and insulin resistance. *J Clin Invest*, 116, 1793-801.

Thuerauf, D. J., Arnold, N. D., Zechner, D., Hanford, D. S., DeMartin, K. M., McDonough, P. M., Prywes, R. & Glembotski, C. C. 1998. p38 Mitogen-activated protein kinase mediates the transcriptional induction of the atrial natriuretic factor gene through a serum response element. A potential role for the transcription factor ATF6. *J Biol Chem*, 273, 20636-43.

Tsukumo, D. M., Carvalho-Filho, M. A., Carvalheira, J. B., Prada, P. O., Hirabara, S. M., Schenka, A. A., Araujo, E. P., Vassallo, J., Curi, R., Velloso, L. A. & Saad, M. J. 2007. Loss-of-function mutation in Toll-like receptor 4 prevents diet-induced obesity and insulin resistance. *Diabetes*, 56, 1986-98.

Urano, F., Wang, X., Bertolotti, A., Zhang, Y., Chung, P., Harding, H. P. & Ron, D. 2000. Coupling of stress in the ER to activation of JNK protein kinases by transmembrane protein kinase IRE1. *Science*, 287, 664-6.

Weisberg, S. P., McCann, D., Desai, M., Rosenbaum, M., Leibel, R. L. & Ferrante, A. W., Jr. 2003. Obesity is associated with macrophage accumulation in adipose tissue. *J Clin Invest*, 112, 1796-808.

Wu, J., Ruas, J. L., Estall, J. L., Rasbach, K. A., Choi, J. H., Ye, L., Bostrom, P., Tyra, H. M., Crawford, R. W., Campbell, K. P., Rutkowski, D. T., Kaufman, R. J. & Spiegelman, B. M. 2011. The unfolded protein response mediates adaptation to exercise in skeletal muscle through a PGC-1alpha/ATF6alpha complex. *Cell Metab*, 13, 160-9.

Xue, X., Piao, J. H., Nakajima, A., Sakon-Komazawa, S., Kojima, Y., Mori, K.,

Yagita, H., Okumura, K., Harding, H. & Nakano, H. 2005. Tumor necrosis factor alpha (TNFalpha) induces the unfolded protein response (UPR) in a reactive oxygen species (ROS)-dependent fashion, and the UPR counteracts ROS accumulation by TNFalpha. *J Biol Chem*, 280, 33917-25.

Yi, L., He, J., Liang, Y., Yuan, D., Gao, H. & Zhou, H. 2007. Simultaneously quantitative measurement of comprehensive profiles of esterified and non-esterified fatty acid in plasma of type 2 diabetic patients. *Chem Phys Lipids*, 150, 204-16.

Yuan, M., Konstantopoulos, N., Lee, J., Hansen, L., Li, Z. W., Karin, M. & Shoelson, S. E. 2001. Reversal of obesity- and diet-induced insulin resistance with salicylates or targeted disruption of Ikkbeta. *Science*, 293, 1673-7.

Yuzefovych, L., Wilson, G. & Rachek, L. 2010. Different effects of oleate vs. palmitate on mitochondrial function, apoptosis, and insulin signaling in L6 skeletal muscle cells: role of oxidative stress. *Am J Physiol Endocrinol Metab*, 299, E1096-105.

Zhang, K. & Kaufman, R. J. 2008. From endoplasmic-reticulum stress to the inflammatory response. *Nature*, 454, 455-62.

Zhang, K., Shen, X., Wu, J., Sakaki, K., Saunders, T., Rutkowski, D. T., Back, S. H. & Kaufman, R. J. 2006. Endoplasmic reticulum stress activates cleavage of CREBH to induce a systemic inflammatory response. *Cell*, 124, 587-99.

Zhang, Y., Li, F., Liu, S., Wang, H., Mahavadi, S., Murthy, K. S., Khalili, K. & Hu, W. 2012. MEKK1-MKK4-JNK-AP1 pathway negatively regulates Rgs4 expression in colonic smooth muscle cells. *PLoS One*, 7, e35646.